

1-1-1993

# Cometary molecules.

Weiguo, Ge

*University of Massachusetts Amherst*

Follow this and additional works at: [https://scholarworks.umass.edu/dissertations\\_1](https://scholarworks.umass.edu/dissertations_1)

---

## Recommended Citation

Ge, Weiguo, "Cometary molecules." (1993). *Doctoral Dissertations 1896 - February 2014*. 1885.  
[https://scholarworks.umass.edu/dissertations\\_1/1885](https://scholarworks.umass.edu/dissertations_1/1885)

This Open Access Dissertation is brought to you for free and open access by ScholarWorks@UMass Amherst. It has been accepted for inclusion in Doctoral Dissertations 1896 - February 2014 by an authorized administrator of ScholarWorks@UMass Amherst. For more information, please contact [scholarworks@library.umass.edu](mailto:scholarworks@library.umass.edu).



312066008193082

# COMETARY MOLECULES

A Dissertation Presented

by

WEIGUO GE

Submitted to the Graduate School of the  
University of Massachusetts in partial fulfillment  
of the requirements for the degree of

DOCTOR OF PHILOSOPHY

February 1993

Department of Physics and Astronomy

©Copyright by Weiguo Ge 1993

All Rights Reserved

# COMETARY MOLECULES

A Dissertation Presented

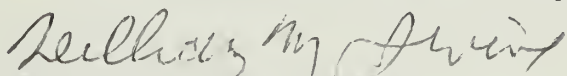
by

WEIGUO GE

Approved as to style and content by:



F. Peter Schloerb, Committee Chairperson



William M. Irvine, Member



Ronald L. Snell, Member



David J. van Blerkom, Member



Edward Chang, Outside Member



Robert B. Hallock, Department Head

Department of Physics and Astronomy

## ACKNOWLEDGEMENTS

I wish there were a better word than "thanks" to express my appreciation of Pete's help and guidance in making me through the toughest time in my life. Finishing a dissertation is not easy, especially for foreign students like me.

I did not have chance studying in high school when the culture revolution started in China. It was six years later since graduated from elementary school I could sit in the classroom of the university. English language was a big barrier that I had to overcome when I started studying astronomy in USA. I did not make sure I could finish the dissertation when faced all the difficulties. Fortunately, I got a lot of help from the people around me. For such guidance and support, I would like to thank Peter, Bill, David, and Ronald. I got a lot of encouraging from Peter and learned from him about how to do research and the scientific methods during my studying in here. We got important observation data that used in this thesis in Hawaii and we also had a lot of fun in there. Bill did a great deal for me throughout the course of my graduate career and especially corrected my thesis in carefully. The first person I met in the department is David and he gave me a warm welcome and helped me through some rough times when I first came here. I also thank Dr. Jaques Crovisier who mailed me the line strength data of  $\text{H}_2\text{CO}$  and enable me

build a excitation model of the molecule. I will remember all these help and kindness in my life.

My parents have been supportive and encouraging throughout my entire education. Unfortunately, I lost my dad forever during my studying in UMass. Sorry Mom. I thank and love you.

Finally, I love and thank my wife, Lijing. She has been, and continues to be, a source of joy to me. She has offered me support, advice, friendship, and compassion. There is no doubt that I owe the completion of this thesis to her. It is for that reason I dedicate this thesis to her.

ABSTRACT  
COMETARY MOLECULES  
FEBRUARY 1993  
WEIGUO GE  
B.S., BEIJING UNIVERSITY  
Ph.D., UNIVERSITY OF MASSACHUSETTS  
Directed by: Professor F. Peter Schloerb

A comprehensive model of the excitation and kinematics of cometary molecules has been developed and used to analyze data obtained on comet Levy (1990c). This work builds on previous studies to develop models of the excitation and distribution of HCN and H<sub>2</sub>CO in the coma and to apply these models to comet Levy in order to determine the physical parameters of the cometary coma and test models of the possible origin of H<sub>2</sub>CO in comets.

The collisional cross sections as a function of  $\Delta J$  have been considered in the excitation models for both molecules, based on quantum mechanical calculations. The vectorial model has been adopted for consideration of possible daughter species and a Monte Carlo calculation technique has been applied to develop both parent and daughter molecule models for H<sub>2</sub>CO so that we can calculate its production rate and discuss its original source.



With the high quality of spectra for both HCN and H<sub>2</sub>CO molecules in comet Levy, we are able to use our models to constrain their abundance and some physical parameters of the coma. These new observational results confirm that microwave spectroscopy is an efficient tool to study cometary parent molecules, and help us understand the formation of our solar system.

# TABLE OF CONTENTS

	Page
ACKNOWLEDGEMENTS.....	iv
ABSTRACT.....	vi
LIST OF TABLES.....	x
LIST OF FIGURES.....	xi
Chapter	
1. INTRODUCTION.....	1
1.1 Importance of Cometary Observations at Radio Wavelengths.....	1
1.1.1 Studies of Composition of the Coma.....	1
1.1.2 Physical Properties of the Coma.....	5
1.2 This Thesis.....	12
2. EXCITATION MODELS FOR HCN AND H <sub>2</sub> CO.....	15
2.1 General Remarks.....	15
2.2 HCN Molecule.....	18
2.2.1 Radiative Excitation.....	18
2.2.2 Collisional Excitation.....	25
2.2.3 Discussion.....	34
2.3 H <sub>2</sub> CO Molecule.....	39
2.3.1 Radiative Excitation.....	41
2.3.2 Collisional Excitation.....	44
2.3.3 Discussion.....	45
2.4 Conclusion.....	49

3. THE COMA MODEL.....	50
3.1 Model Description.....	50
3.2 Spectra Simulation.....	56
3.3 Conclusions.....	59
4. OBSERVATIONS.....	62
5. RESULTS.....	72
5.1 HCN Molecule.....	72
5.1.1 Spectrum.....	72
5.1.2 Map.....	78
5.1.3 Outflow Velocity of the Coma.....	83
5.1.4 Conclusion.....	96
5.2 H <sub>2</sub> CO Molecule.....	99
5.2.1 Spectrum.....	101
5.2.2 Map.....	106
5.2.3 Conclusion.....	109
6. SUMMARY.....	110
BIBLIOGRAPHY.....	114

## LIST OF TABLES

Table	Page
2.1 Rotational population distribution at fluorescence equilibrium.....	25
2.2 Fractions of Total De-excitation.....	27
2.3 The summary of used model.....	33
2.4 HCN integrated intensity (in units of $\text{K km s}^{-1}$ ).....	37
2.5 Parameters of the molecular bands of $\text{H}_2\text{CO}$ .....	43
2.6 Integrated intensities of $\text{H}_2\text{CO}$ for 10-m and 30-m telescope.....	48
4.1 The values of HCN $J=3-2$ integrated intensities for Comet Levy.....	64
5.1 Parameters in The model fitting.....	78
5.2 HCN Lifetime and position offset of the nucleus.....	83
5.3 Parameters of Velocity Laws.....	91
5.4 Parameters in Model fitting.....	106

## LIST OF FIGURES

Figure	Page
2.1 Possible vibrational levels $\nu_2$ , $2\nu_2$ , and $\nu_3$ involved in radiative excitation of HCN and the excitation rates by the solar radiation field at heliocentric distance $R_h = 1$ AU.....	19
2.2 Sample of HCN ro-vibrational levels and possible transition, $\Sigma$ - $\Sigma$ and $\Pi$ - $\Sigma$ .....	23
2.3 The rotational distributions of HCN in a cometary coma as a function of $r$ , the distance from the nucleus.....	31
2.4 The ratios of HCN $J=3-2/J=1-0$ and $J=4-3/J=3-2$ integrated intensities as a function of temperature, and the total cross section as a parameter.....	38
2.5 Sample of ortho- $H_2CO$ rotational energy levels.....	40
2.6 The vibrational levels of $H_2CO$ and the radiative excitation rates due to the solar infrared field.....	42
2.7 The $H_2CO$ rotational populations in the coma as a function of distance from the nucleus.....	46
3.1 The antisun and antiearth coordinate systems.....	53
3.2 The sample spectra by using parent model (full line) and daughter model (dashed line), respectively.....	61
4.1 HCN $J=3-2$ spectrum of Comet Levy(1990c) obtained at $0.1 \text{ km s}^{-1}$ resolution.....	66
4.2 HCN $J=3-2$ Map of Comet Levy(1990c). The spectra are sampled on a 30 arcsec grid about the "nucleus" position tracked by the telescope.....	67

4.3 HCN J=4-3 Spectrum of Comet Levy(1990c) obtained on August 30, 1990.....	68
4.4 H <sub>2</sub> CO 5 <sub>15</sub> -4 <sub>14</sub> spectrum of Comet Levy(1990c).....	69
4.5 H <sub>2</sub> CO 5 <sub>15</sub> -4 <sub>14</sub> Map of Comet Levy(1990c).....	71
5.1 fit to the HCN J=3-2 spectrum of Comet Levy(1990c) by using the model with constant outflow velocity.....	74
5.2 $\chi^2$ , contour map in V <sub>p</sub> -AP space.....	76
5.3 Fit to the HCN J=3-2 spectrum of Comet Levy(1990c) by using the model with constant outflow velocity.....	77
5.4 $\chi^2$ , contour map in x <sub>off</sub> -y <sub>off</sub> space.....	81
5.5 Observed distribution of HCN J=3-2 emission compare to that of the model.....	82
5.6 Four derived velocity laws with the theoretical velocity curve (filled line) calculated by Combi and scaled for the heliocentric distance of comet Levy.....	86
5.7 Fit to the HCN J=3-2 spectrum of Comet Levy(1990c) by using the model with the velocity as a step function (See equation 5.2).....	87
5.8 Fit to the HCN J=3-2 spectrum of Comet Levy(1990c) by using the model with the velocity law $V(r) = V_0 r^a$ (See equation 5.3).....	88
5.9 Fit to the HCN J=3-2 spectrum of Comet Levy(1990c) by using the model with the velocity law $V(r) =$ $V_0[1-(r/r_n)^{1/r_0}] + 0.2$ (See equation 5.4).....	89
5.10 Fit to the HCN J=3-2 spectrum of Comet Levy(1990c) by using the model with the velocity law $V(r) =$ $V_0[1-(r/r_n)^{1/r_0}]$ (See equation 5.5).....	90
5.11 $\chi^2$ , contour map in V <sub>1</sub> -V <sub>2</sub> space.....	92
5.12 $\chi^2$ , contour Map in a-b space. The equation (5.3) is used as a velocity law .....	93

5.13 $\chi^2_v$ contour Map in a-b space. The equation (5.4) is used as a velocity law.....	94
5.14 $\chi^2_v$ contour Map in a-b space. The equation (5.5) is used as a velocity law.....	95
5.15 The HCN particle number as a function of r, the distance from the nucleus.....	97
5.16 Fit to H <sub>2</sub> CO 5 <sub>15</sub> -14 <sub>14</sub> spectrum of Comet Levy(1990c) obtained on August 30, 1990.....	103
5.17 Fit to H <sub>2</sub> CO 5 <sub>15</sub> -14 <sub>14</sub> spectrum of Comet Levy(1990c) obtained on August 31, 1990.....	104
5.18 Fit to H <sub>2</sub> CO 5 <sub>15</sub> -14 <sub>14</sub> spectrum of Comet Levy(1990c) obtained on two days average.....	105
5.19 Observed distribution of H <sub>2</sub> CO 5 <sub>15</sub> -14 <sub>14</sub> emission compared to that of both the parent model (solid line) and the daughter models.....	108

# CHAPTER 1

## INTRODUCTION

### 1.1 Importance of Cometary Observations at Radio Wavelengths

#### 1.1.1 Studies of Composition of the Coma

The most pristine material surviving from the original solar nebula is believed to be in comets, and one of the main purposes of cometary studies is to determine the composition of the volatile species contained in the nucleus. These species may have remained unchanged since their original condensation, during or before the formation of the comets. Therefore, the composition of cometary nuclei may be representative of the primitive solar nebula and bear witness to the formation of the solar system.

Observations indicate that the nuclei of comets are ice-dust conglomerates and are very fragile entities. According to the Whipple's icy conglomerate model (1950), a comet nucleus is a mixture of ices of the abundant species, H, C, N, and O with H<sub>2</sub>O being the most abundant constituent and the dust embedded in the icy conglomerate. When a comet enters the inner solar system, its volatile species are released by solar heating and an expanding atmosphere of gas and dust develops



around the nucleus. This atmosphere is referred to as the coma and can be studied by ground based observations. Molecules released directly from the subliming ices have a variety of lifetimes against photodissociation in the solar radiation field. The secondary products formed by the photodissociation process of sublimed parents are radicals (Daughter molecules), atoms, and ions and can be observed in the ultraviolet and optical windows. The CN radical is one of these daughter molecules in cometary atmospheres, and the optical spectral lines of the CN radical are among the strongest features observed in the visible spectra of comets (Huggins 1882). However, despite observations of these fragments, any knowledge of the chemical composition of the nuclear ices must remain extremely model-dependent unless direct samples of cometary ices or direct observations of parent molecules are obtained.

The spectroscopy of comets at UV and visible wavelengths provides little help to determine the nature of their parent volatile species. These species generally do not have strong features at these wavelengths because they are destroyed by UV and visible photons rather than excited. Since most parent molecules in comets do not have strong electronic transitions in the visible and UV spectral ranges, one has to search for these species at other wavelengths. The low energy rotational transitions of these parent molecules usually fall in the radio range, so radio telescopes have become a useful tool for cometary studies.

It has long been proposed that HCN is one of the CN radical parent molecules based on the fact that HCN is abundant in interstellar clouds (Snyder and Buhl 1971) and has been detected in comets. The J(1-0) rotational lines of hydrogen cyanide at 89 GHz were detected in comet Halley by three independent groups (Bockelée-Morvan et al. 1987; Schloerb et al. 1987; Winnberg et al. 1987). This was the first unambiguous detection of HCN in a comet after several unsuccessful searches were carried out in other comets (Bockelée-Morvan et al. 1984), although an earlier detection was claimed in comet Kohoutek 1973 XII (Huebner et al. 1974). According to the data analysis (Schloerb et al. 1987; Bockelée-Morvan et al. 1987; and Crovisier et al. 1990), HCN is a relatively minor constituent with 0.1% of the abundance of H<sub>2</sub>O and may be one of the important parent molecules of the CN radical.

Since the Halley observations, many efforts have been made to search for the HCN molecule and other parent molecules in various comets. Searches for millimeter transitions of HCN in comets Austin, Machholtz, Brorsen-Metcalf, Okazaki-Levy-Rudenko and Wilson were carried out using the Five College Radio Astronomy Observatory (FCRAO) 14-m antenna. The fluorescence of the A-X bands of H<sub>2</sub>CO in optical band was reported in comet IRAS-Araki-Alcock (1983 VII) by Cosmovici and Ortolani (1984) and in comet Austin by Valk et al. (1992). During the fly-by of comet P/Halley by the IKS-VEGA instrument,

Combes et al. (1988) observed the infrared spectrum at  $3.6 \mu\text{m}$  and suggested that the observed emission should come from the  $\nu_1$  and  $\nu_5$  vibrational bands of  $\text{H}_2\text{CO}$ . Snyder et al. (1989) reported a detection of the  $1_{11}-1_{10}$  transition of  $\text{H}_2\text{CO}$  at 4829.695 MHz (6 cm wavelength) from comet Halley. The millimeter observations with the IRAM 30-m telescope have obtained important new molecular discoveries in the past years (Crovisier 1991). As a result, the HCN J(1-0) and J(3-2) transitions were detected in comets P/Brosen-Metcalf (1989o), Austin (1989c1) and Levy (1990c);  $\text{H}_2\text{CO}$  rotational transition  $3_{12}-2_{11}$  in comets P/Brosen-metcalf (1989o) and Levy (1990c). Hydrogen sulfide  $\text{H}_2\text{S}$  and methanol  $\text{CH}_3\text{OH}$  were first detected in comet Austin (1989c1). As many cometary molecular transitions fall at submillimeter wavelengths, this effort has expanded to submillimeter wavelengths with the search for parent molecules at the CSO (Caltech Submillimeter Observatory) in comets Austin (1989c1) and Levy (1990c). The comet Levy (1990c) observations were especially significant since they yielded good detections of HCN,  $\text{H}_2\text{CO}$ , and  $\text{CH}_3\text{OH}$  and provided high quality spectra and the first-ever maps of a parent molecule in the coma of the comet.

Another advantage of radio observations of molecules in the cometary coma is that high spectral resolution is obtainable. High spectral resolution permits radio observations to directly measure the line of sight velocity distribution of molecules in the coma and provides a

constraint on the outflow velocity of molecules in the coma. Moreover, high resolution resolves individual rotational transitions and the molecules can be unambiguously identified in cometary atmospheres by radio spectroscopy. This technique is now a proven means to study the composition of comets and their behavior. Therefore, it offers us the possibility of reconstructing the conditions under which comets formed and may help in tracing the history of the solar system.

### **1.1.2 Physical Properties of the Coma**

Knowledge of the physical nature of the coma is essential to the proper interpretation of cometary data at all wavelengths, including radio wavelengths. Radio observations of parent molecules in comets offer a direct means to monitor the production rates and kinematics of these parent molecules. Nevertheless before quantitative compositional knowledge can be realized, we must fully understand both the physical structure of the coma and the excitation of the molecules within it.

Because the integrated intensity of an optically thin molecular line in the coma is directly related to molecular column density in the upper level of that transition, it is important to have detailed models of the molecular excitation state so that observations may be interpreted to

obtain the abundances of these parent molecules. Excitation models of the cometary atmosphere have been developed for some parent molecules, such as hydrogen cyanide (Crovisier and Encrenaz 1983; Weaver and Mumma 1984; Bockelée-Morvan 1984); water molecule (Crovisier 1984; Bockelée-Morvan 1987); and formaldehyde (Bockelée-Morvan and Crovisier 1992). Two models of formaldehyde infrared fluorescence also were developed by Brooke et al. (1989) and Reuter et al. (1989) in order to derive synthetic spectra to be compared with available infrared spectra.

The possible excitation mechanisms of parent molecules in comets are radiative excitation of the vibrational bands in the medium infrared or of the electronic bands in the UV, and thermal excitation by collisions. Collisions with neutral species in the coma is expected to be the dominant collisional process. Excitation of parent molecules can also occur by collisions with ions and electrons, although it can be expected that these collisions are negligible compared with collisions with water since the densities of ions and electrons are lower than that of the H<sub>2</sub>O molecule. Collisional excitation prevails in the inner coma and forces the parent molecules to be at thermal equilibrium. Unfortunately, collisional excitation is not easy to calculate because it depends on two uncertain parameters: the collisional cross-sections and the coma temperature. In previous models, the effects of collisions on the rotational level

distribution of a molecule as a function of the distance from the nucleus of the comet has been calculated by assuming that each collision redistributes the molecule in the rotational levels according to a Boltzmann distribution (Crovisier 1984; Crovisier 1987 and Bockelée-Morvan and Crovisier 1992). Thus, only the total collisional cross-section as a model parameter is needed in the excitation calculation. However, this treatment is only approximate, because the actual cross-sections for molecules such as HCN are generally a function of  $\Delta J = J_{\text{upper}} - J_{\text{lower}}$ .

The radius of the collisional region in a typical bright comet is only on the order of a few  $10^3$  km. Outside this region, the rotational population distribution is governed by fluorescence equilibrium, the balance between the excitation of the vibrational bands by infrared radiation fields and radiative decay due by spontaneous emission. The excitation of electronic bands for most molecules in comets by solar radiation leads primarily to photodissociation instead of fluorescence, and so does not affect the population distribution within the ground electronic state.

Several radiation fields exist in the cometary environment that may contribute to the molecular excitation. They are direct solar radiation, solar radiation scattered by the nucleus or dust particles, and thermal emission of the nucleus or dust particles. It can be shown (Crovisier and Encrenaz 1983) that excitations due to the scattered solar radiation and

thermal emissions of the nucleus or dust particles are negligible with respect to those due to direct solar radiation.

Radio observations in comets can lead to measurements of the outflow velocities of the parent molecules, which are a necessary feature of coma models as well as a clue to the thermodynamics of the coma, and enable us to obtain information on cometary composition and kinematics. As mentioned above, hydrogen cyanide has now been observed in a few comets and the kinematic behavior of gas in the coma can be characterized through the direct HCN observations of parent outflow velocities. The HCN line width is directly related to the parent outflow velocity, and in comet P/Halley, it was shown to increase with decreasing heliocentric distance (Schloerb et al. 1987). Information about the origin of CN might also be obtained from the HCN outflow velocity. For example, comparison of the HCN velocity (Schloerb et al. 1987) and the CN shell velocities (Schlosser et al. 1986) in P/Halley suggests that the CN shell velocity may be less than the HCN velocity. This would be difficult to explain if the observed CN were produced directly from HCN, since the photodissociation process should add an additional velocity to the daughter. Thus, the CN in the shells must either arise from parent molecules with a lower velocity or must be thermalized as discussed by Delsemme (1982). The former case would be consistent with a grain

origin for some CN in the coma as proposed by A'Hearn et al. (1986), since the grain velocities are expected to be less than those of the gas.

Most cometary models assume that water ice is dominant in the cometary nucleus, but the H<sub>2</sub>O molecule cannot be easily observed because it has no strong spectral lines at visible wavelengths. Snyder (1982) summarized a number of searches for H<sub>2</sub>O and other molecules at radio wavelengths. Combes et al. (1986) identified possible fluorescence signatures of H<sub>2</sub>O with the IKS experiment on board VEGA 1. The first indisputable, direct detection of H<sub>2</sub>O in any comet was made during IR observations of comet Halley from the NASA Kuiper Airborne Observatory (Mumma et al. 1986), and high resolution spectra of the (001-000) and (011-010) bands of H<sub>2</sub>O near 2.65  $\mu\text{m}$  were obtained. Thus, high resolution spectra suitable for kinematic analyses have been used to measure the expansion velocity (Larson et al. 1987), spatial anisotropy (Weaver et al. 1987), and temporal variability (Larson et al. 1990) in the neutral gas outflow. In comet Halley, the derived H<sub>2</sub>O outflow velocity was 0.9 km s<sup>-1</sup> pre-perihelion and 1.4 km s<sup>-1</sup> post-perihelion (Weaver et al. 1987). From infrared observations of the water molecule, the gas kinetic temperature in the coma can be derived by using a thermodynamical model.

The OH radical has been studied in the optical regions, the 0-0 (3085 Å) and 1-1 (3135 Å) bands of the A <sup>2</sup>Σ<sup>+</sup> - X <sup>2</sup>Π transition, and in the



radio region  $\Lambda$ -doublet transitions at 18-cm wavelength (Schloerb et al. 1987; Claussen and Schloerb 1987). The high spectral resolution and high signal to noise ratio of the radio OH spectra have been used to study the kinematics of OH in the cometary coma (Tacconi-Garman et al. 1990). The shape of the OH radio lines places significant constraints on the velocity of gas in the coma and clearly demonstrates that OH is a daughter species. Thus, the OH line studies demonstrate the potential of high resolution spectroscopy to resolve the question of the origin of a particular species in the coma. The OH molecules are excited from the hyperfine levels of the ground state by solar UV. Since the excitation is caused by the Doppler shifted solar spectrum, the resulting relative populations of the hyperfine levels depend on the heliocentric velocity of the comet. If an upper level becomes overpopulated, the background radiation causes maser emission of the corresponding 18 cm OH line. We can see the OH in absorption against the background if the comet's heliocentric velocity is such that a lower level becomes overpopulated. During a comet's perihelion passage, its heliocentric velocity changes drastically, and the cometary OH lines are changed from absorption to emission and back again (Crovisier and Schloerb 1990). Thus, using theoretical models, one can predict the OH behavior of the comet as a function of heliocentric velocity.

The observational radio data of cometary atmospheres can be used to compare with the data obtained in the optical and UV ranges, and more than that, their high spectral resolution allows a direct measurement of the line of sight velocity distribution of molecules in the coma that enables one to discuss the kinematics of cometary comae. In principle, radio observations themselves can constrain the models of molecular excitation and molecular origin, for example, through maps of the extent of the emission or through multi-transitional studies of molecules. In the case of the VLA  $\text{H}_2\text{CO}$   $1_{11}-1_{10}$  spectral line observed in comet Halley, Snyder et al. (1989) had to assume an  $\text{H}_2\text{CO}$  scale length of  $10^4$  km in order to fit the spectrum and compute the  $\text{H}_2\text{CO}$  production rate. Because the photodissociation scale length was about  $10^3$  km, their data analysis suggested that cometary  $\text{H}_2\text{CO}$  was produced from an extended source in the coma as well as directly from the nucleus. The observations of the 226 GHz  $\text{H}_2\text{CO}$  line obtained by Colom et al. (1990) also suggest a distributed source for  $\text{H}_2\text{CO}$ . Their line intensity data at offset positions can not be explained by assuming that  $\text{H}_2\text{CO}$  comes directly from the nucleus, as formaldehyde is a short-lived molecule with its photodissociation rate of  $2.8 \times 10^4 \text{ s}^{-1}$  at 1 AU from the Sun.

Generally, an important goal of the analysis of radio observations is to improve the models of cometary comae, both to improve the quantitative interpretation of compositional information, and to improve

our understanding of the physical processes in comets in order to determine the type of cloud in which the solar system formed.

## 1.2 This Thesis

In this thesis, a comprehensive model of the excitation and kinematics of molecules in cometary comae has been developed and used to analyze the data obtained on Comet Levy (1990c). We develop detailed models of the excitation and distribution of HCN and H<sub>2</sub>CO in the coma and apply these models to comet Levy (1990c) in order to determine the physical parameters in the cometary coma and test models of the possible origin of H<sub>2</sub>CO in comets.

For HCN, new theoretical excitation calculations, which extend previous work through more detailed consideration of collisional cross sections, have been developed. Quantum mechanical calculations (Green and Thaddeus 1974) show that the HCN cross sections depend on  $\Delta J$  and have a large preference for  $\Delta J=2$  collisions. Thus, we have treated collisions in the inner coma by assuming that the cross section is a function of  $\Delta J$ , based on calculations of the collisional cross section of HCN on He (Green and of Thaddeus 1974). A similar treatment for the H<sub>2</sub>CO excitation model has been carried out by using collisional cross

sections based on the calculations for rates of excitation of  $\text{H}_2\text{CO}$  by collisions with He (Green et al. 1978).

In addition to molecular excitation studies, we have also discussed the coma kinematics. For parent molecules, the kinematics are simple: essentially radial outflow of molecules from the nucleus. For daughter molecules, however, the behavior is more complex. Daughter molecular kinematics are described by the vectorial model in which each daughter molecule is released in a random direction from its parent. The additional velocity is added vectorially to the original parent velocity to produce the final daughter velocity after the parent molecule photodissociation. In this work, both parent and daughter models have been used to analyze the maps and spectral line shapes obtained in comet Levy in order to investigate the origin of the species. With the use of Monte Carlo calculation techniques, the vectorial model has been successfully used in the calculation of synthetic spectra (Bockelée-Morvan and Gérard 1984) and gas dynamical models (Combi and Smyth 1988b). We have adopted the vectorial model for consideration of possible daughter species and apply a Monte Carlo calculation technique to develop both parent molecule and daughter molecule models for  $\text{H}_2\text{CO}$  observed at radio wavelengths so that we may calculate its production rate and constrain its original source.

With the high quality of spectra for both HCN and H<sub>2</sub>CO molecules in Comet Levy, we are able to use our model to constrain their total production rates, the distribution of gas production from the nucleus, the gas velocity within the coma, and to discuss the origin of these molecules. Using different gas velocity laws to fit the observed data, we are also able to discuss the acceleration of gas in the coma. These new observational results confirm that microwave spectroscopy is an efficient tool to study cometary parent molecules, which may in turn help us understand the formation of the Sun and our solar system.

## CHAPTER 2

### EXCITATION MODELS FOR HCN AND H<sub>2</sub>CO

#### 2.1 General Remarks

In order to estimate the abundance of a particular molecule in the coma of a comet, it is necessary to have a model of its excitation to derive the relative population of the rotational levels of the ground vibrational and electronic state. In this chapter, we develop such a model for two parent species, HCN and H<sub>2</sub>CO, that have been observed recently in comets.

Interpretation of rotational line observations in terms of molecular column densities and production rates must be based on a comprehensive excitation model. The main excitation mechanisms which need to be considered are thermal excitation by collisions with H<sub>2</sub>O in the inner coma and excitation via the fundamental bands of vibration by the infrared solar field in the outer coma (Crovisier and Encrenaz 1983). In carrying out the calculation, several simplifying assumptions have to be made, and these are summarized and discussed below.

The balance between solar infrared excitation and spontaneous decay that tends to establish equilibrium of the population distribution of the ground state rotational levels is called fluorescence equilibrium. The typical excitation rates for this mechanism are on order of  $10^{-4} \text{ s}^{-1}$  at a

heliocentric distance  $r_h = 1$  AU. In contrast with radicals which have strong signals resulting from visible or UV excitation, most parent molecules are not likely to be significantly excited by this process. In some cases, these transitions do not exist or are weak in the visible range. In other cases, these transitions lead to dissociation and not fluorescence. Thus, the excitation by the UV solar radiation field can be neglected and only radiative excitation in the fundamental vibrational bands of a molecule is included in the model. The excitation of any harmonic bands is neglected because their strengths and excitation rates are generally at least an order of magnitude smaller than those of the fundamental bands.

We assume that the populations of excited vibrational levels are much smaller compared with that of the ground vibrational level and may be neglected. The vibrational Einstein spontaneous emission coefficients ( $< 1 \text{ s}^{-1}$ ) are much larger than the excitation rate ( $\sim 10^{-4} \text{ s}^{-1}$ ) and collisional excitation to vibrational levels is not important due to the low coma temperature. Thus, the excitation rates are too small to populate the vibrational states significantly. Moreover, we have neglected rotational spontaneous decay within excited vibrational levels in this model and assumed that virtually all cometary HCN would be in the  $00^0_0$  ground vibrational state.

Other radiation fields might also have been considered, such as solar radiation scattered off the nucleus or dust particles and thermal

emission of the nucleus or dust particles. An accurate estimation of these fields would require the knowledge of the dust distribution and size distribution, the nucleus and dust composition, and the temperature distribution. Since such data were lacking, Crovisier and Encrenaz (1983) made order of magnitude estimations based on crude assumptions about the dust size and distribution. Their results show that the excitation due to scattered solar radiation is completely negligible; the excitation due to nucleus emission is negligible with respect to that due to dust emission; the excitation due to dust emission is negligible for wavenumber greater than  $1,500 \text{ cm}^{-1}$ , and for low wavenumbers, it is also negligible for distances to the nucleus  $r$  greater than  $10^3 \text{ km}$ . Thus, our excitational model is simplified so that only the excitation due to direct solar radiation is considered.

Finally, all molecular transitions are assumed to be optically thin in the coma, and radiative trapping effects are neglected. This assumption, which is not valid for the strong rotational lines of  $\text{H}_2\text{O}$  (Crovisier 1984; Bockelée-Morvan and Crovisier 1986), is fully justified for minor species, even in active comets. For molecules like  $\text{HCN}$  and  $\text{H}_2\text{CO}$ , whose abundances relative to water are usually believed to be 0.1% and 1.0% respectively, the assumption of optical thin transitions is appropriate except within 100 km of the nucleus.



## 2.2 HCN Molecule

### 2.2.1 Radiative Excitation

HCN is a linear molecule, and it is relatively straightforward to model its radiative excitation. Its rotational line frequencies and strengths for the  $\Sigma$  state depend only on two parameters, the moment of inertia and the permanent dipole moment. The  $\Pi$  vibrational states are degenerate and need an additional quantum number  $l$  to describe.

As discussed in the last section, the radiative excitation by the solar infrared field is only considered for the fundamental bands of vibration and most molecules are in the ground vibrational state. But, one of the HCN harmonic vibrational bands  $2\nu_2$  is involved in the calculation as its radiative excitation rate is comparable to other two fundamental bands shown in Figure 2.1. Thus, we need to consider rotational decay within the ground vibrational level; excitation and fluorescence of parallel vibrational bands ( $\Sigma$ - $\Sigma$  type, stretching mode and non-degenerate with  $\Delta l = 0$ ); and excitation and fluorescence of perpendicular vibrational bands ( $\Pi$ - $\Sigma$  type, bending mode and double-degenerate with  $\Delta l = \pm 1$ ) as shown in Figure 2.1. Fundamental bands of vibration other than those shown in Figure 2.1 are negligible since their band strengths are smaller and lead to smaller excitation rates. Figure 2.1 also gives the values of band

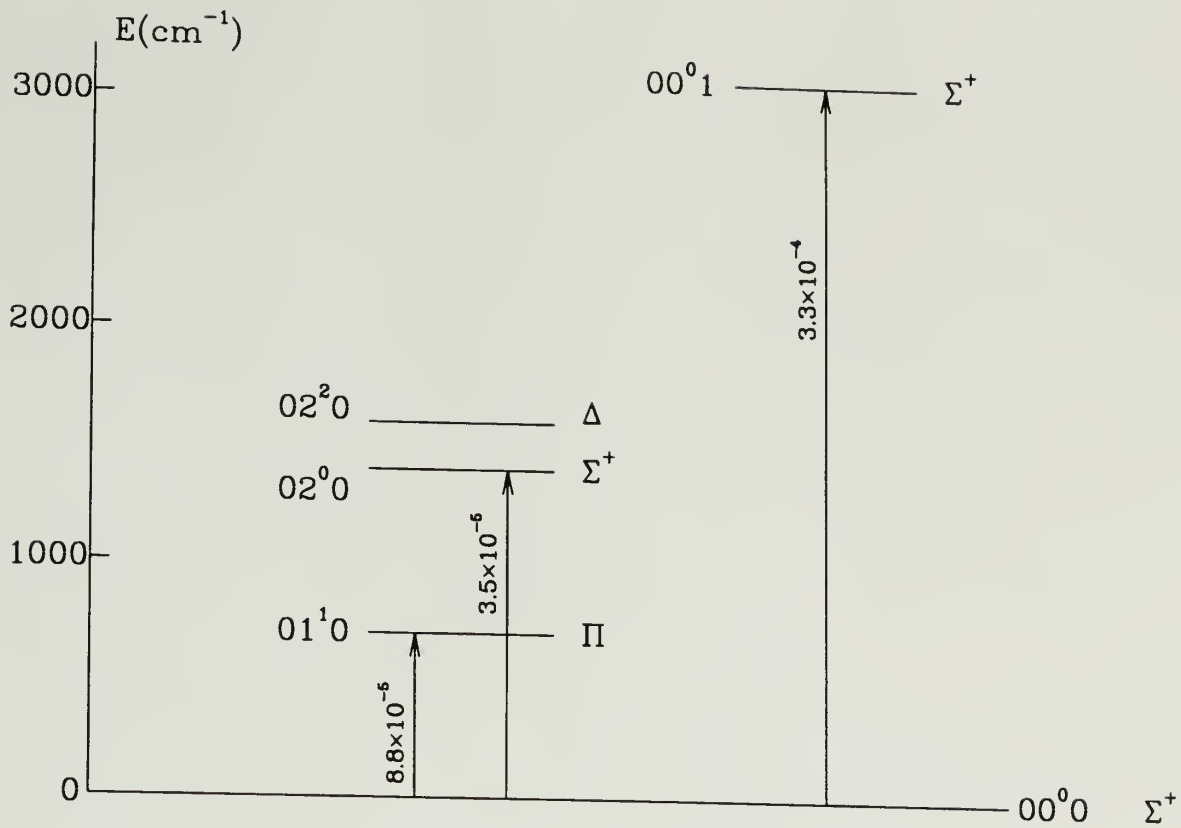


Figure 2.1 Possible vibrational levels  $v_2$ ,  $2v_2$ , and  $v_3$  involved in radiative excitation of HCN and the excitation rates by the solar radiation field at heliocentric distance  $R_h = 1 \text{ AU}$ .

excitation  $g_{v'}$  at  $R_h = 1$  AU defined by Crovisier and Encrenaz (1983):

$$g_{v'} = \frac{\Omega_{bb}}{4\pi} A_{v',v} [e^{hc\sigma_{v'}/kT_{bb}} - 1]^{-1} \quad (2.1)$$

where  $\Omega_{bb}$  is the solar solid angle,  $\sigma_{v'}$  the line frequency in  $\text{cm}^{-1}$ , and  $A_{v',v}$  the band Einstein spontaneous emission coefficient given by

$$A_{v',v} = 3.08 \times 10^{-8} \times \sigma_{v',v}^2 \times S \quad (2.2)$$

where  $S$ , in  $\text{cm}^{-2} \text{atm}^{-1}$ , is the total band strength.

The approximation that all the HCN molecules are in their ground vibrational state, as discussed in the last section, allows us to simplify the detailed fluorescence computation. Considering rotational level  $J$  in the ground vibrational state, we only need to calculate the probabilities that the transitions lead back to another rotational level  $J'$  after radiative excitation by the solar radiation field to an excited vibrational state. For example, the probability for transition from an excited vibrational level  $(v, J+1)$  back to a ground vibrational level  $(0, J)$  should be  $A_{J+1,J}^{v,0} / (A_{J+1,J}^{v,0} + A_{J+1,J+2}^{v,0})$  for  $\Sigma$ - $\Sigma$  type transitions, where  $A$  is the Einstein spontaneous emission coefficient. Similar way, we can calculate the probability for  $\pi$ - $\Sigma$  type transitions.

Now, we can write down the statistical equilibrium equations by only considering the radiative excitation of the vibrational bands and radiative decay due to spontaneous emission as

$$\begin{aligned}
\frac{dp_J}{dt} = & p_{J-2} \sum_J G_{J-2,J-1} \frac{A_{J-1,J}}{A_{J-1,J} + A_{J-1,J-2}} \\
& - p_J [A_{J,J-1}^{0,0} + \sum_J (G_{J,J-1} \frac{A_{J-1,J-2}}{A_{J-1,J-2} + A_{J-1,J}} + G_{J,J+1} \frac{A_{J+1,J+2}}{A_{J+1,J+2} + A_{J+1,J}})] \\
& + p_{J+1} A_{J+1,J}^{0,0} \\
& + p_{J+2} \sum_J G_{J+2,J+1} \frac{A_{J+1,J}}{A_{J+1,J} + A_{J+1,J+2}}
\end{aligned} \quad (2.3)$$

where  $p_J$  is the relative population of the rotational level  $J$  in the vibrational ground state.  $A_{J,J'}$  is the Einstein coefficient for  $(v',J') \rightarrow (v'',J'')$  spontaneous emission, and  $G_{J'',J'}$  is the excitation rate of the  $(v'',J'') \rightarrow (v',J')$  transition by the solar radiation field. The selection rules are  $\Delta J = \pm 1$  for parallel vibrational transitions ( $\Sigma \rightarrow \Sigma$  transition). The Einstein coefficients and the excitation rates that can be found in the appendix of Bockelée-Morvan and Crovisier (1985) are given as the following:

$$A_{J-1,J} = A_{v,0} \frac{J}{2J-1} \quad , \quad (2.4)$$

$$A_{J+1,J} = A_{v,0} \frac{J+1}{2J+3} \quad , \quad (2.5)$$

where  $A_{v,0}$  is the total spontaneous emission rate of the band, defined in equation 2.2. Similarly for the excitation rate,

$$G_{J,J-1} = g_v \frac{J}{2J+1} \quad , \quad (2.6)$$

$$G_{J,J+1} = g_v \frac{J+1}{2J+1} , \quad (2.7)$$

where  $g_v$  is the total excitation rate of the band and  $g_v = g_{0,v}/R_h^2$  with  $g_{0,v}$  given in equation (2.1). The  $R_h$  is the heliocentric distance of the comet. The selection rules are  $\Delta J = 0, \pm 1$  for the upper vibrational level with double degeneracy ( $\Sigma$ - $\Pi$  transition). We have

$$A_{J-1,J} = A_{v,0} \frac{J-1}{2J-1} , \quad (2.8)$$

$$A_{J,J} = A_{v,0} , \quad (2.9)$$

$$A_{J+1,J} = A_{v,0} \frac{J+2}{2J+3} , \quad (2.10)$$

and

$$G_{J,J-1} = 0.5g_v \frac{J-1}{2J+1} , \quad (2.11)$$

$$G_{J,J} = 0.5g_v , \quad (2.12)$$

$$G_{J,J+1} = 0.5g_v \frac{J+2}{2J+1} . \quad (2.13)$$

In Figure 2.2, we show a sample of ro-vibrational energy levels of HCN and a partial set of possible transitions among these levels. For the  $\Sigma$ - $\Sigma$  transition, the rotational level  $J=2$  in the ground vibrational state is

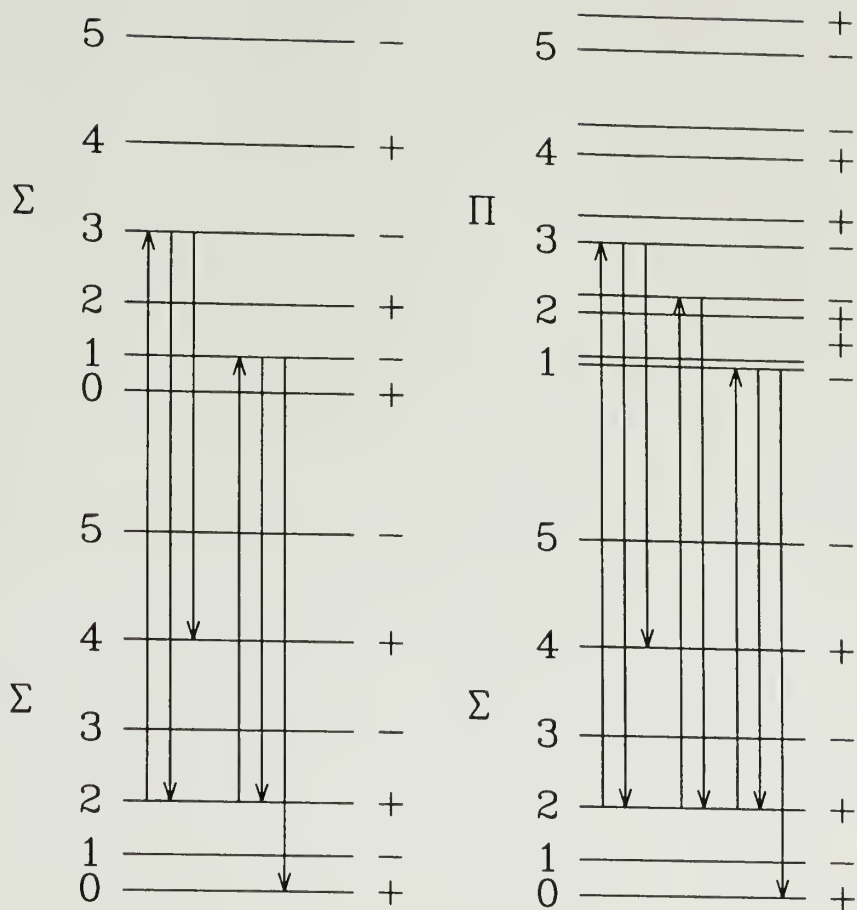


Figure 2.2 Sample of HCN ro - vibrational levels and possible transitions,  $\Sigma$ - $\Sigma$  and  $\Pi$ - $\Sigma$ . The possible transitions for the rotational level  $J=2$  in the ground vibrational state have been demonstrated.

populated by the solar radiation according to the selection rules. Thus, as shown in Figure 2.2, there are two ways that the molecule can go back to  $J=2$  rotational level in the ground vibrational state from the excited vibrational state and we can calculate the probabilities corresponding to these two transitions. Similarly, we can calculate the probabilities among the  $\Pi$ - $\Sigma$  transition and the only difference is the selection rules.

As we can see from the excitation rates given in the equations, the HCN relative population of the rotational levels only depends on the heliocentric distance if solar radiation is the only excitation mechanism. The equation 2.3 has been solved by using the Gaussian elimination method and selecting 20 rotational levels. The results are shown in Table 2.1, which gives the relative populations  $p_J$  at different heliocentric distance. We can see from this table that the excitation of higher rotational levels is enhanced when  $R_h$  decreases since the radiative excitation rates increase as a function of  $R_h^{-2}$ .

Table 2.1

Rotational population distribution at fluorescence equilibrium

$R_n(\text{AU}) \setminus P$ (J)	P(0)	P(1)	P(2)	P(3)	P(4)	P(5)
1.8	.1960	.5710	.1840	.0440	.0048	.0005
1.4	.1380	.5340	.2430	.0725	.0109	.0014
1.0	.0994	.4250	.3150	.1260	.0290	.0049
0.6	.0744	.2470	.3340	.2210	.0920	.0261
0.2	.0872	.0913	.1430	.1860	.1950	.1620

### 2.2.2 Collisional Excitation

Collisional excitation is not as straightforward to calculate because it depends on two uncertain parameters: the collisional cross-sections and the coma temperature. Lack of accurate collision cross-sections is a major obstacle to understanding the excitation of a particular molecule. Under conditions in a typical comet, most molecules are in their lowest electronic and vibrational level and only a handful of rotational levels are significantly populated. Since the radiative and collisional excitations may



have comparable rates, but obey different "selection rules", the rotational levels are generally not in equilibrium with either the radiation temperature or the ambient kinetic temperature. Thus, detailed knowledge of both radiative and collisional rates is necessary to understand the physics in these regions and to interpret the observational data.

In previous models (Crovisier and Encrenaz 1983; Weaver and Mumma 1984; Bockelée-Morvan 1984), the effects of collisions on the rotational level distribution of a molecule as a function of its distance from the nucleus of comet has been calculated by assuming that each collision redistributes the molecule in the rotational levels according to a Boltzmann distribution. However, the quantum mechanical calculation of HCN cross sections (Green and Thaddeus 1974) shows that a large preference for  $\Delta J=2$  collisions may exist. Thus, in our model, we have treated collisions in the inner coma by assuming that the cross section is a function of  $\Delta J$ , based on calculations of the collisional cross section of HCN with He and HC<sub>3</sub>N with He (Green and of Thaddeus 1974). Table 2.2 summarizes these two groups of collisional cross sections. The fractional de-excitation rates of the HCN model in Table 2.2 are the averaged results of the HCN - He collisional rates listed in Table 2 of Green and Thaddeus' article (1974) for different temperatures from 5 K to 100 K for  $\Delta J$  from 1 to 7. The same method has been used to get the

de-excitation rates of the HC<sub>3</sub>N model from the HC<sub>3</sub>N-He collisional rates (Green and Chapman 1977).

Table 2.2

Fractions of Total De-excitation		
$\Delta J$	HCN model	HC <sub>3</sub> N model
1	0.129	0.472
2	0.616	0.213
3	0.048	0.131
4	0.152	0.085
5	0.020	0.054
6	0.036	0.030
7	0.006	0.015
>7	0.000	0.000

The total cross-section  $\sigma_c$  for rotational transitions induced by collisions with H<sub>2</sub>O is also a poorly known physical parameter, and since H<sub>2</sub>O and HCN are polar molecules, their collisional cross-section could be much larger than their geometric cross-section ( $\sim 10^{-15}$  cm<sup>2</sup>). For the purpose of this work, we have assumed values of  $\sigma_c \sim 10^{-14}$  cm<sup>2</sup> and  $10^{-15}$  cm<sup>2</sup> in the model to span the likely range of  $\sigma_c$ .

The temperature of the gas, which must be specified in a collisional model, depends on thermodynamical models of the coma. Most such models predict a decrease in the temperature from 200 K at the nucleus

to a few 10's K, or even less, at about 100 km from nucleus, due to the nearly adiabatic expansion of the gas. Beyond this point, the gas temperature is expected to rise again due to photolytic heating. We have adopted for the excitation model a constant expansion velocity of 0.8 km s<sup>-1</sup> and a temperature law derived from fitting Crovisier's temperature model (1986). It is similar to that used by Crovisier (1987),

$$\text{Log } T = 0.77[\text{Log } r - 1.9]^{1.2} + 1.0 \quad (2.14)$$

where  $r$  is the distance from the nucleus.

Once all the physical parameters of the coma are specified, the collision rate may be determined for all parts in the coma.

The global collision rate

$$C = \sigma_c n_{H_2O} V \quad , \quad (2.15)$$

where  $\sigma_c$  is the collisional cross-section and the mean velocity between H<sub>2</sub>O and HCN molecules is

$$V = \left( \frac{8kT}{\pi} \left( \frac{1}{m_{H_2O}} + \frac{1}{m_{HCN}} \right) \right)^{1/2} \quad (2.16)$$

and

$$n_{H_2O} = \frac{Q_{H_2O}}{4\pi r^2 V_{exp}} \quad (2.17)$$

where  $Q(H_2O)$  is the H<sub>2</sub>O production rate in molecule per second.

Now, using the radiative and collisional excitation models and for the radiative part putting equations (2.4)-(2.13) into (2.3), we may directly write down the statistical equilibrium equations as

$$\begin{aligned}
\frac{dP_J}{dt} = & \sum_i C_{\Delta_i} (P_{J+1} + \frac{g_J}{g_{J-i}} \exp(-\frac{\Delta E_i}{kT}) P_{J-i}) \\
& - P_J \sum_i C_{\Delta_i} (1 + \frac{g_{J+i}}{g_J} \exp(-\frac{\Delta E_i}{kT})) \\
& + P_{J-2} G \frac{J(J-1)}{(2J-1)(2J-3)} \\
& + P_J [-\frac{3J^4}{2J+1} A_{10} - G \frac{2J^2+2J-2}{(2J+3)(2J-1)}] \\
& + P_{J+1} \frac{3(J+1)^4}{2J+3} A_{10} \\
& + P_{J+2} G \frac{(J+1)(J+2)}{(2J+3)(2J+5)}
\end{aligned} \tag{2.18}$$

where  $P_J$  is the relative population of the rotational level  $J$  in the vibrational ground state.  $G$  is the total excitation rate of the three involved band transitions by the solar radiation field as defined in equation (2.1).  $g_J = 2J+1$  is the statistical weight, and  $\Delta E_i = E_J - E_{J-i}$ ,  $\Delta E'_i = E_{J+i} - E_J$ , are the energy differences between levels. The first term in equation (2.18) represents the collisional excitation into level  $J$  from other levels and the second one treats the removal of molecules from level  $J$  by collisions, and  $C_{\Delta_i}$  is the collision rate and is given by the total collisional cross-section times the fraction shown in the Table 2.2. The other terms represent vibrational excitation and radiative decay within rotational levels as shown in equation (2.3).

The population distribution at equilibrium is obtained by solving

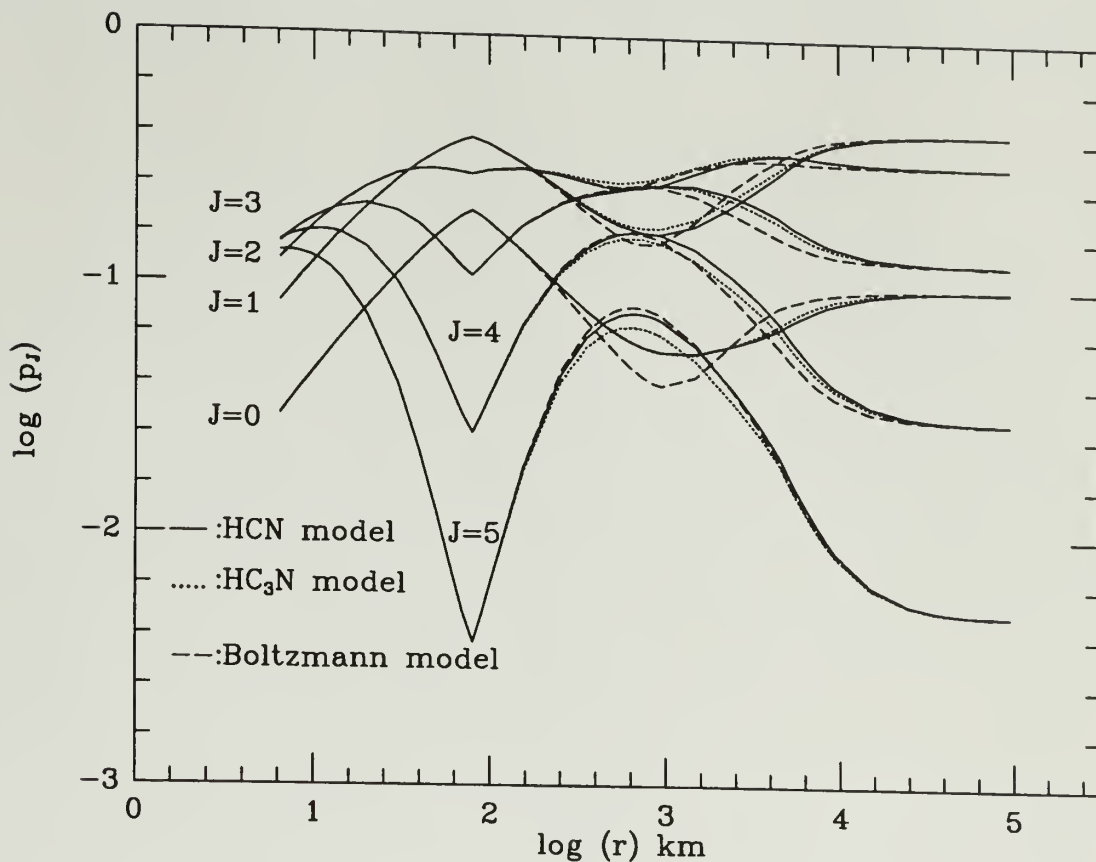
$$\frac{dP_J}{dt} = 0 \quad (2.19)$$

and

$$\sum_J P_J = 1 \quad (2.20)$$

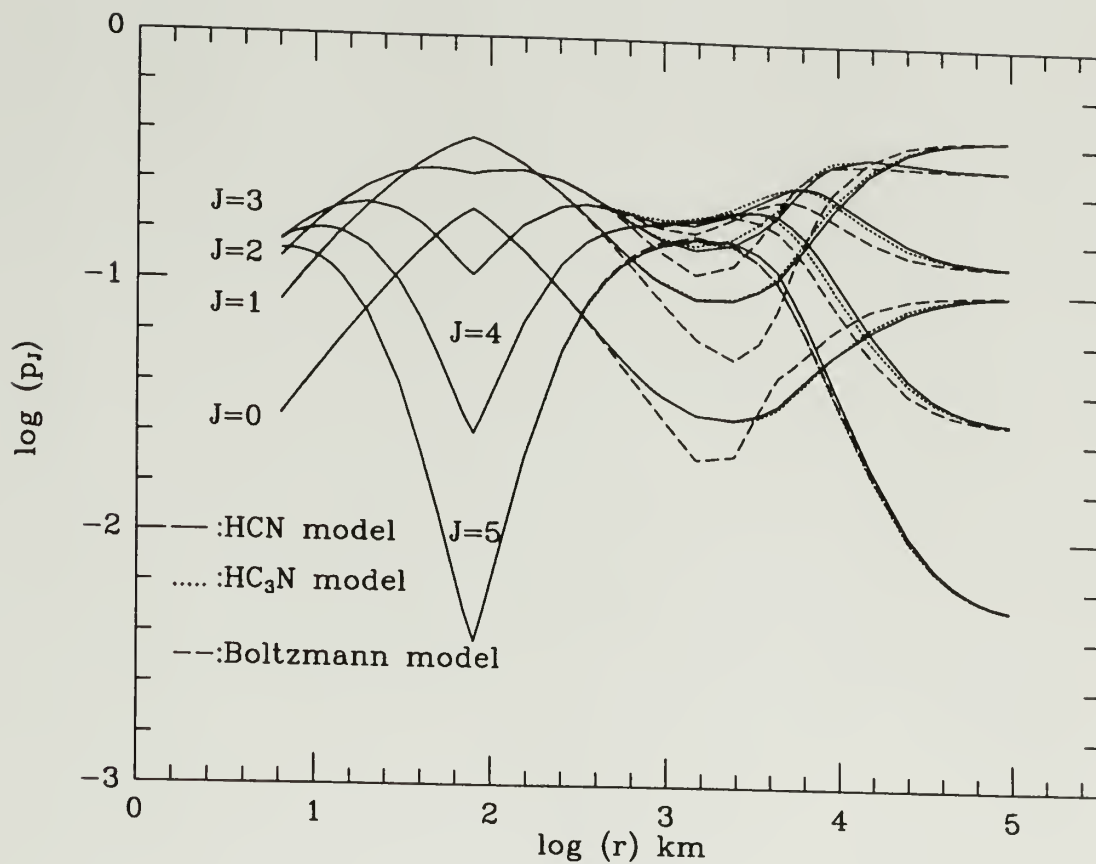
We solve the statistical equilibrium equations by selecting 20 rotational levels since the HCN molecule has big rotational constants and 20 levels are sufficient for accuracy. The gaussian elimination method is used in the calculations. The steady state approximation for each point in the coma is only strictly true if the HCN molecule undergoes several excitations while it is at the radius under consideration. Thus, it is completely valid in the inner ( $< 10^3$  km) and outer ( $> 10^5$  km) coma. However, at intermediate distances, the steady state distribution can only be regarded as an approximation to the real distribution. Fortunately, comparison with the results of full time dependent solutions obtained from the Gear method (Gear 1971; Crovisier 1987), shows that the use of the approximation does not lead to very different results.

Figure 2.3a and 2.3b illustrates our results for the rotational distribution of HCN as a function of  $r$ , the distance from the nucleus of the comet for two values of total collisional cross-section:  $10^{-15}$  and  $10^{-14}$ . Table 2.3 lists the parameters that we used in the calculation and we also



(a)

Figure 2.3 The rotational distributions of HCN in a cometary coma as a function of  $r$ , the distance from the nucleus. Three collisional models are used. Statistical equilibrium is assumed in the calculation. a: The total HCN-H<sub>2</sub>O cross-section is  $10^{-15}$ ; b: The total HCN-H<sub>2</sub>O cross-section is  $10^{-14}$ . Continued on following page.



(b)

Figure 2.3 Continued from previous page.

summarize in the table the assumptions that we made in the model. Both the HCN-He (HCN model) and HC<sub>3</sub>N-He (HC<sub>3</sub>N model) collisional cross-section rates in Table 2.2 have been used in the calculation. It seems that the rotational population of HCN is rather insensitive to the explicit  $\Delta J$  dependence of the cross sections since no big difference is found between the HCN and the HC<sub>3</sub>N models, as long as the total cross section remains fixed. The results of models which redistribute population according to a Boltzmann distribution are also shown in Figure 2.3 in order to compare with our results. The biggest divergence occurred in the lowest  $J=0$  level and the divergences decrease as  $J$  increase.

Table 2.3

The summary of used model. a: Parameters used in model;

b: Summary of assumptions made in model. Continued on following page.

a:

Parameter	Value
Production rate $Q(\text{H}_2\text{O})$	$2.0 \times 10^{29} \text{ molec s}^{-1}$
Heliocentric $R_h$	1 AU
Total cross-section	$5.0 \times 10^{-15} \text{ cm}^2$



Table 2.3

Continued from previous page.

b:

1. UV excitation by solar radiation field is negligible.
2. Excitation only occurs in fundamental bands.
3. Population in excited vibrational levels is negligible.
4. Only radiative excitation by solar radiative field is considered.
5. All HCN lines are optically thin.
6. Collisional cross-section of HCN-He can be used as that of HCN-H<sub>2</sub>O.

### 2.2.3 Discussion

Given the rotational population distribution and the spatial distribution of HCN within the coma, the integrated intensities of the rotational lines for a given telescope can be readily evaluated as these are directly related to the HCN column density of the upper levels of the involved transition (Schloerb et al. 1986).

In order to estimate the uncertainties introduced by uncertainties in the total cross section and the difference between our collisional

redistribution models and the Boltzmann model used by Crovisier, we evaluate the HCN integrated intensities for  $J=1-0$ ,  $J=2-1$ ,  $J=3-2$ , and  $J=4-3$  transitions of the molecule by using these three models with different total collision-sections. The 1-0 and 3-2 transitions have been observed in several comets (Bockelée-Morvan et al. 1990; Colom et al. 1992). Since both the HCN  $J=1-0$  and  $J=3-2$  transitions were detected in comet Levy by using 30-m telescope of the Institut de Radio Astronomie Millimétrique (IRAM)(Bockelée-Morvan et al. 1991) when the comet was at 1.4 AU heliocentric distance and 0.43 AU distance between the comet and the earth, these values are used in the calculation of integrated intensities. The relevant beam sizes are 28" for  $J=1-0$ , 14" for  $J=2-1$ , 10" for  $J=3-2$ , and 7" for  $J=4-3$  transitions. HCN production rate  $2.0 \times 10^{26}$  and  $H_2O$  production rate  $2.0 \times 10^{29}$  molecules  $s^{-1}$  are assumed in the calculation.

The results given in Table 2.4a show that the total cross-section has the biggest effect on the integrated intensities and that the HCN model and  $HC_3N$  model give us similar integrated intensity results. The differences between the results of our redistribution model and the Boltzmann model are 10% for  $J=1-0$ , 15% for  $J=2-1$  and  $J=3-2$ , and 5% for  $J=4-3$ , with the Boltzmann model requiring somewhat larger HCN production rates in order to get the same integrated intensity as the other models. The total cross-section can in principle be determined by the

integrated intensity ratio of the  $J=1-0$  and  $J=3-2$  transitions. The observed integrated intensities in comet Levy are  $0.40 \text{ K km s}^{-1}$  and  $3.87 \text{ K km s}^{-1}$  respectively, and the calculated results in Table 2.4a show that the total cross-section is likely around  $10^{-14} \text{ cm}^2$ . The HCN population and the integrated intensities have also been calculated by using three different temperature values for the cometary coma in order to check out the effect of temperature on the results, as the temperature law is uncertain in comets. The results listed in Table 2.4b are calculated by using the HCN model and the total cross-section of  $10^{-14}$ . It shows that the integrated intensity of HCN depends on the coma temperature. The integrated intensity at  $T=100 \text{ K}$  is closest to the observed data, and this might be reasonable because the beam size at  $89 \text{ GHz}$  corresponds to a distance of  $10^3 \text{ km}$  from the nucleus, where the temperature is about  $100 \text{ K}$ . Considering both the HCN production rate and the total cross-section are unknown parameters, we have calculated the ratios of  $J=3-2/J=1-0$  and  $J=4-3/J=3-2$  integrated intensities as a function of  $T$ , and the  $\sigma$  as a parameter, where  $\sigma$  is the total cross-section and  $T$  the temperature of the coma. The results are shown in Figure 2.4 and we can determine these parameters from observed line ratios. From Figure 2.4, we can see that both the ratios of  $J=3-2/J=1-0$  and  $J=4-3/J=3-2$  integrated intensities do not depend too strongly on the coma temperature and the total cross-section can be found from the ratio of  $3-2/1-0$ .

Table 2.4

HCN integrated intensity (in units of K km s<sup>-1</sup>).  
 a: using different collisional excitation models  
 b: using different temperature values

a:

Frequency (GHz)	$\sigma = 1.0 \quad 10^{-15}$				$\sigma = 1.0 \quad 10^{-14}$			
	89	177	266	355	89	177	266	355
HCN model	0.71	2.85	5.29	5.35	0.40	1.97	4.68	7.65
HC <sub>3</sub> N model	0.72	2.93	5.07	4.81	0.41	2.04	4.80	7.71
Boltzmann model	0.63	2.54	4.57	4.84	0.36	1.75	4.65	7.62

b:

Frequency (GHz)	88.63	177.26	265.89	354.65
T <sub>1</sub> = 40 K	0.656	2.540	4.786	6.917
T <sub>2</sub> = 60 K	0.567	2.245	4.643	7.658
T <sub>3</sub> = 80 K	0.512	2.030	4.376	7.670
T <sub>4</sub> = 100K	0.475	1.873	4.126	7.475

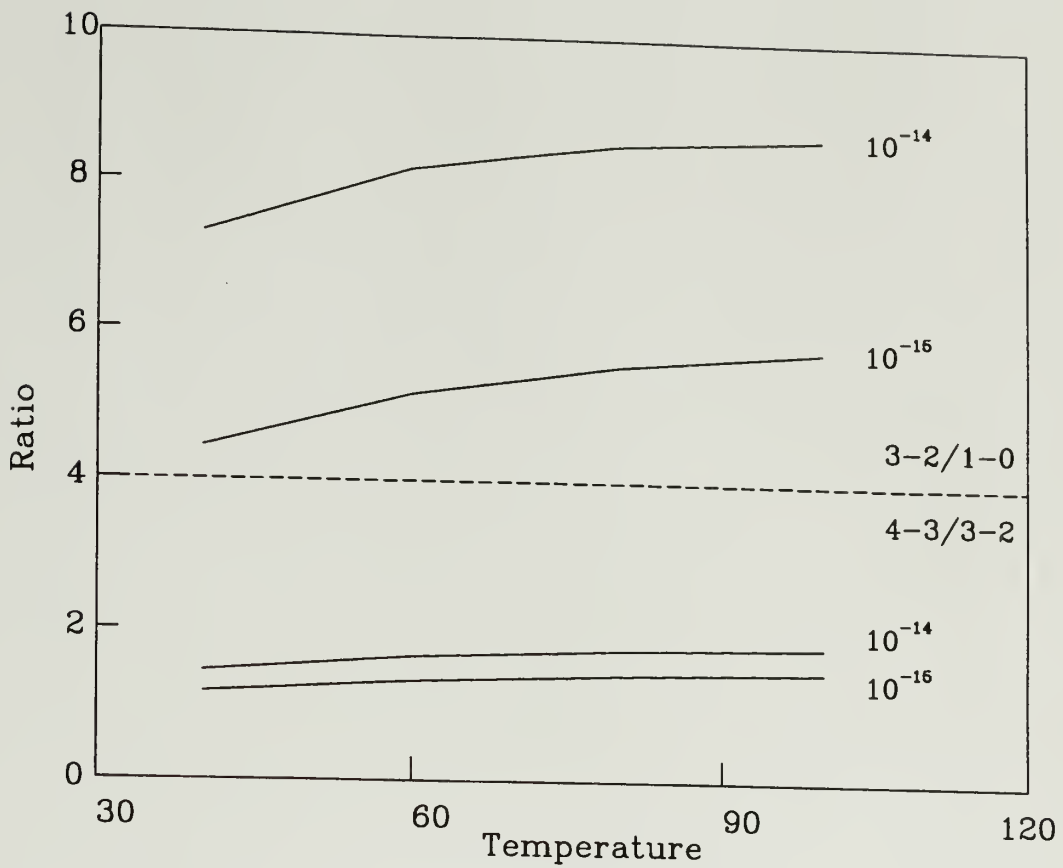


Figure 2.4 The ratios of HCN  $J=3-2/J=1-0$  and  $J=4-3/J=3-2$  integrated intensities as a function of temperature, and the total cross section as a parameter.

### 2.3 H<sub>2</sub>CO Molecule

We have also developed an excitation model for H<sub>2</sub>CO in order to analyze the millimeter-wave data obtained in comets. This model uses the same characteristics of the coma discussed in the previous section, but has been modified for H<sub>2</sub>CO. Formaldehyde is a slightly asymmetric rotor with Ray's asymmetry parameter  $K = -0.96$  and an electric dipole moment of 2.331 debyes along the axis of the smaller moment of inertia (Clouthier and Ramsay 1983). Figure 2.5 shows part of its rotational energy level structure. As the figure shows, the rotational levels are labelled by  $J_{K_a K_c}$ , where  $J$  is the total quantum number and  $K_a$  and  $K_c$  are subquantum numbers for the prolate and oblate symmetric rotor, respectively. The selection rules for pure rotational transitions are  $\Delta J = 0, \pm 1$ ,  $\Delta K_a = \text{even}$  and  $\Delta K_c = \text{odd}$ . The statistical weights due to the nuclear spins of hydrogen atoms in the molecule are 3 for the ortho-states corresponding to  $K_a$  odd and 1 for the para-states with  $K_a$  even. The formaldehyde molecule may exist in the ortho or para state and the transitions between these two states by collisions or radiative processes are strictly forbidden. The only possibility of transition is through chemical reactions, so the abundance ratio of ortho and para for formaldehyde in the coma should be the same as that when H<sub>2</sub>CO was created. The knowledge of this ratio in comets would be highly desirable since it might be a clue to the formation temperature of H<sub>2</sub>CO. In the

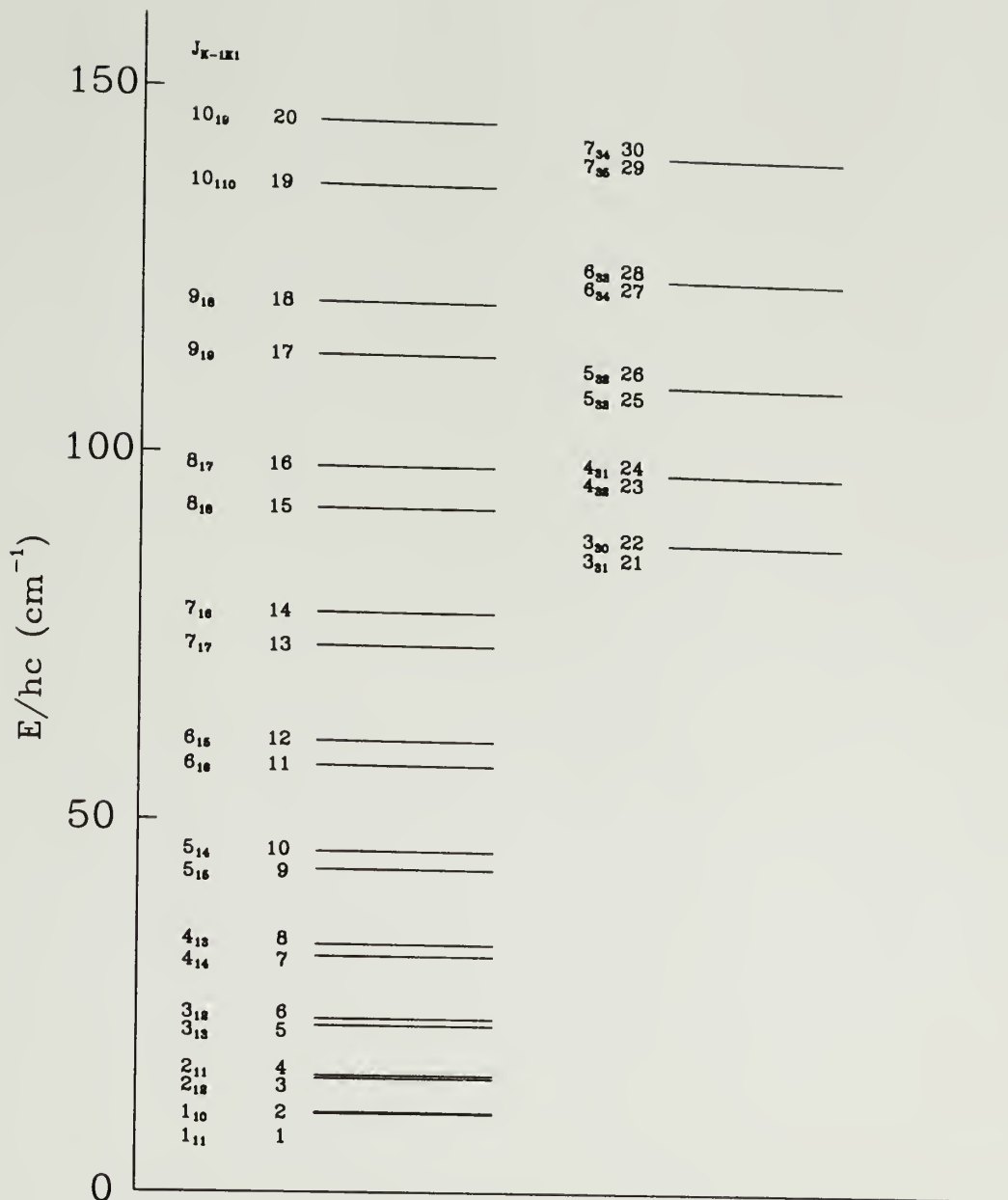


Figure 2.5 Sample of ortho-H<sub>2</sub>CO rotational energy levels.

absence of any information about this ratio at present, we will assume that formaldehyde in comets is distributed among the ortho and para states according to the equilibrium ratio 3:1. The physical parameters, like the rotational energy levels, line frequencies, and Einstein A-coefficients, have been published by Jaruschewski (1986) and have been used in our calculations. The possible excitation mechanisms of the H<sub>2</sub>CO molecule in comets are radiative excitation of the vibrational bands by the solar infrared field and thermal excitation by collision with the H<sub>2</sub>O molecule.

### 2.3.1 Radiative Excitation

We now evaluate the fluorescence rate of each vibrational band of H<sub>2</sub>CO by the solar radiation field by assuming that all the excitation transitions start from  $\nu(0,0,0,0,0,0)$  level. The 6 possible vibrational bands are shown in Figure 2.6 with their calculated fluorescence rates, which also are listed in Table 2.5. The rates are calculated by using equation (2.1). We see from the table that 95% of the total excitation rate comes from the  $\nu_1$ ,  $\nu_2$  and  $\nu_3$  fundamental bands. Thus, only radiative excitations of the  $\nu_1$ ,  $\nu_2$ , and  $\nu_3$  fundamental bands are included in the model.

As for the treatment of HCN in the last section, the probabilities for transitions back to the ground vibration state from the excited



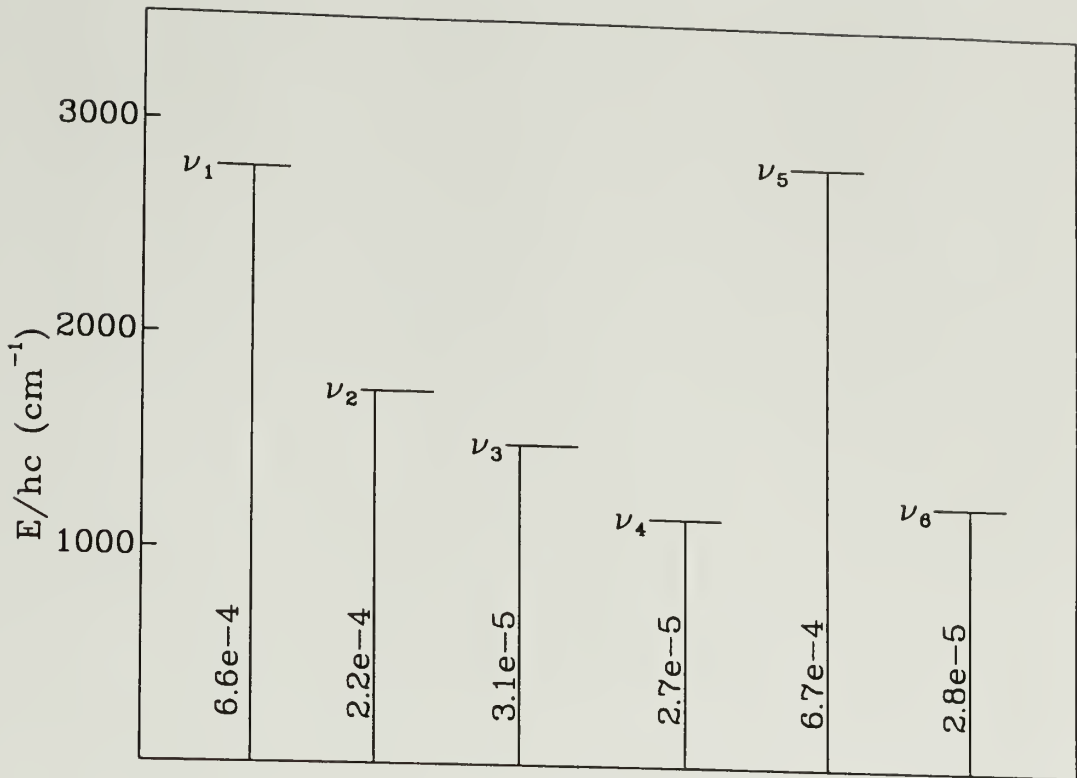


Figure 2.6 The vibrational levels of H<sub>2</sub>CO and the radiative excitation rates due to the solar infrared field.

vibrational states after radiative excitation by the solar radiative field from the ground vibrational state have been calculated, and the line strengths are given by the GEISA molecular data base (kindly supplied by J. Crovisier). These probabilities will be used in the radiative excitation part of the statistical equilibrium equation.

Table 2.5

Parameters of the molecular bands of H<sub>2</sub>CO

	$\sigma_{v''v'}$ cm <sup>-1</sup>	$S_{v''v'}$ km/mol	$A_{v''v'}$ s <sup>-1</sup>	$g_{v''v'}$ s <sup>-1</sup>	Fraction of total g-rates %
$\nu_1$	2783	75.51	73.2	$3.92 \times 10^4$	40.5
$\nu_2$	1746	73.98	28.1	$2.56 \times 10^4$	13.3
$\nu_3$	1500	11.15	3.1	$3.66 \times 10^5$	1.9
$\nu_4$	1167	6.49	1.1	$1.75 \times 10^5$	1.6
$\nu_5$	2843	87.60	88.6	$4.60 \times 10^4$	41.0
$\nu_6$	1249	9.95	1.9	$2.80 \times 10^5$	1.7

### 2.3.2 Collisional Excitation

There are no data on the collisional cross-sections of  $\text{H}_2\text{CO}$  with  $\text{H}_2\text{O}$ ; therefore, to be consistent with the treatment of HCN, we have used the rates of excitation of  $\text{H}_2\text{CO}$  by collisions with He published by Green et al. (1978) in our model calculations. In Table 4 of their paper, Green et al. (1978) listed these collision rate constants calculated in the temperature ranges from 10 K to 80 K.

Statistical equilibrium equations similar to equation (2.18) need to be solved in order to calculate the  $\text{H}_2\text{CO}$  rotational population distribution. In order to estimate how many rotational levels should be involved, we have evaluated the relative population in rotational levels according to a Boltzmann distribution under the range of temperatures likely to be found in comets. The results show that a total of 68 rotational levels are required for the calculation. This large number of rotational levels is necessary to get correct populations at thermal and fluorescence equilibrium, because of their small energy separation and their large radiative lifetime. These 68 rotational levels with energies up to  $450\text{ cm}^{-1}$  in the ground vibrational state include  $J=1$  to 16 for ladder  $K_a=1$ ,  $J=3$  to 14 for  $K_a=3$ , and  $J=5$  to 10 for  $K_a=5$ .

The time scale for establishment of equilibrium is about  $10^3$  sec, and it may not be possible for formaldehyde in the coma to reach

equilibrium due to its short lifetime ( $10^3$  sec at  $r_h = 1$  AU) by photodissociation. Thus, the adoption of a steady state model must be regarded as an approximation to the actual behavior.

### 2.3.3 Discussion

The evolution of the population distribution as a function of the distance from the nucleus is derived assuming that formaldehyde expands throughout the coma with an outflow velocity of  $0.8 \text{ km s}^{-1}$ .

Figure 2.7 shows the fractional population of different  $\text{H}_2\text{CO}$  levels within the coma. The results were calculated at the heliocentric distance of 1 AU with a water production rate  $Q(\text{H}_2\text{O}) 2.0 \times 10^{29} \text{ s}^{-1}$ , a constant kinetic temperature of 50 K in the coma, and the life time scale 2,860 seconds derived by Huebner and Carpenter (1979). At 3,000 km, where formaldehyde molecules emitted directly from the nucleus are dissociated, the population distribution is far from thermal and does not resemble a Boltzmann distribution. Rotational levels like  $4_{13}$ ,  $5_{15}$  and  $5_{14}$ , have begun to decrease as they have small radiative lifetimes and inefficient collisional excitation. On the other hand, the rotational levels with large radiative lifetimes have increased their populations by the successive spontaneous cascades from the upper levels. This happens for

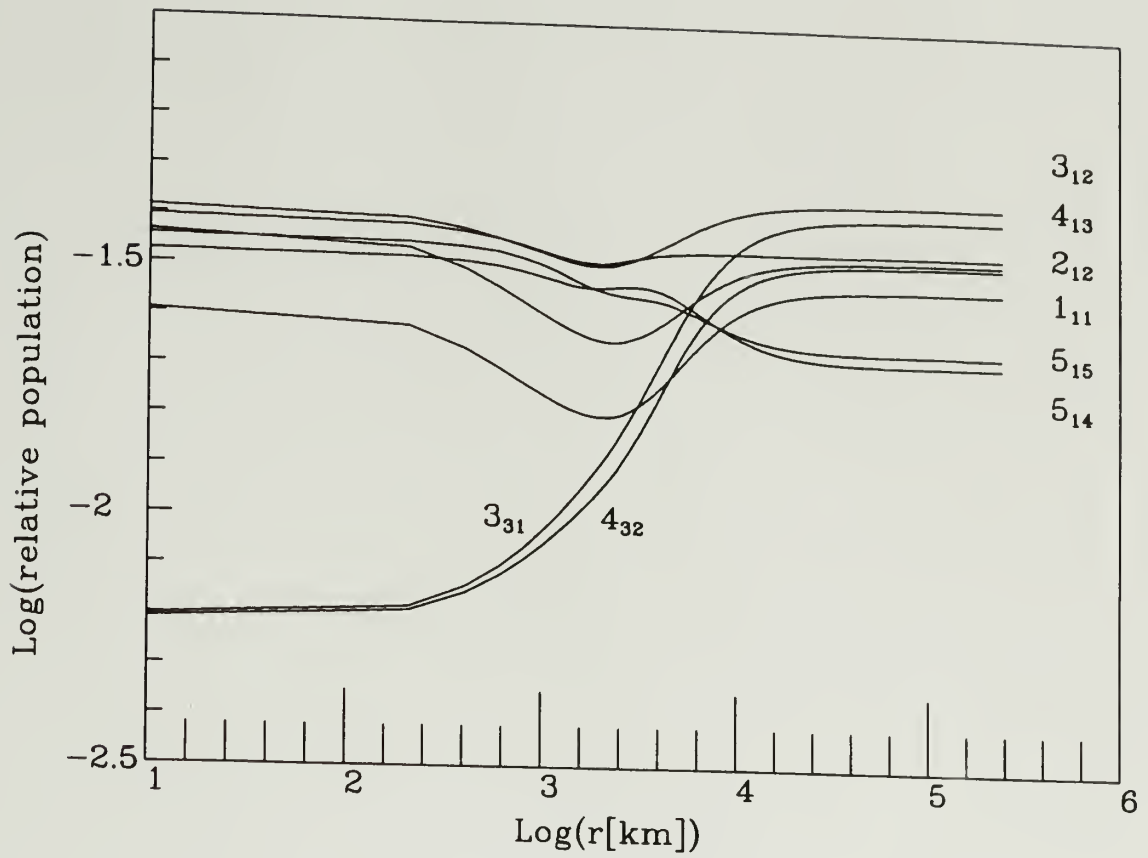


Figure 2.7 The H<sub>2</sub>CO rotational populations in the coma as a function of distance from the nucleus. Constant temperature is used and details of model described in text.

energy levels within the  $K=3$  ladder. The fluorescence equilibrium is reached at typical distance of  $2 \times 10^4$  km from the nucleus.

Since the  $\text{H}_2\text{CO } 3_{12}-2_{11}$  and  $5_{15}-4_{14}$  transitions were observed in comet Levy at IRAM (Bockelée-Morvan et al. 1990) and CSO (Schloerb and Ge 1990), we have used the results of the rotational population distribution to evaluate rotational lines for these two telescope diameters.

Calculations are performed with a  $\text{H}_2\text{CO}$  production  $4 \times 10^{26} \text{ s}^{-1}$ , a water production rate  $2.5 \times 10^{29} \text{ s}^{-1}$ ,  $r_h = 1.4$  AU from the Sun,  $\Delta = 0.4$  AU from the Earth, and a coma kinetic temperature of 50 K. The lifetime has been assumed to be  $2.86 \times 10^3$  sec. The results are listed in Table 2.6 and show that, if the abundance of  $\text{H}_2\text{CO}$  is at a 0.2% level in cometary atmospheres, both  $3_{12}-2_{11}$  and  $5_{15}-4_{14}$  rotational lines should be detected in comets with a  $Q(\text{H}_2\text{O})$  value of  $10^{29} \text{ s}^{-1}$ . The table shows that the formaldehyde line at 6-cm could not be detected according to our calculation. We have used our model to analyze the tentative detection of the  $\text{H}_2\text{CO}$  6-cm line in P/Halley by Snyder et al. (1989) with the VLA. The integrated intensity calculated by our model is about  $10^{-4} \text{ K km s}^{-1}$  even if a production rate of  $10^{28} \text{ s}^{-1}$  is used. Thus, the model can not reproduce the VLA data observed by Snyder (1989).

Table 2.6

Integrated intensities of H<sub>2</sub>CO for 10-m and 30-m telescope

Transition	Frequency GHz	$\int T dv$ [K km s <sup>-1</sup> ]	
		d = 10 m	d = 30 m
1 <sub>10</sub> - 1 <sub>11</sub>	4.83	$2.32 \times 10^{-7}$	$2.09 \times 10^{-6}$
2 <sub>11</sub> - 2 <sub>12</sub>	14.49	$1.18 \times 10^{-5}$	$1.05 \times 10^{-4}$
3 <sub>12</sub> - 3 <sub>13</sub>	28.97	$4.78 \times 10^{-5}$	$4.12 \times 10^{-4}$
4 <sub>13</sub> - 4 <sub>14</sub>	48.28	$1.19 \times 10^{-4}$	$9.80 \times 10^{-4}$
5 <sub>14</sub> - 5 <sub>15</sub>	72.41	$2.05 \times 10^{-4}$	$1.62 \times 10^{-3}$
6 <sub>15</sub> - 6 <sub>16</sub>	101.33	$2.81 \times 10^{-4}$	$2.10 \times 10^{-3}$
7 <sub>16</sub> - 7 <sub>17</sub>	135.03	$3.37 \times 10^{-4}$	$2.38 \times 10^{-3}$
2 <sub>12</sub> - 1 <sub>11</sub>	140.84	$1.41 \times 10^{-2}$	$8.81 \times 10^{-2}$
2 <sub>11</sub> - 1 <sub>10</sub>	150.50	$1.98 \times 10^{-2}$	$1.15 \times 10^{-1}$
8 <sub>17</sub> - 8 <sub>18</sub>	173.46	$3.59 \times 10^{-4}$	$2.35 \times 10^{-3}$
3 <sub>13</sub> - 2 <sub>12</sub>	211.21	$6.75 \times 10^{-2}$	$3.76 \times 10^{-1}$
9 <sub>18</sub> - 9 <sub>19</sub>	216.57	$3.27 \times 10^{-4}$	$1.88 \times 10^{-3}$
3 <sub>12</sub> - 2 <sub>11</sub>	225.70	$8.44 \times 10^{-2}$	$4.50 \times 10^{-1}$
4 <sub>14</sub> - 3 <sub>13</sub>	281.53	$1.53 \times 10^{-1}$	$8.18 \times 10^{-1}$
4 <sub>32</sub> - 3 <sub>31</sub>	291.38	$2.09 \times 10^{-2}$	$8.19 \times 10^{-2}$
4 <sub>13</sub> - 3 <sub>12</sub>	300.84	$1.82 \times 10^{-1}$	$9.32 \times 10^{-1}$
5 <sub>15</sub> - 4 <sub>14</sub>	351.77	$2.27 \times 10^{-1}$	$1.06 \times 10^0$
5 <sub>33</sub> - 4 <sub>32</sub>	364.28	$3.83 \times 10^{-2}$	$1.58 \times 10^{-1}$
5 <sub>14</sub> - 4 <sub>13</sub>	375.89	$2.78 \times 10^{-1}$	$1.39 \times 10^0$

## 2.4 Conclusion

We have developed two models for the excitation of cometary hydrogen cyanide and formaldehyde in order to interpret their rotational lines observed in comets. The main excitation mechanisms in cometary coma are thermal excitation by collision and radiative excitation by infrared solar radiation.

The main difference with previous models is in the calculations of collisional excitation. In our model, we have utilized the cross-sections based on quantum mechanical calculations. However, the results of our model show only modest difference from previous models.

The total collisional cross-section of HCN can be determined from the observed ratio of  $J=3-2/J=1-0$  integrated intensities. The temperature in the cometary atmosphere does not affect strongly on both the  $3-2/1-0$  and the  $4-3/3-2$  ratios from our model calculations.

The results derived from the model for excitation of formaldehyde show that both rotational transitions,  $3_{12}-2_{11}$  and  $5_{15}-4_{14}$ , can be observed in comets according to our model. We will use this model to analyze the observed data in comet Levy in order to determine the formaldehyde abundance in comet Levy and its lifetime against photodissociation.



## CHAPTER 3

### THE COMA MODEL

#### 3.1 Model Description

One of the main purposes for studying comets is to understand the physics of the cometary atmosphere, and radio techniques provide high spectral resolution that enables us to probe some important aspects of the physical behavior of the coma. Knowledge of the distribution of parent molecules in the cometary coma is needed in order to interpret the observed integrated intensity in terms of the molecular column density. The Haser model (Haser 1957, 1966) and the vectorial model (Combi and Delsemme 1980a; Festou 1981 a, b) are often used to describe the gas distribution and kinematics of cometary comae. As mentioned in chapter 1, the vectorial model provides a more realistic model of the behavior of daughter molecules in cometary comae. Thus, we have adapted an existing model program to generate synthetic spectra of both parent molecules and possible daughter molecules, since some species may be daughter species. The program uses a Monte Carlo technique to perform the calculations. A detailed description of the calculation is given below:

- A parent molecule (HCN or H<sub>2</sub>CO) is generated at some time  $t_i$  which lies in the range  $0 \leq t_i \leq t_{\text{obs}}$ .  $t_{\text{obs}}$  is chosen to be three to five times the

parent molecule lifetime against photodissociation. The length of time,  $t_{\text{obs}}$ , during which parent molecules may be generated before observations start, is chosen to be sufficiently long to sample the parent molecule distribution. For the  $\text{H}_2\text{CO}$  molecule, the observations (Snyder et al. 1989; Bockelée-Morvan and Crovisier 1991) suggest that  $\text{H}_2\text{CO}$  comes from a distributed source. Thus, in order to determine the origin of  $\text{H}_2\text{CO}$  in comets,  $\text{H}_2\text{CO}$  is also treated as a daughter molecule in our model and an assumed parent molecule is assigned to  $\text{H}_2\text{CO}$ . A constant production rate of parent molecule on the nucleus is assumed during each process so that we can chose a random distribution of parent creation times over the length of each simulation. Thus, since all parent creation times have equal probability, we can use a random number  $r$ , in the interval  $[0,1)$ , to determine the creation time as  $t_i = rt_{\text{obs}}$  such that the  $t_i$  value falls uniformly within the range  $0 \leq t_i < t_{\text{obs}}$ .

- After the parent molecule is produced at the time  $t_i$ , it will fly out until photodissociation by solar radiation happens at time  $t_d$ .  $t_d$  is discussed by Tacconi-Garman (1990) and given in the molecular simulation by

$$t_d = t_i - \tau_{\text{parent}} \ln(r) \quad , \quad (3.1)$$

where  $r$  is a random number between 0 and 1 which can be produced automatically by a computer program and  $\tau_{\text{parent}}$  is the parent lifetime against photodissociation by the solar radiation field. For HCN, we

adopted a lifetime value of  $8 \times 10^4$  sec to be roughly in agreement with those given by Huebner and Carpenter (1979) and Jackson (1976). A value of  $2.86 \times 10^3$  sec is adopted for the  $\text{H}_2\text{CO}$  lifetime according to the calculation by Huebner and Carpenter (1979). These values can also be adjusted as model parameters in order to best fit the observed spectra in comets. Once again, if  $\text{H}_2\text{CO}$  is a daughter molecule, a value for its parent photodissociation rate has to be assumed and checked by the model.

- If  $t_d$  for the parent molecule is greater than  $t_{\text{obs}}$ , the parent molecule exists at the time of observation. The next step is to determine its position and velocity in the cometary coma so that we can calculate the contribution of this particular parent to the spectrum from the knowledge of the fractional population in molecular upper level obtained from our excitation model.

Two coordinate systems, the antisun (unprimed) and the antiearth (primed) systems, are used to describe the position of molecules in the coma. These systems are shown in Figure 3.1. The center of the comet is located at the origin of the systems. The +z-axis in the unprimed system points in the antisun direction, while the +y-axis lies perpendicular to the sun-comet-earth plane. The antiearth coordinate can be obtained by rotating a phase angle about the y-axis. The phase angle is defined as the sun-comet-earth angle.

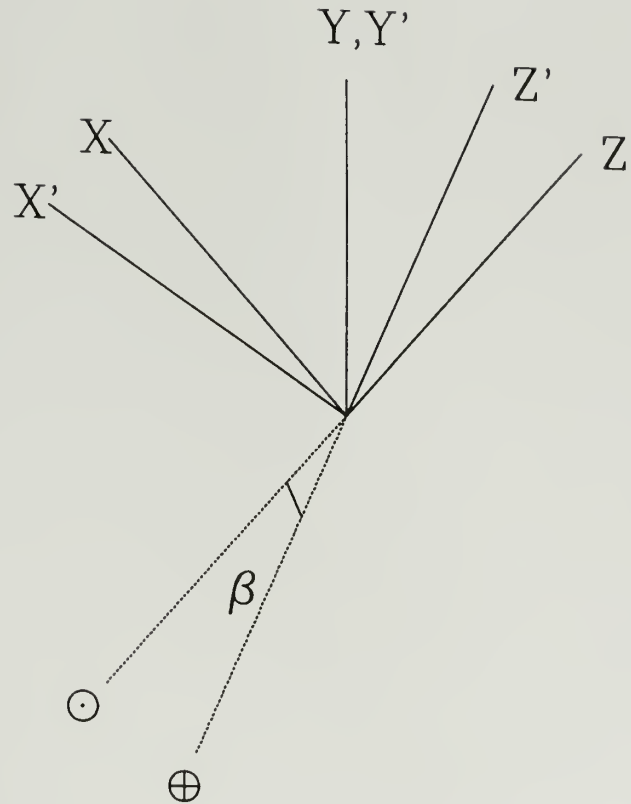


Figure 3.1 The antisun and antiearth coordinate systems.

The origin is the nucleus of the comet. The  $x$ ,  $x'$ ,  $z$ , and  $z'$  axes all lie in the sun-earth-comet plane.

The angle  $\beta$  is the phase angle.

A more sophisticated treatment in the simulation is to divide the nucleus of the comet into day and night hemispheres and permit the gas production from day and night sides to depend on a parameter called the anisotropy parameter (hereafter referred to as AP). This parameter is defined as

$$AP = \log[Q_{day}/Q_{night}] \quad (3.2)$$

where  $Q_{day}$  and  $Q_{night}$  are the production rates into the day and night hemisphere, respectively. We can use a random number  $r$  to judge whether the parent goes either to the day side if  $f_n < r < 1$  or to the night side if  $r \leq f_n$ , where  $f_n$  is defined as the fraction of all molecules which enter the night hemisphere.

Thus, we can determine the direction which the parent travels in the two hemispheres. The spherical angle for the day hemisphere is given by

$$\cos\theta = \frac{1-r(1+f)}{f} \quad , \quad (3.3)$$

where  $f = 10^{AP}$  is the ratio of day and night hemisphere production rates.

For the night hemisphere we have

$$\cos\theta = 1-r(1+f) \quad , \quad (3.4)$$

and for pure isotropic emission ( $f = 1$ ), both equations reduce to

$$\cos\theta = 1-2r \quad . \quad (3.5)$$

The azimuthal angle is given by

$$\phi = r'(2\pi) \quad (3.6)$$

where  $r'$  is another random number.

After the direction is obtained, we need knowledge of the velocity of the parent molecule in order to determine its position. The velocity can be determined from either a constant velocity or a velocity law, depending on which can best fit the observed spectrum. If a constant velocity is used, it is simple to determine the velocity components in the antisun coordinate system by using the knowledge of its direction angles obtained above. The position can be located by the velocity components and the time interval between the time when it is produced and the time  $t_{\text{obs}}$ . A program to integrate the velocity is needed in order to obtain the position if a velocity law is assumed. The doppler velocity along the line of sight can be obtained from a coordinate transformation if the phase angle is known; then we can put and record the parent molecule into different velocity bins.

We need go to the beginning and generate another parent molecule if  $t_d$  is smaller than  $t_{\text{obs}}$ , since the parent is destroyed before the observation. For a daughter molecule, however,  $t_d$  has to be smaller than  $t_{\text{obs}}$  in order that the daughter molecule be present at the time of

observation. After the daughter molecule is produced, its photodissociation time can be modelled by using equation (3.1) and the daughter's lifetime. If the photodissociation time still is smaller than  $t_{\text{obs}}$ , we can go to the next step to calculate the daughter's velocity, position, and its spectrum in a manner similar to that for the parent molecule, otherwise it is not present and the process is repeated with the generation of another candidate parent molecule.

The statistical nature of a Monte Carlo simulation requires the generation of many candidate parent molecules to achieve an accurate result. In this work, as many as  $2.0 \times 10^5$  parent molecules are used in each simulation to reduce the statistical fluctuations inherent in the Monte Carlo method.

### 3.2 Spectra Simulation

A link is needed to connect the parent simulation in the coma developed in last section with observable quantities like integrated intensity and antenna temperature.

Radiation transfer equation under the assumption of optically thin emission is given by

$$\frac{dI_\nu}{ds} = \frac{h\nu}{4\pi} A_{ul} n_u \varphi_\nu \quad (3.7)$$

where  $A_{ul}$  is the Einstein spontaneous emission coefficient,  $n_u$  is the upper level density, and  $\varphi_\nu$  the line profile. Integrating the equation, we have

$$I_\nu = \frac{h\nu}{4\pi} A_{ul} \int n_u \varphi_\nu ds \quad (3.8)$$

Using the Rayleigh-Jeans approximation and integrating equation 3.7 over frequency and over solid angle weighted by beam pattern, then

$$\int T_A d\nu = \frac{c^3 h}{8\pi k\nu^2} A_{ul} \frac{1}{\Delta\Omega_B \Delta^2} \iint A(x,y) \int f_u n(x,y,s) ds dx dy \quad (3.9)$$

where  $A(x,y)$  is the beam pattern,  $\Delta\Omega_B$  the antenna beam solid angle,  $n(x,y,s)$  the parent molecule density, and  $f_u$  the fractional population of upper level of the transition and can be obtained from our excitation models in chapter 2. The total number of parent molecules is given by

$$\iiint n(x,y,s) dx dy ds = N = \frac{Q}{\tau} \quad (3.10)$$

where  $N$  is the total number of the parent molecules,  $Q$  the production rate in molecule  $s^{-1}$ , and  $\tau$  the lifetime against photodissociation. Define  $M$  and  $M'$  as



$$M = \frac{\iint A \int f n d s d x d y}{N} \quad (3.11)$$

and

$$M' = \frac{\int d v \iint A d x d y \int f n d s}{N} , \quad (3.12)$$

where  $M$  represents the fraction of total molecules that contribute to the line strength and can be calculated by the Monte Carlo method discussed in the last section.  $M'$  is same as  $M$  but is the fraction in a given velocity channel.

Putting equation 3.10 and 3.11 into equation 3.8, we have

$$\int T_A d v = \frac{h c^3}{8 \pi k v} A_{ul} \frac{M Q \tau}{\Delta \Omega_B \Delta^2} \quad (3.13)$$

for integrated intensity, or for channel we have

$$T_A = \frac{h c^3}{8 \pi k v} A_{ul} \frac{Q \tau M'}{\Delta v \Delta \Omega_B \Delta^2} \quad (3.14)$$

where  $\Delta v$  is the spectra resolution.

Thus, we can use the Monte Carlo method to calculate the integrated intensity or the spectrum of parent or daughter molecules in comets by using the above equations. We are able to generate a spectral

line map with as many as five beams with offsets expressed in the anti-earth coordinate system. This can be done by determining the beam weights for each molecule and transforming its coordinate to the plane of the sky ( $x'y'$ -plane). The beam weights in the above equation are given by

$$beamweight = \exp\left(-4\ln(2)\sum_j \frac{off_{ij}^2}{B_{ij}^2}\right) \quad (3.15)$$

where  $off_{ij}$  is the  $j$ th coordinate of the  $i$ th beam offset and  $B_{ij}$  is the  $j$ th dimension of beam  $i$ .

### 3.3 Conclusions

A set of physical parameters in equations 3.12 and 3.13 must be determined in the simulation process. These are listed in below:

The parameters that determine the upper level fraction  $f_u$  are:

- The water production rate
- The total collisional cross-section
- The temperature in the cometary atmosphere

The total collisional cross-section has been discussed and may be determined as in the last chapter. Other parameters in the equations are:

- The parent production rate
- The outflow velocity of the observed molecule
- The parent lifetime against photodissociation

- The daughter lifetime against photodissociation
- AP value

All the above parameters can be determined by using the observed data of integrated intensity and rotational spectral line shape of molecules in comets, given the comet orbital parameters, like distance to the earth, heliocentric distance, and the phase angle.

In order to demonstrate the results obtained from using both parent and daughter models, sample spectra are shown in Figure 3.2. In the parent model, we have assumed  $0.7 \text{ km s}^{-1}$  parent velocity,  $10,000 \text{ sec}$  lifetime against photodissociation, and  $200,000$  molecules put in the calculation. For daughter model,  $0.75 \text{ km s}^{-1}$  daughter velocity and  $10,000 \text{ sec}$  lifetime are used. The positions where on and off the nucleus are selected to calculate the spectra. From Figure 3.2, we can see that the spectra of the daughter model can be distinguished from that of the parent model. Thus, the origin of molecule in the coma can be examined by using these models to fit observed spectrum.

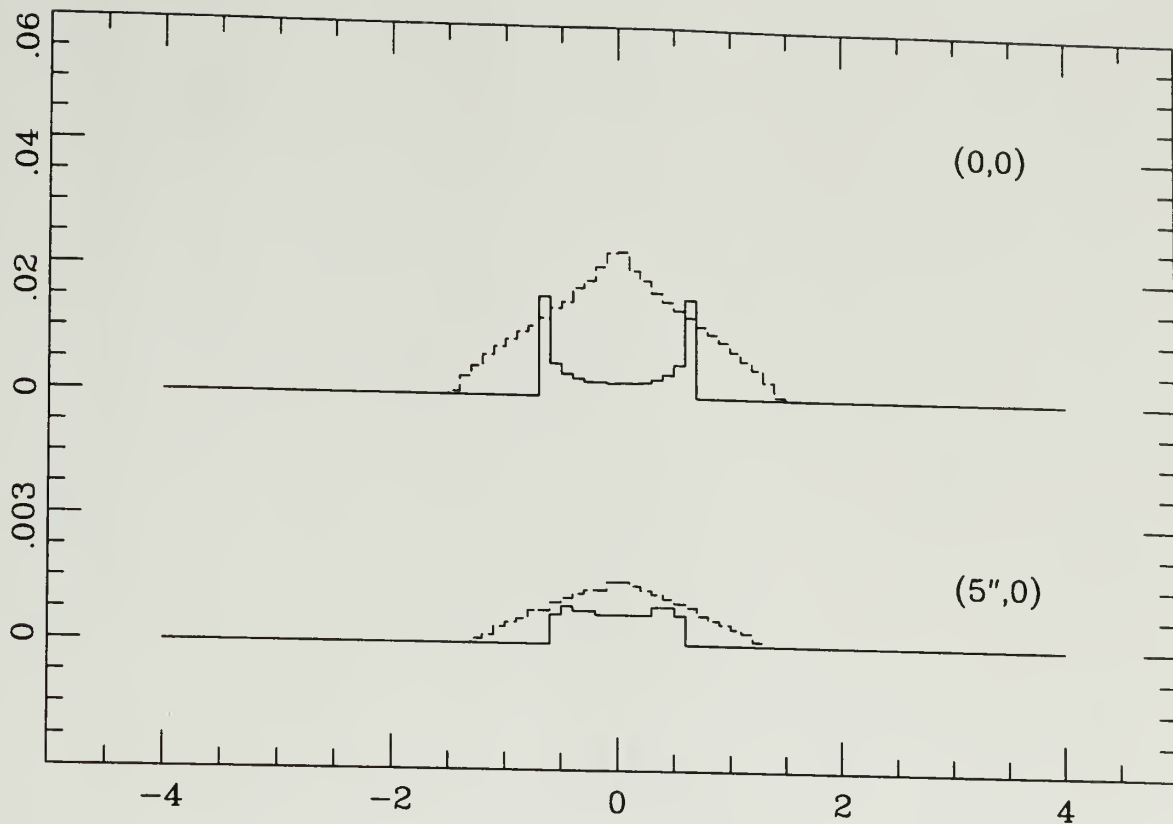


Figure 3.2 The sample spectra by using the parent model (full line) and the daughter model(dashed line), respectively.

## CHAPTER 4

### OBSERVATIONS

Observations of HCN and H<sub>2</sub>CO in Comet Levy (1990c) were obtained at the Caltech Submillimeter Observatory using the 10m antenna during 29 August - 1 September 1990 at  $r_h = 1.4$  AU from the Sun and  $\Delta = 0.4$  AU from the Earth. An SIS receiver was used for the HCN J=3-2 observations at 266 GHz; the single sideband system temperature measured on the sky by the chopper wheel method was approximately 700 K during the observations. For the HCN J=4-3 (354 GHz) and H<sub>2</sub>CO (352 GHz) observations, the two lines were observed simultaneously by placing them in opposite receiver side bands of the SIS receiver. The SSB system temperature of this receiver was approximately 1400 K, as measured on the sky during the observations. Two Acousto-Optic Spectrometers (AOS) were used to detect the spectral lines. The AOS bandwidths were 500 MHz and 50 MHz, which yielded 0.5 MHz and 50 KHz resolution, respectively. Antenna pointing was verified on Saturn, which was relatively close to Comet Levy in the sky; the pointing uncertainties are estimated to be 3 arcsec rms. The antenna beam width is 28 arcsec at 266 GHz and 22 arcsec at 353 GHz. The beam efficiency at both frequencies is approximately 0.55.

Cometary observations pose a special problem for radio observers since typically the comet must be tracked blind. For these observations, we used orbital elements kindly supplied by D. Yeomans, JPL, at the beginning of our run to predict the position of the comet. However, subsequent improvements in the orbit, published in *Minor Planets Circular (MPC) 16841*, indicated that we tracked a position about 13 arcsec NE of the actual position of the nucleus. This illustrates the need for good orbital solutions to support radio observations.

The HCN  $J=3-2$  rotational line was measured at high spectral resolution ( $0.1 \text{ km s}^{-1}$ ) and mapped at 13 points over a region of approximately 1.5 arcmin. These results are shown in Figures 4.1 and Figure 4.2. Figure 4.1 shows a high resolution ( $0.1 \text{ km s}^{-1}$ ) spectrum of the line and indicates the positions and relative strengths of the 6 hyperfine components of this transition. This interesting line shape is due to both the hyperfine structure and the line of sight velocity distribution of HCN in the coma, which is due primarily to the outflow morphology and speed of the coma gas. Figure 4.2 displays a set of low resolution spectra obtained at 13 positions on a 30 arcsec grid around the "nucleus" position that was tracked by the telescope during our observations. The map shows an apparent asymmetry towards the south and west of this position in the direction of the offset between the ephemeris used for these observations and that of MPC 16841. The integrated intensity for each spectrum is

given in Table 4.1. The  $I_{\text{int}}$  in the third column of the table represents observed HCN integrated intensity at each of 13 different positions and its error is given in the fourth column.

Table 4.1

The values of HCN J=3-2 integrated intensities for Comet Levy

$X_{\text{off}}$ (arcsec)	$Y_{\text{off}}$ (arcsec)	$I_{\text{int}}$ (K km s <sup>-1</sup> )	$I_{\sigma}$
0.0	0.0	0.980	0.0194
30.0	0.0	0.073	0.0572
0.0	30.0	0.270	0.0464
-30.0	30.0	0.840	0.0672
-30.0	0.0	0.810	0.0598
-30.0	-30.0	0.730	0.0604
0.0	-30.0	0.720	0.0541
30.0	-30.0	0.120	0.0769
0.0	-60.0	0.240	0.0510
-60.0	0.0	0.380	0.0590
-60.0	-60.0	0.600	0.0709
-90.0	0.0	0.006	0.0752
-90.0	-90.0	-0.38	0.1250

Observations of the HCN J=4-3 and H<sub>2</sub>CO 5<sub>15</sub>-4<sub>14</sub> transitions were obtained on two days following the HCN J=3-2 measurements. These transitions are the first submillimeter spectral lines to be detected in a comet. The HCN J=4-3 and H<sub>2</sub>CO 5<sub>15</sub>-4<sub>14</sub> transitions at the "nucleus" position tracked during our observations are shown in Figure 4.3 and

Figure 4.4 respectively. The results for the H<sub>2</sub>CO spectral line at 352 GHz presented in Figure 4.4 were obtained on August 30, and 31, 1990, respectively and display significant day-to-day variations in the strength of the line. In addition to observations at the nominal nucleus position, the HCN J=4-3 and H<sub>2</sub>CO spectra were also obtained at four positions offset by 30 arcsec in the cardinal directions from the nucleus. The distribution of brightness in the HCN J=4-3 transition is consistent with that observed in the J=3-2 maps, which provides verification of the pointing of the telescope with respect to the comet during these observations and confidence in the derived results. The H<sub>2</sub>CO five pointing map is shown in Figure 4.5. Due to the poor quality of the map, the spectra at south and north offsets were averaged with those at west and east offsets respectively, and the resulting three points map were used to determine the radial distribution of the H<sub>2</sub>CO molecule. The apparent extended emission in this map is not easy to reconcile with a model that the formaldehyde directly emanated from the nucleus, since the molecule has a short lifetime against photodissociation. At the distance  $\Delta = 0.4$  AU from the Earth, its lifetime of 2,860 second and a H<sub>2</sub>CO outflow velocity of 0.8 km s<sup>-1</sup> corresponds to a photodissociation scale length of 8 arcsec from the nucleus before photodissociation is expected to occur.



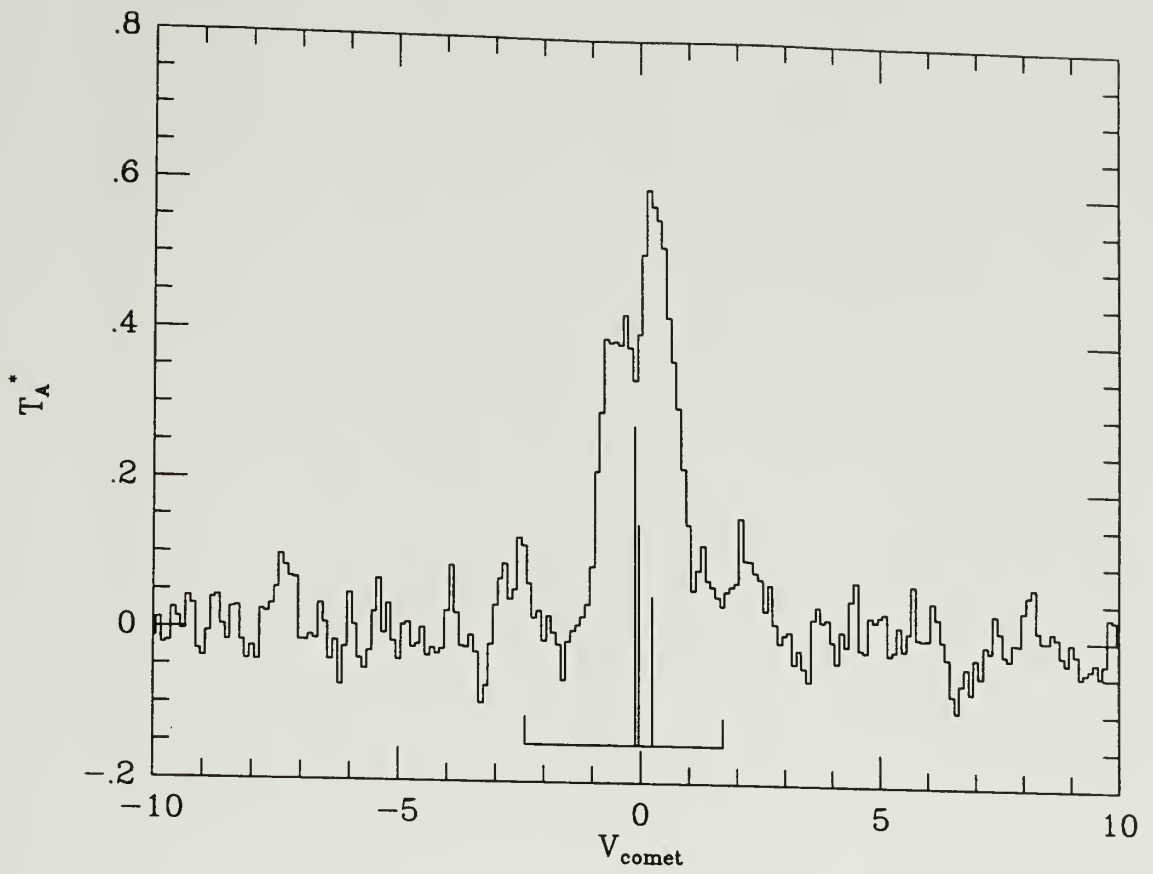


Figure 4.1 HCN J=3-2 spectrum of Comet Levy(1990c)  
obtained at  $0.1 \text{ km s}^{-1}$  resolution.

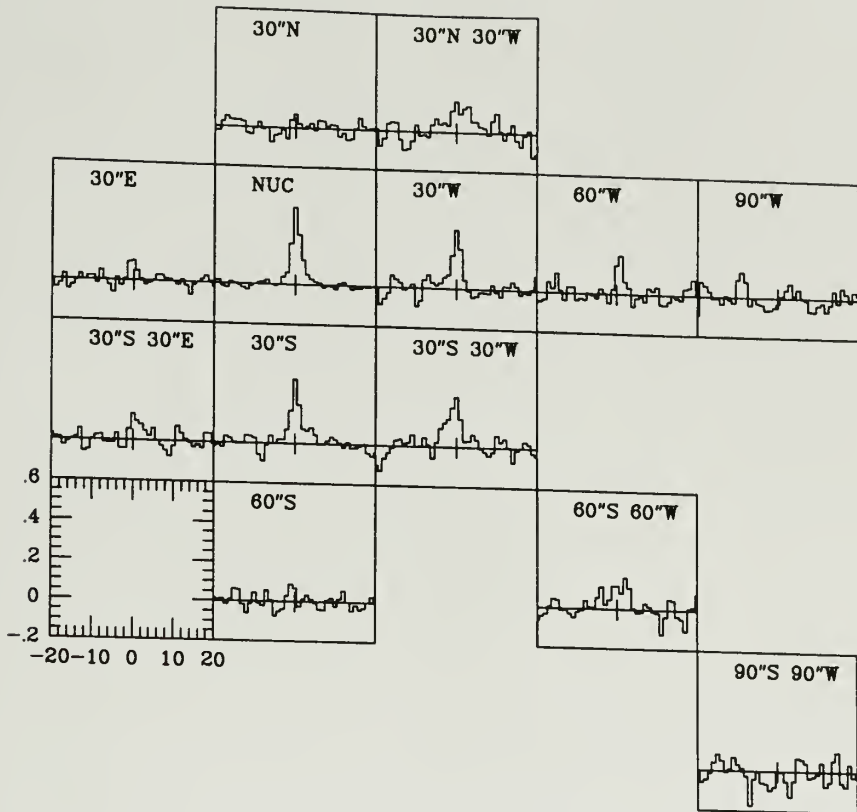


Figure 4.2 HCN J=3-2 Map of Comet Levy(1990c). The spectra are sampled on a 30 arcsec grid about the "nucleus" position tracked by the telescope.

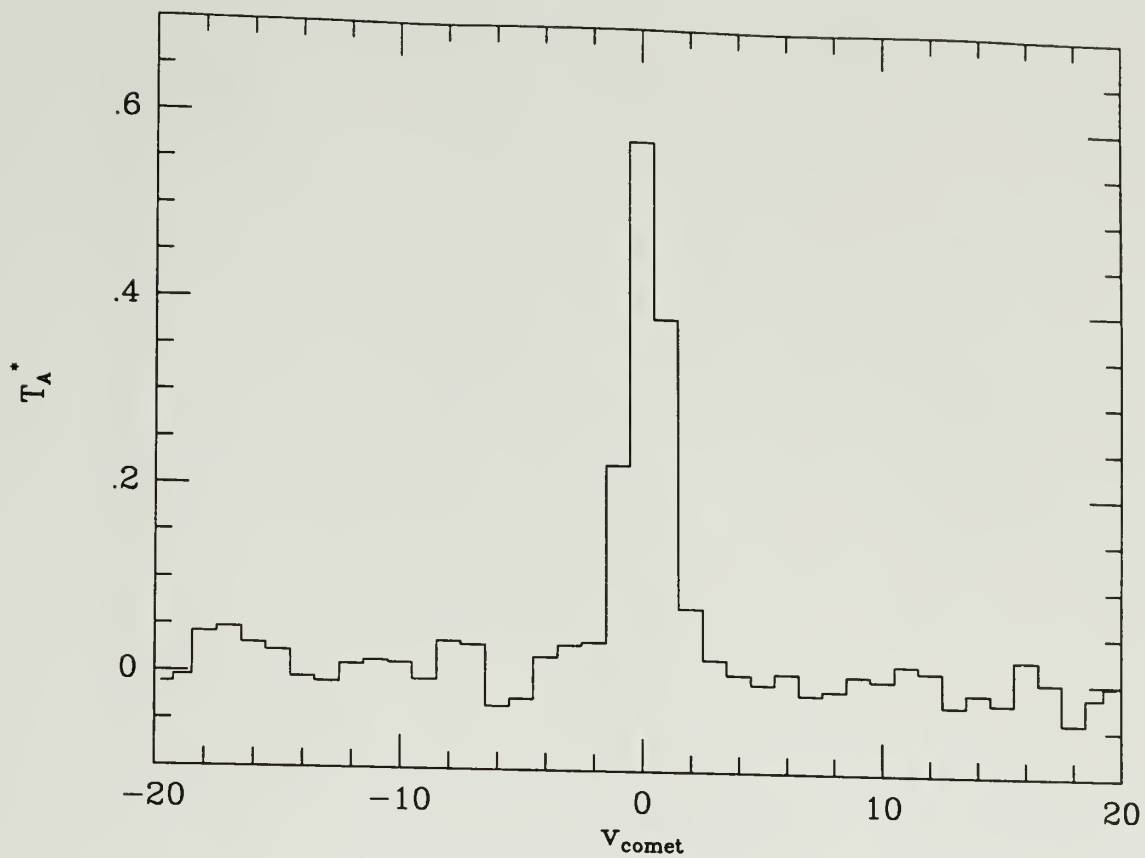
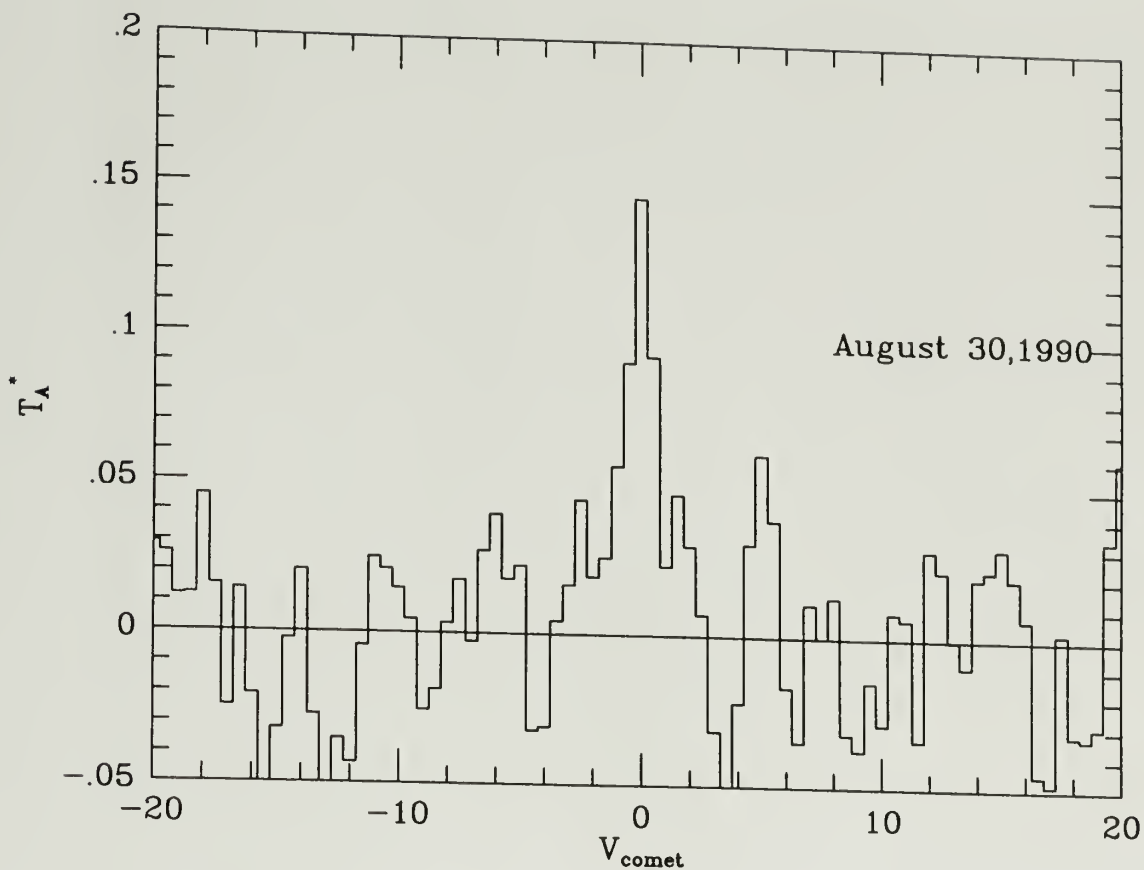


Figure 4.3 HCN J=4-3 spectrum of Comet Levy(1990c) obtained on August 30, 1990.



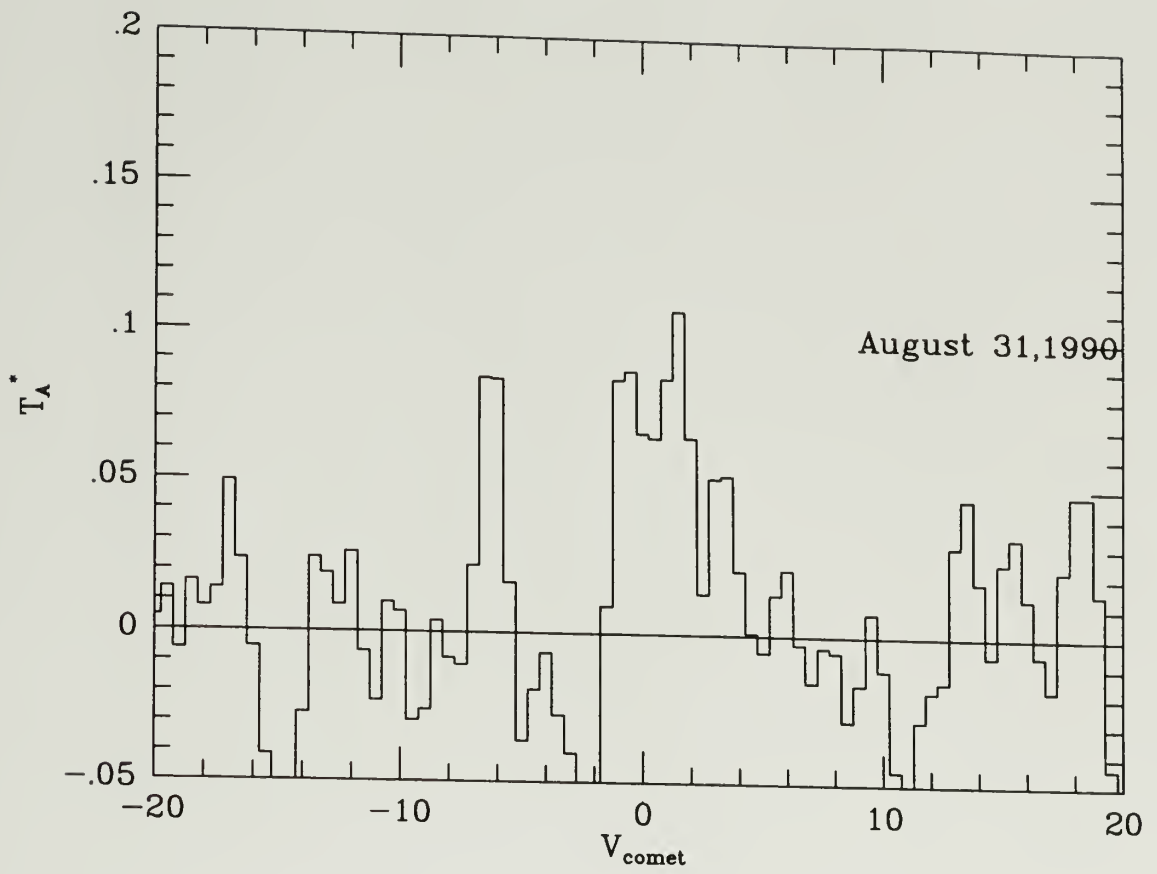
(a)

Figure 4.4  $\text{H}_2\text{CO } 5_{15}-4_{14}$  spectrum of Comet Levy(1990c).

a: obtained on August 30, 1990;

b: obtained on August 31, 1990.

Continued on following page.



(b)

Figure 4.4 Continued from previous page.

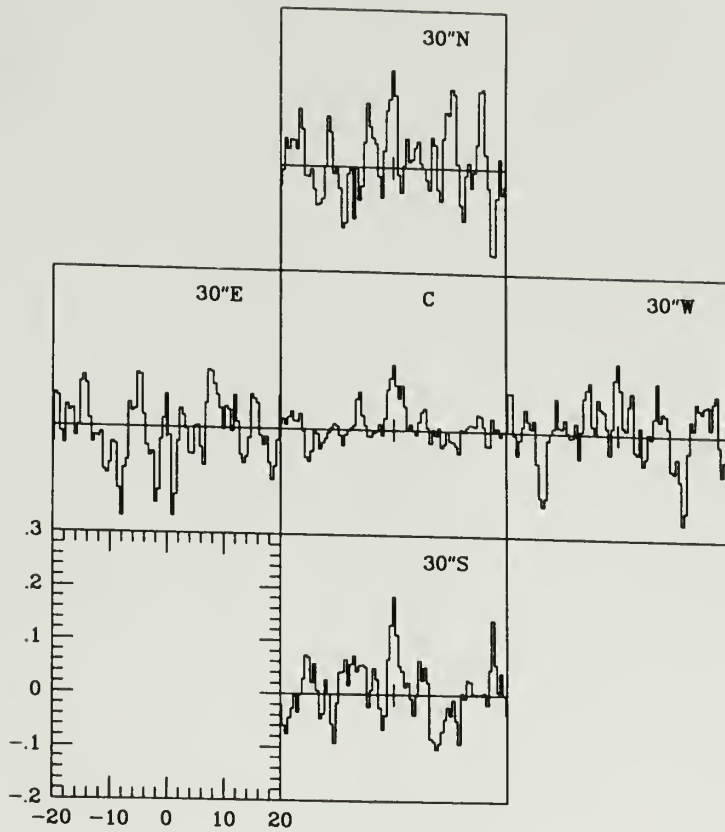


Figure 4.5  $\text{H}_2\text{CO } 5_{15}-4_{14}$  Map of Comet Levy(1990c). The spectra are sampled on a 30 arcsec grid about the "nucleus" position tracked by the telescope.

## CHAPTER 5

### RESULTS

The HCN and H<sub>2</sub>CO rotational lines that have been observed in comet Levy may be used to study the composition of its nucleus and the kinematics of its coma. In chapter 2 and chapter 3, the necessary models of the excitation and kinematics of these molecules were developed. In this chapter, these models are used to analyze the comet Levy data that were obtained at the CSO.

#### 5.1 HCN Molecule

##### 5.1.1 Spectrum

In order to model the HCN J=3-2 line profile shown in Figure 4.1, several parameters must be specified:

- Total HCN production rate  $Q_{\text{HCN}}$
- Parent outgassing velocity  $V_p$
- Parent lifetime against photodissociation
- Distribution of the HCN production from the nucleus.

We have chosen to parameterize the last feature of the model, the distribution of HCN production from the nucleus, by using the Anisotropy

Parameter AP (Tacconi-Garman et al 1987) which is defined to be

$$AP = \log[Q_{day}/Q_{night}] \quad (5.1)$$

where  $Q_{day}$  and  $Q_{night}$  are the production rates into the day and night hemisphere respectively, so the AP value is relative to the ratio of the comet night side and day side production rates.

To illustrate the sensitivity of the data to the various model parameters, we begin with the simplest case, which assumes HCN outflows isotropically with a constant velocity. Thus, AP is fixed with a value of 0 and the HCN lifetime at 1 AU is assumed to be  $8 \times 10^4$  sec. As discussed in chapter 3, the molecular populations in rotational levels have to be known in order to calculate the spectrum. The water production rate is needed in the collisional part of the excitational model. We adopted, in comet Levy,  $2.5 \times 10^{29} \text{ s}^{-1}$  as the value of water production rate that obtained from the OH 18 cm observations (Bockelée-Morvan et al. 1990). The outflow velocity and production of HCN are determined from a fit to the spectrum. Figure 5.1 shows the fitting results for the velocity of  $0.79 \pm 0.17 \text{ km s}^{-1}$  obtained from searching for the least value of  $\chi^2$ . The relevant HCN production rate is  $2.08 \pm 0.24 \times 10^{26} \text{ s}^{-1}$  and is listed in Table 5.1 with the  $\chi^2$  value.

The HCN J=3-2 line profile shown in Figure 4.1 has a slight redshift in the line position which could be due to a small deviation from isotropic gas emission from the nucleus. Thus, a grid of model covering



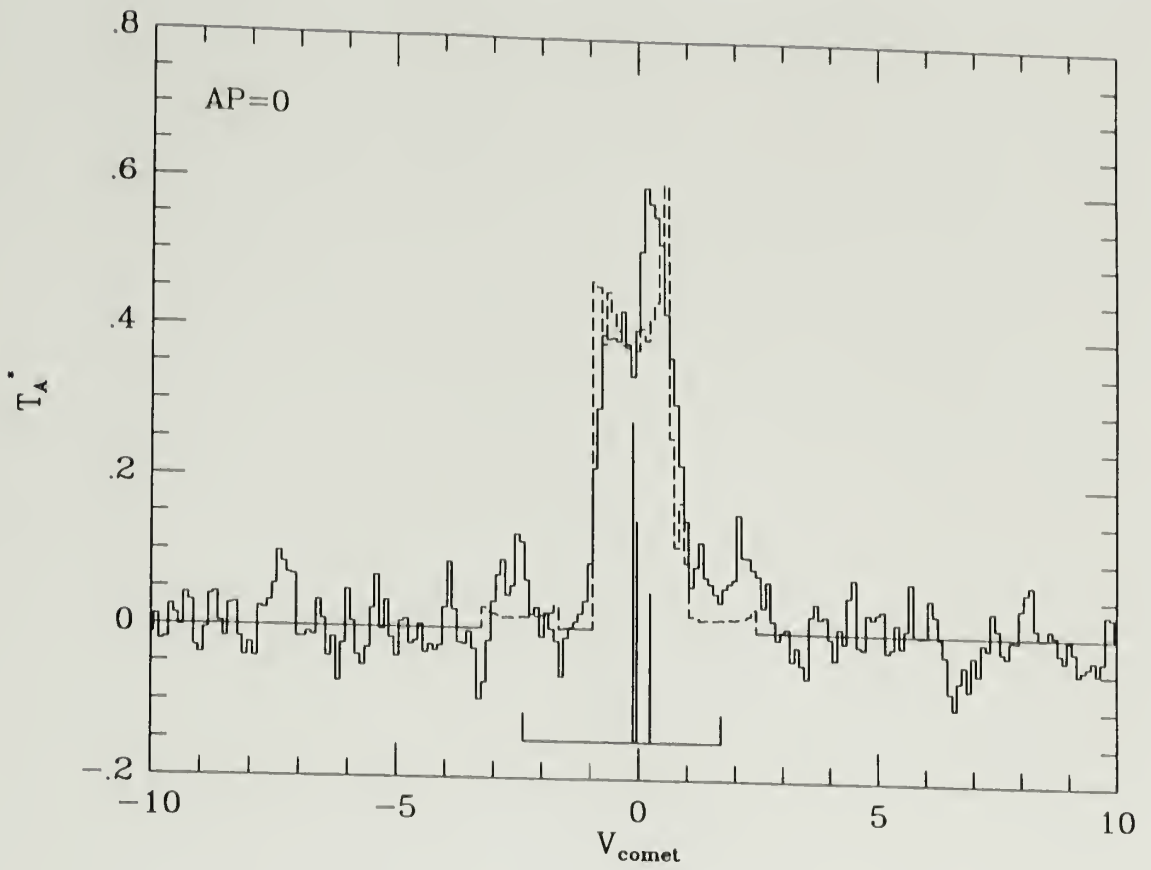


Figure 5.1 Fit to the HCN  $J=3-2$  spectrum of Comet Levy (1990c) by using the model with constant outflow velocity.

AP- $V_p$  parameter space has been carried out. The grid spacing for AP values is in unit of 0.2, or roughly a factor of 1.5 in the ratio of day-to-night emission. The parent outflow velocity grid spacing is characteristically  $0.2 \text{ km s}^{-1}$ . Both parameters are allowed to vary until a best fitting solution is obtained. For each combination of AP and  $V_p$ , the model spectrum has been calculated and fit to the spectrum. A best fitting result comes out when the  $\chi^2$  value reaches its minimum. Our resulting  $\chi^2$  is shown in Figure 5.2. The HCN outflow velocity  $V_p$  from the calculation is  $0.78 \pm 0.14 \text{ km s}^{-1}$  and the AP value is about  $-0.21 \pm 0.09$ . The spectrum fitting results are shown in Figure 5.3 and in Table 5.1. The AP value of -0.2 formally means that the night side emission rate could be enhanced over the day side rate by approximately 20%. The results of  $\chi^2$  values listed in Table 5.1 have been improved by using anisotropic model.

We have noted that both the outflow velocity and the production rate of HCN shown in Table 5.1 are independent of the AP value. Comparing with the two spectra shown in Figure 5.1 and in Figure 5.3, the AP value is directly related to the shape of the spectrum. At the phase angle of  $34^\circ$ , the parent molecules on the night side hemisphere have positive Doppler velocities along the line of sight and have negative values of velocity if they are on the day side. Thus, different AP values only change the shape of the spectrum instead of the production rate and

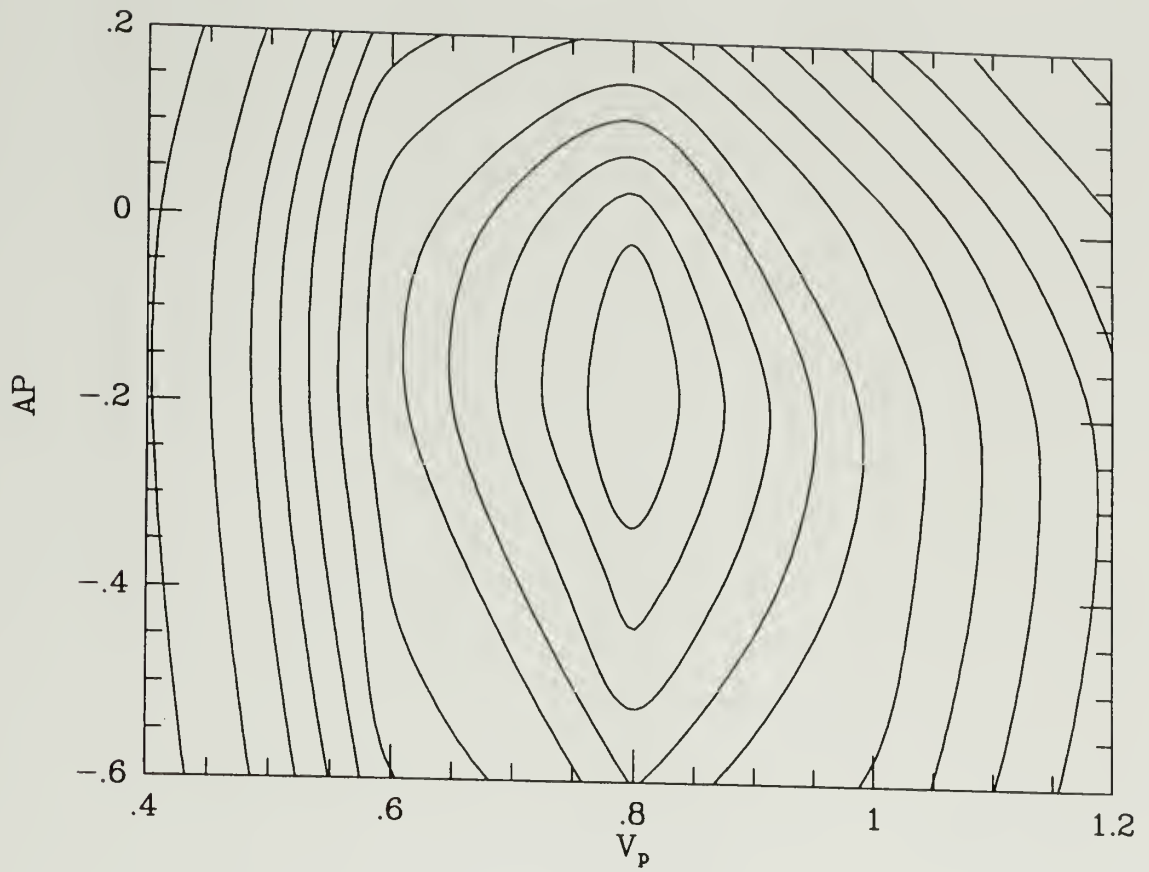


Figure 5.2  $\chi^2$ , contour map in  $V_p$ -AP space. The grid spacing of AP is in unit of 0.2 and the grid spacing of velocity is 0.2 km s<sup>-1</sup>. The contour spacing is 0.06.

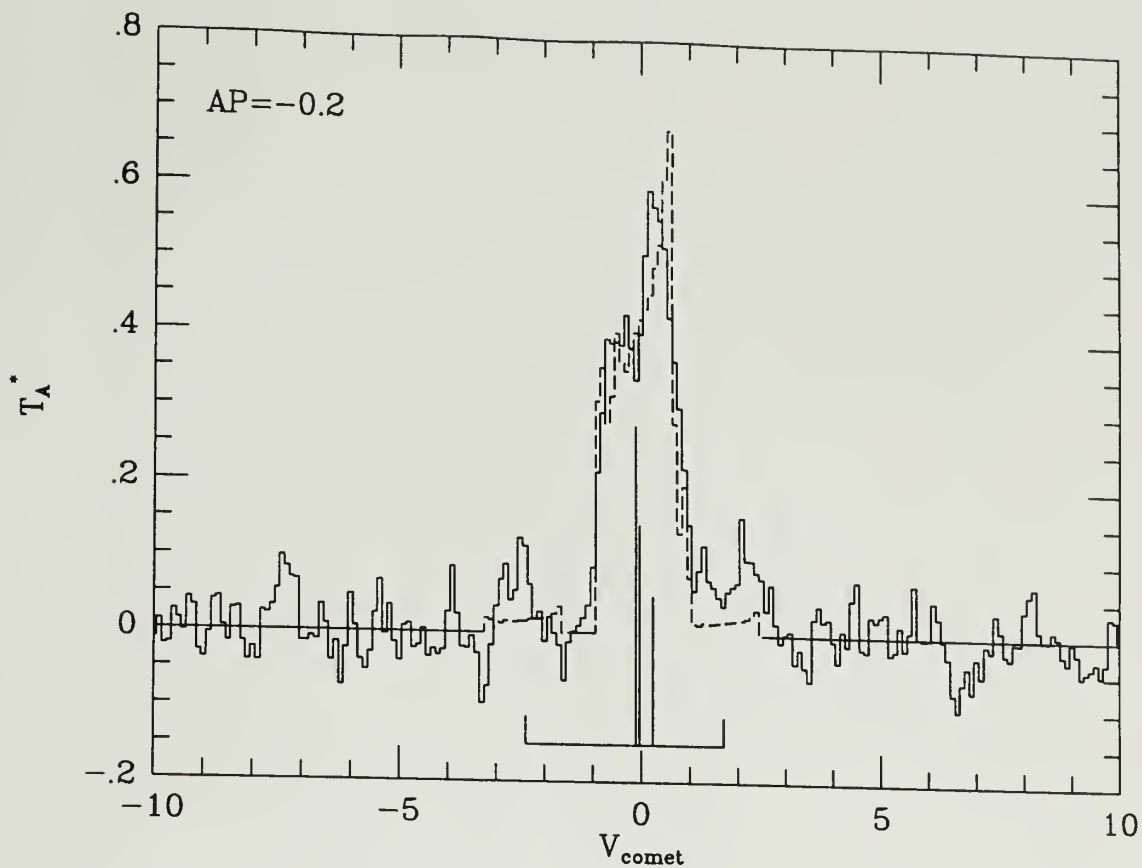


Figure 5.3 Fit to the HCN  $J=3-2$  spectrum of Comet Levy (1990c) by using the model with constant outflow velocity. The AP value of -0.2 is used in model.

spectrum width. The HCN abundance relative to water in comet Levy is about 0.1%, which is roughly in agreement with that in P/Halley (Schloerb et al. 1986).

Table 5.1

Parameters in The model fitting

	V	$\sigma_v$	AP	$\sigma_{AP}$	$Q_{\text{HCN}}$	$\chi^2_v$
	km s <sup>-1</sup>				$\times 10^{26}$	
monokinetic, isotropic	.79	.17			2.08	1.69
monokinetic, anisotropic	.78	.14	-.20	$\pm .09$	2.15	1.50

### 5.1.2 Map

In order to track the comet, we used orbital elements supplied by D. Yeomans at the beginning of the observations. However, subsequent improvements in the orbit indicated that the position tracked was displaced from the actual position of the nucleus. Fortunately, the comet Levy observations provided us high quality spectra which offer the opportunity to determine the actual position of the nucleus and constrain

other parameters of the coma using the two dimensional distribution of the HCN emission shown in Table 4.1.

Several parameters are required to model the two dimensional distribution of HCN emission. First, since the actual position of the nucleus is unknown, it must be determined from the observations. The actual position of the nucleus is located by solving for its position offset  $x_{\text{off}}, y_{\text{off}}$  from the position that the telescope tracked during the observations. The x-axis positive direction is toward the East and the y-axis is defined to be positive North. A remaining important parameter is the HCN lifetime at  $r_h = 1$  AU, which affects the extent of the coma. Thus, the simplest model required to fit the data would include the following parameters

- Position offset  $x_{\text{off}}$  and  $y_{\text{off}}$
- HCN lifetime against photodissociation.

First, the minimum  $\chi^2_v$  is sought in the  $x_{\text{off}} - y_{\text{off}}$  parameter space with a nominal HCN lifetime value in order to calculate these integrated intensities at 13 positions and produce the best fitting model for the observed integrated intensities. Then we repeat the above process by changing the HCN lifetime value until a least  $\chi^2_v$  value is found and the HCN lifetime is determined. In the calculation, a constant velocity of  $0.8 \text{ km s}^{-1}$  has been used from the results of last section. The AP values of 0.0

and -0.2 have been chosen in the model and it has been shown that the final results of  $x_{\text{off}}$  and  $y_{\text{off}}$  are not sensitive to the different AP values.

The position fitting results are given in Figure 5.4 and in Table 5.2 and show that the actual position of the nucleus should be south 6.7 arcsec and west 11.3 arcsec from the tracked one for the best fitting result. Table 5.2 also lists the results derived from the orbital elements published in MPC 16841 and indicated that we tracked a position about 13 arcsec NE of the actual position of the nucleus and our results are close to this value. The HCN lifetime of  $7.9 \pm 0.80 \times 10^4$  sec at heliocentric distance  $r_h = 1$  AU is also close to the value given by Huebner and Carpenter (1979) and Jackson (1976). The HCN production rate obtained from the fit is  $2.4 \pm 0.4 \times 10^{26} \text{ s}^{-1}$  and is consistent with the results obtained in last section. Figure 5.5 shows the observed distribution (dark cross) of HCN emission with the results obtained from the model.

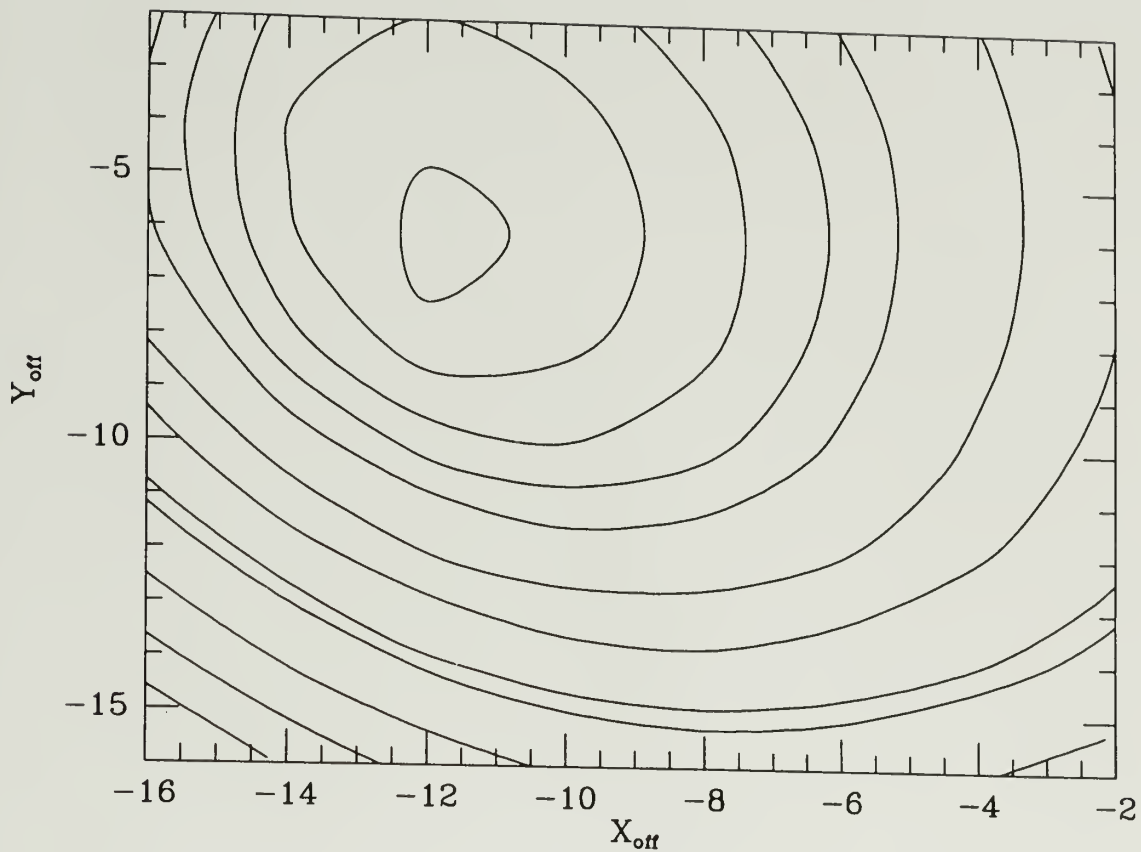


Figure 5.4  $\chi^2_{\nu}$  contour map in  $x_{\text{off}}-y_{\text{off}}$  space. The grid spacings of  $x_{\text{off}}$  and  $y_{\text{off}}$  are in unit of 2 arcsec. The contour spacing is 0.06.



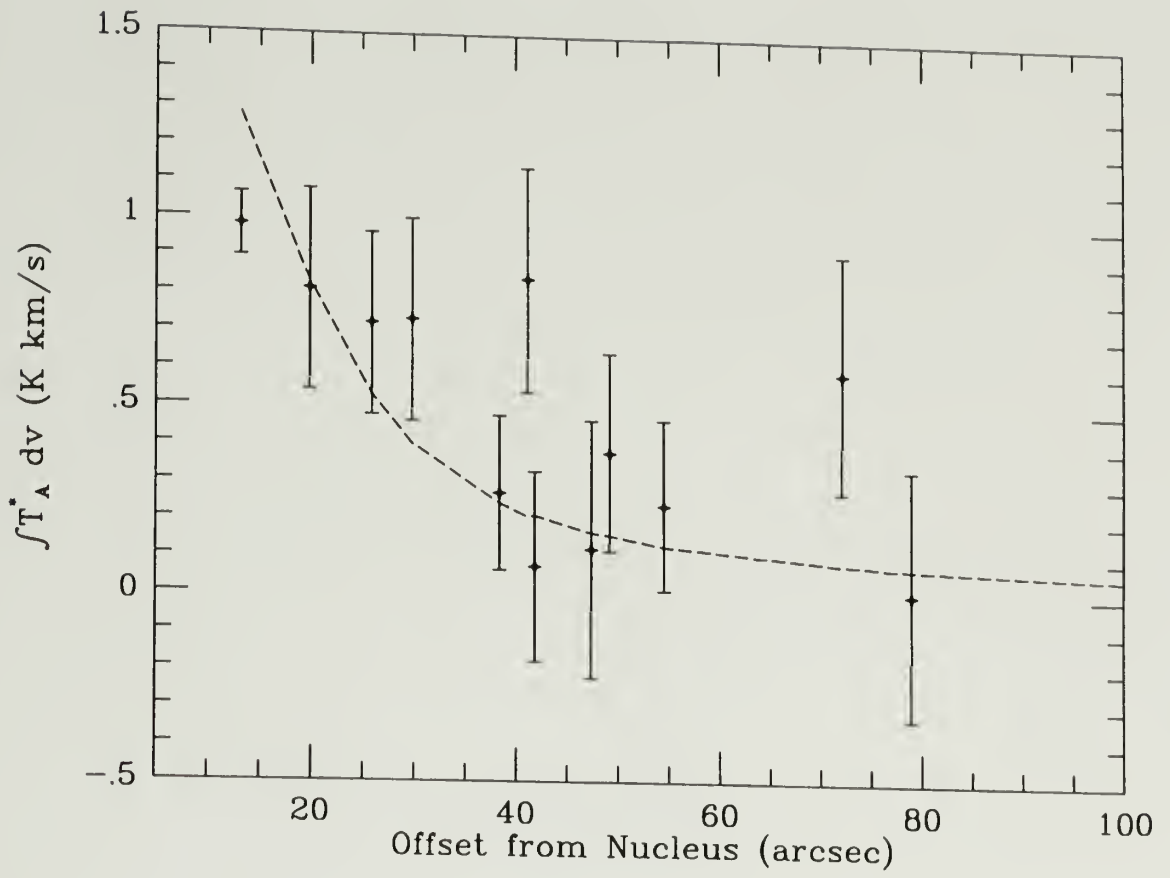


Figure 5.5 Observed distribution of HCN J=3-2 emission  
compare to that of the model.

Table 5.2

HCN Lifetime and position offset of the nucleus

	$X_{\text{off}}$	$\sigma_x$	$Y_{\text{off}}$	$\sigma_y$	$\tau_{\text{HCN}}$	$\sigma_\tau$
Map fitting	-11.3	$\pm 1.14$	-6.7	$\pm 0.86$	79285.0	$\pm 8035.0$
MPC 16841	-10.1		-8.6			

### 5.1.3 Outflow Velocity of the Coma

As we can see from Figure 5.1 and Figure 5.3, the monokinetic isotropic and anisotropic models with constant outflow velocity do not reproduce the HCN  $J=3-2$  line profile completely. Thus, it is worth considering whether the model may be improved to provide a better agreement. One area that is probably oversimplified is the assumption of a constant outflow velocity throughout the coma. Most theoretical calculations demonstrate that the radial velocity of gas increases with distance from the nucleus in bright comets (c.f. Combi 1989). Moreover, such a radial dependence of the outflow speed was actually measured by the in situ Giotto neutral-gas mass spectrometer (NMS) measurements (Lämmerzahl et al. 1986). Combi (1989) has developed a one-dimensional

steady-state model that includes the effects of dust-gas dynamics in the inner coma and photochemical heating of the outer coma, which is in a state of transition from collision-dominated to free molecular flow. This work showed that the model describes the Giotto NMS observations and suggests that the radial gradients should be important in the modeling of doppler resolved velocity spectral lines. Thus, this previous work and that of Crovisier (1985) and Hu (1990) on the radial dependence of outflow velocity suggest a way to improve the model of the kinematics of the coma of comet Levy, and we have added radial gradients to the model in an attempt to improve the fit. Unfortunately, the theoretical calculation of the radial velocity function requires construction of a detailed physical model which would be beyond the scope of the analysis presented here. Thus, we have attempted to determine the coma velocity gradient by fitting a model to it. Since the selection of a particular model is somewhat arbitrary and might systematically bias the fit results, we have adopted 4 different models for the model fitting. The rationale for selecting velocity functions is that they can roughly fit the theoretical speed curve calculated by Combi (1989). The four models of velocity as a function of radial distance from the nucleus are given in equations 5.2 to 5.5:

$$\text{Model 1} \quad \begin{aligned} V &= V_1 & r < r_c \\ &= V_2 & r > r_c \end{aligned} \quad (5.2)$$

$$\text{Model 2} \quad V = V_0 \left( \frac{r}{r_n} \right)^\alpha \quad (5.3)$$

$$\text{Model 3} \quad V = V_0 \left[ 1 - \left( \frac{r}{r_n} \right)^{-1/\alpha} \right] + 0.2 \quad (5.4)$$

$$\text{Model 4} \quad V = V_0 \left[ 1 - \left( \frac{r}{r_n} \right)^{-1/\alpha} \right] \quad (5.5)$$

where  $r$  is the radial distance from the nucleus,  $v_1$ ,  $v_2$ , and  $r_c$  are to be determined from the data, and  $r_n$  is the radius of the nucleus.

Each model is capable of behavior similar to the detailed physical model calculated by Combi, and analysis of the common features of the 4 profiles leads confidence to the basic results.

There are only 2 or 3 parameters in each outflow velocity law to be determined from the data. Figure 5.6 shows these four outflow speed laws that have been fit by the least square method, along with the theoretical velocity curve calculated by Combi (1989). This theoretical curve has been scaled to the heliocentric distance of comet Levy in order to compare with our model results assuming that the velocity decreases with heliocentric distance according to  $r^{-1}$ . The spectral line fits are shown in Figure 5.7 through Figure 5.10 and demonstrate a significant improvement; calculated parameters are given in Table 5.3. The results

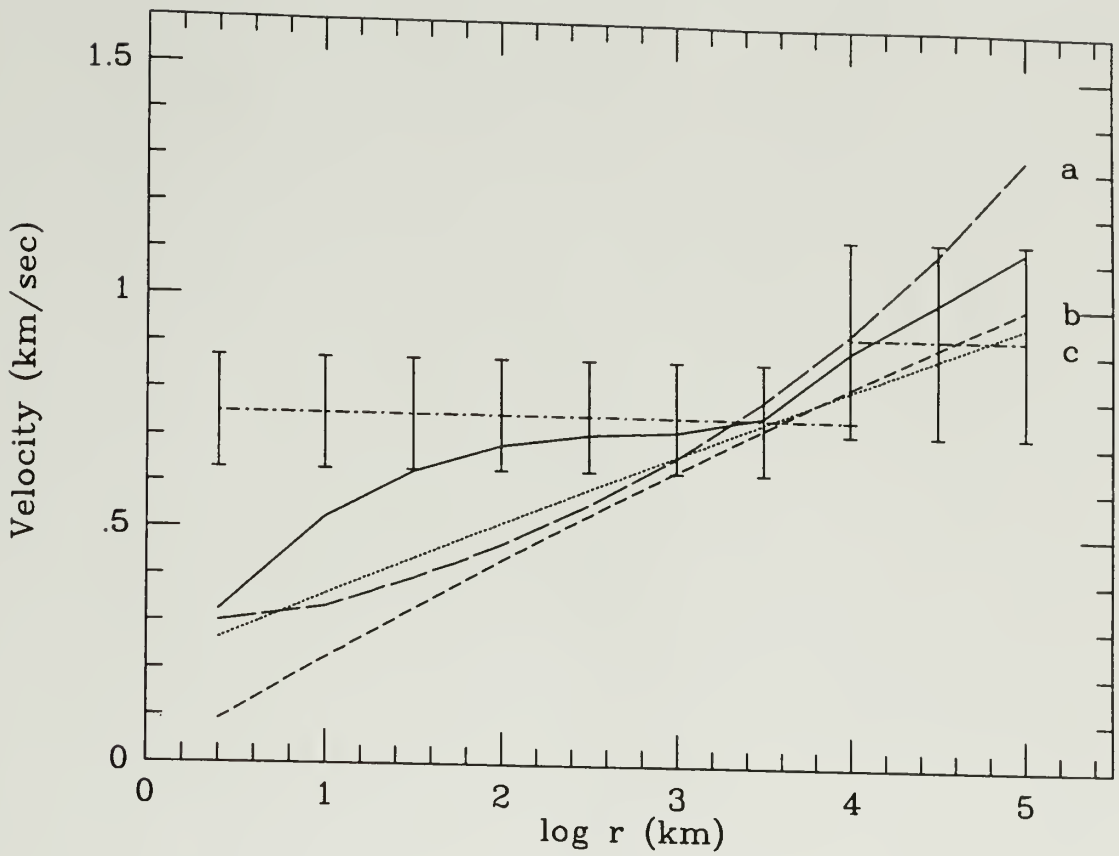


Figure 5.6 Four derived velocity laws with the theoretical velocity curve (filled line) calculated by Combi and scaled for the heliocentric distance of comet Levy. a: model 2; b: model 3; c: model 4; and the step function for model 1.

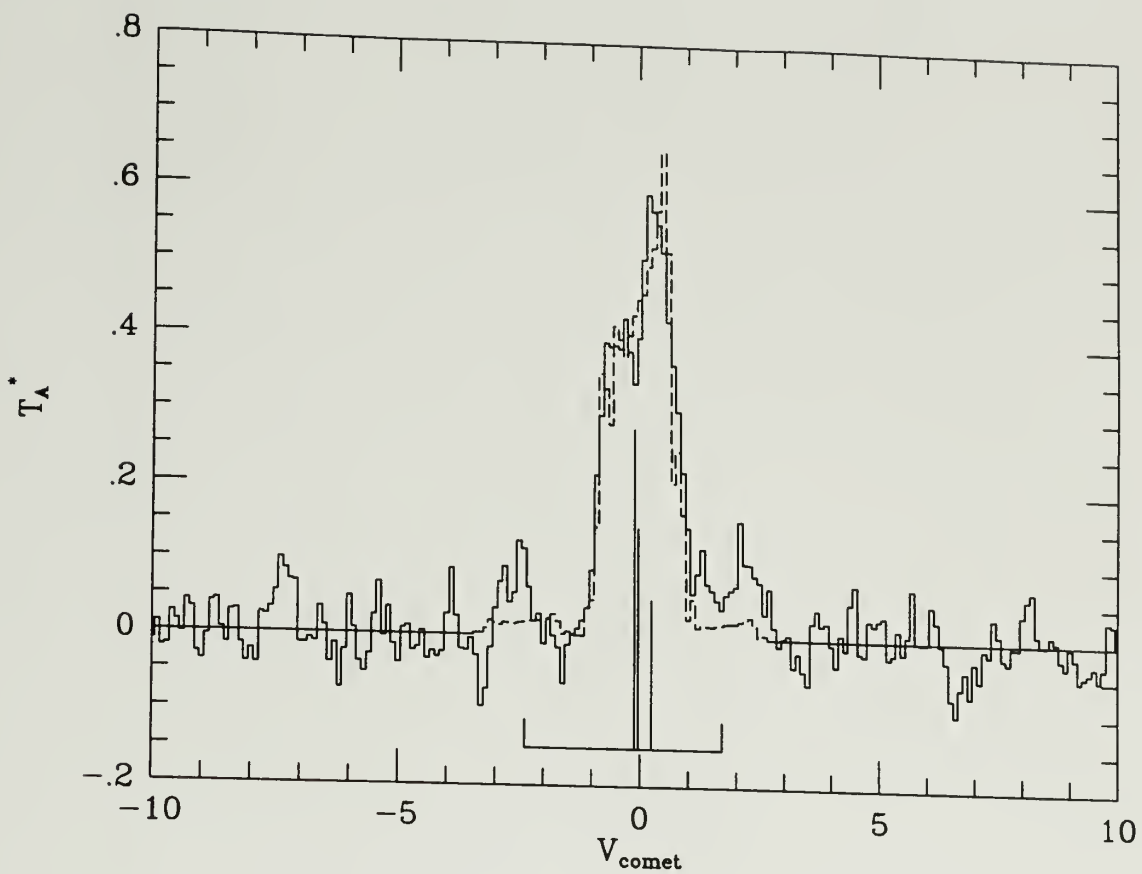


Figure 5.7 Fit to the HCN J=3-2 spectrum of Comet Levy (1990c) by using the model with the velocity as a step function (See equation 5.2).

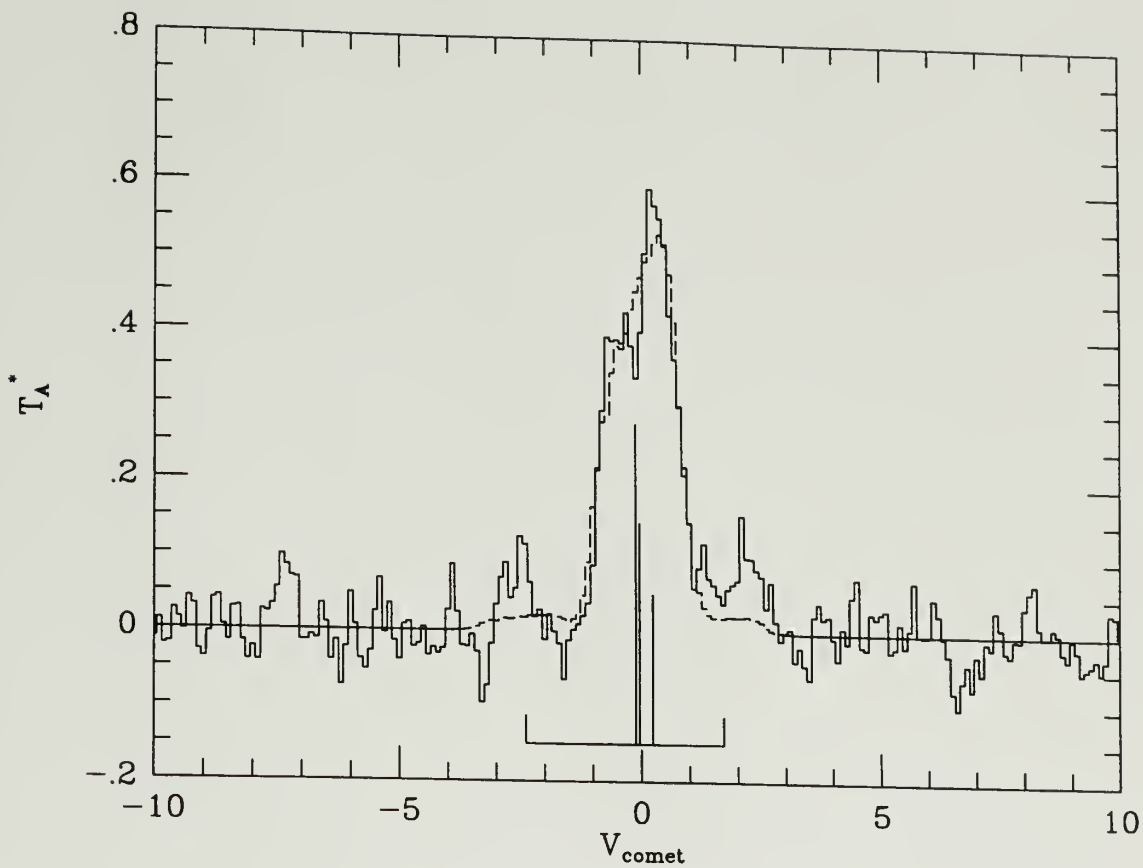


Figure 5.8 Fit to the HCN J=3-2 spectrum of Comet Levy (1990c) by using the model with the velocity law  $V(r) = V_0 r^\alpha$  (See equation 5.3).

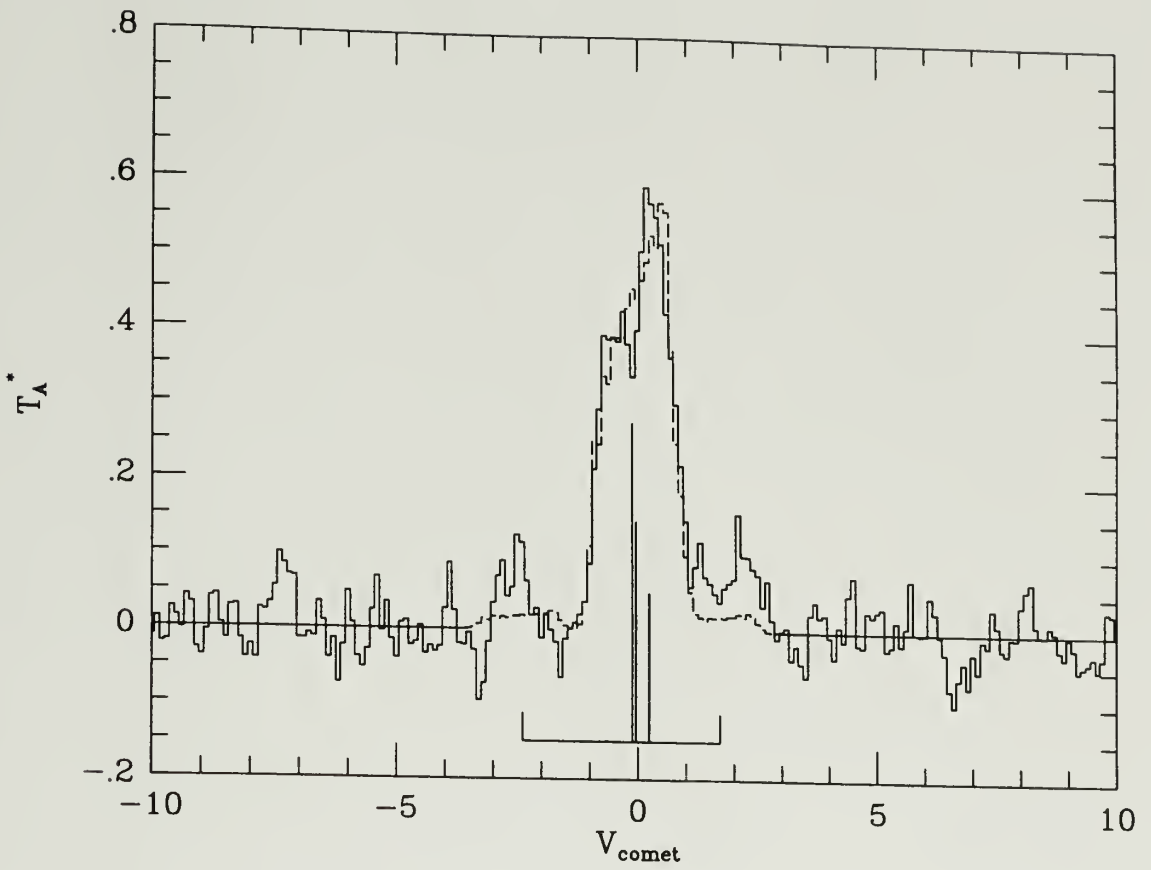


Figure 5.9 Fit to the HCN J=3-2 spectrum of Comet Levy (1990c) by using the model with the velocity law  $V(r) = V_0[1 - (r/r_0)^{1/r_0}] + 0.2$  (See equation 5.4).



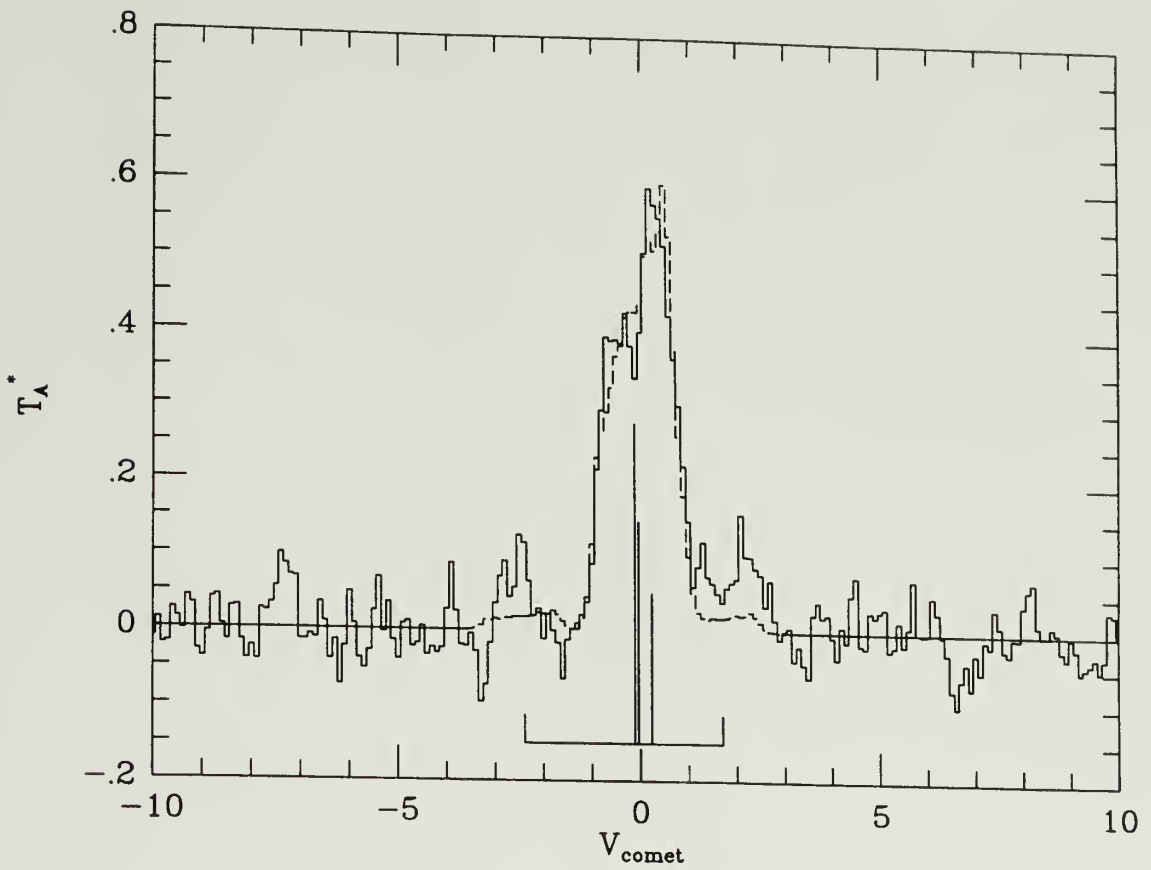


Figure 5.10 Fit to the HCN J=3-2 spectrum of Comet Levy (1990c) by using the model with the velocity law  $V(r) = V_0[1 - (r/r_n)^{1/r_0}]$  (See equation 5.5).

given in Table 5.3 are calculated by using the value of 5 km for the radius of the nucleus  $r_n$ , and an HCN lifetime of  $8 \times 10^4$  sec at  $r_n = 1$  AU has been assumed. The production rate of HCN found for these outflow velocity laws is about  $2.6 \pm 0.32 \times 10^{26}$  molec  $s^{-1}$ . In Table 5.3, the two parameters for each outflow velocity model have been listed with their errors. The value of  $r_c$  is determined by using the same method as in the HCN lifetime determination. Also, the  $\chi^2_v$  values evaluated in a-b parameter space are shown in Figure 5.11 to 5.14.

Table 5.3

Parameters of Velocity Laws

Velocity laws	a	$\sigma_a$	b	$\sigma_b$	$r_c$	$\sigma_r$	$\chi^2_v$
Model 1	.75	$\pm .12$	.93	$\pm .21$	$2.1 \cdot 10^4$	$0.33 \cdot 10^4$	1.24
Model 2	.30	$\pm .03$	.15	$\pm .02$			1.20
Model 3	6.10	$\pm .96$	37.6	$\pm 3.30$			1.21
Model 4	3.90	$\pm .49$	16.9	$\pm 1.77$			1.19

The model with constant outflow velocity is apparently too simple to reproduce the observed HCN data in comet Levy, and the gradient of the molecular outflow velocity plays an important role in controlling the spectral shape. The coma outflow speeds determined from the Giotto NMS data were obtained in the range  $10^3 < r < 10^5$  km where  $r$  is the distance from the nucleus. The data could be fitted by Combi's

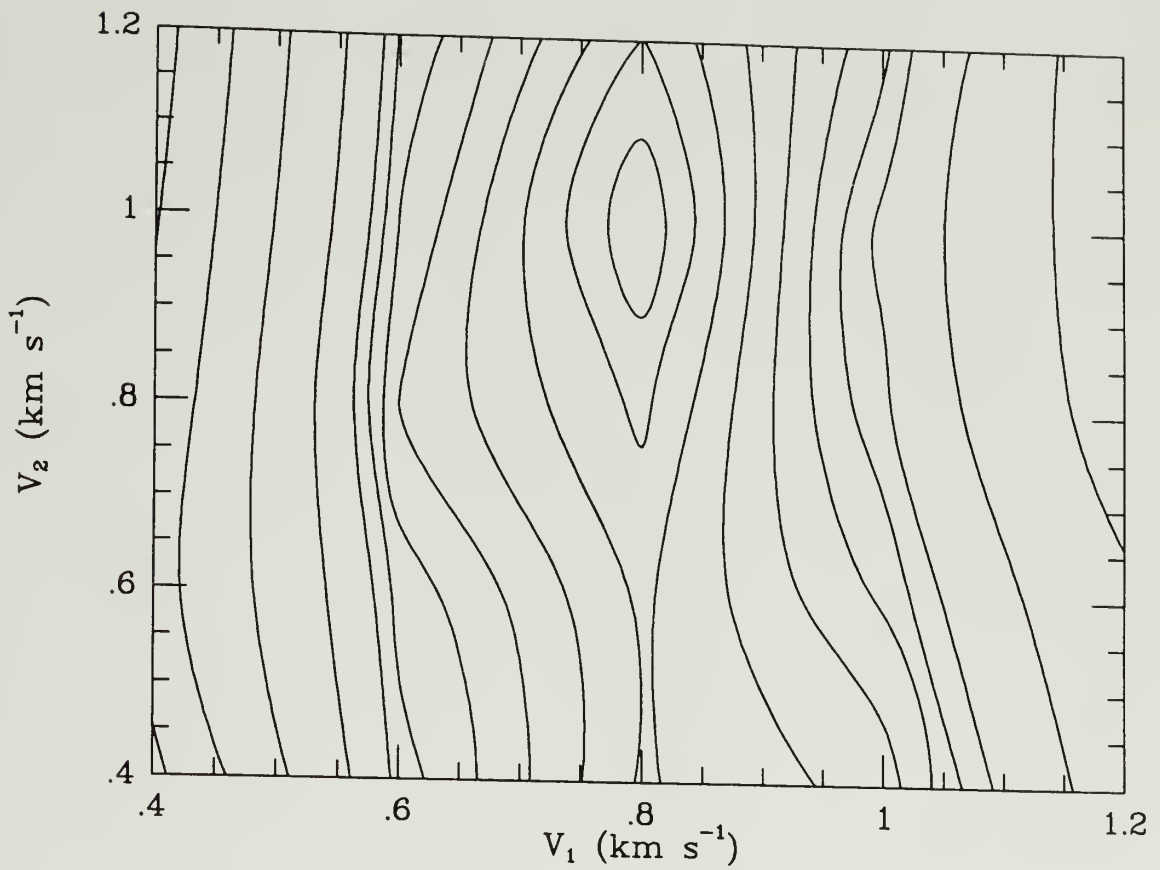


Figure 5.11  $\chi^2_v$  contour map in  $V_1$ - $V_2$  space. The step function of velocity is used. The grid spacings are in unit of 0.2 km s<sup>-1</sup>. The contour spacing is 0.06.

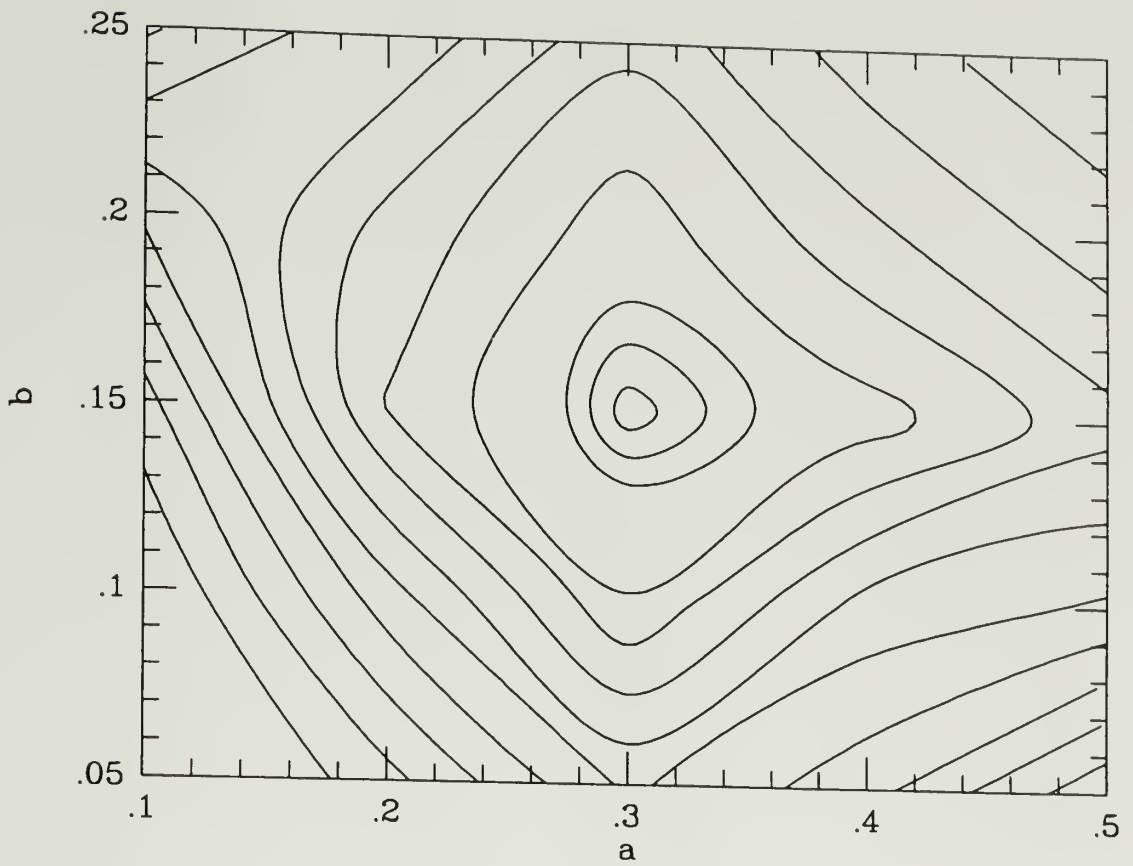


Figure 5.12  $\chi^2$ , contour map in  $a$ - $b$  space. The equation (5.3) is used as a velocity law. The grid spacing of  $a$  is in unit of 0.1 and  $b$  in unit of 0.05. The contour spacing is 0.06.

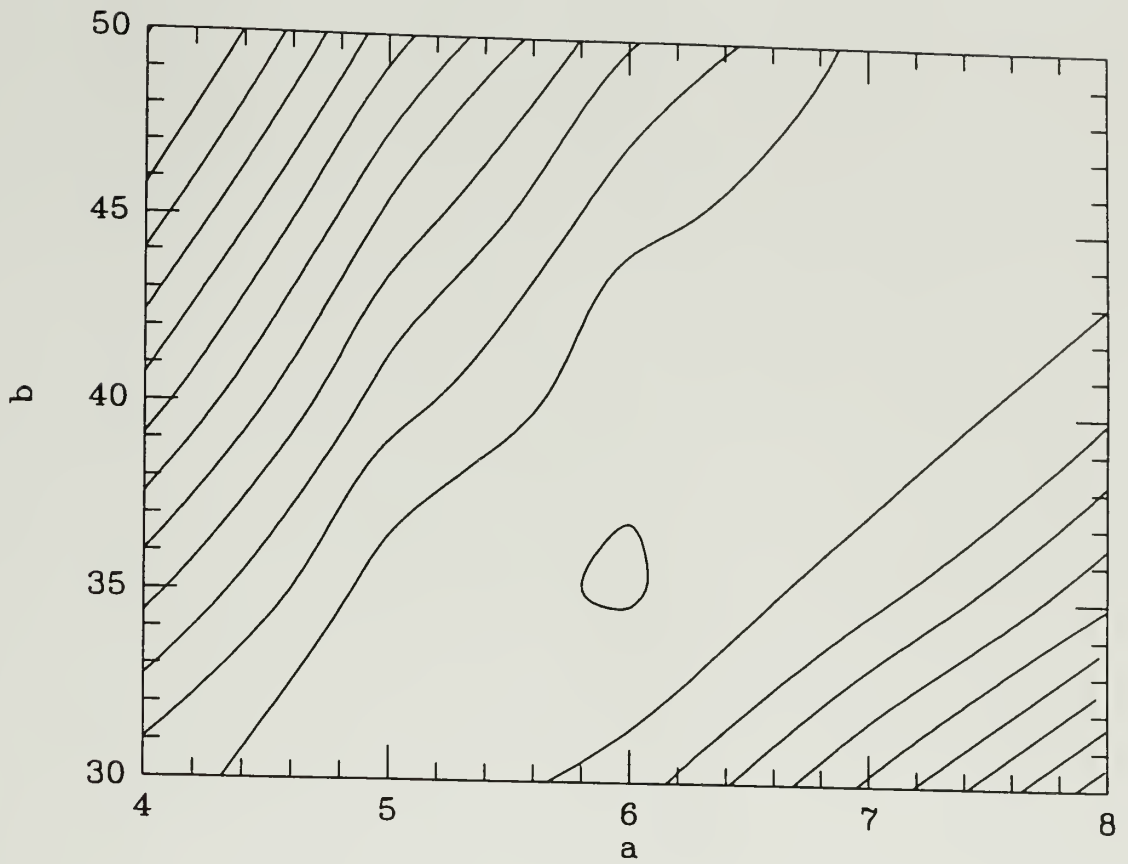


Figure 5.13  $\chi^2$ , contour map in a-b space. The equation (5.4) is used as a velocity law. The grid spacing of a is in unit of 1 and b in unit of 5. The contour spacing is 0.06.

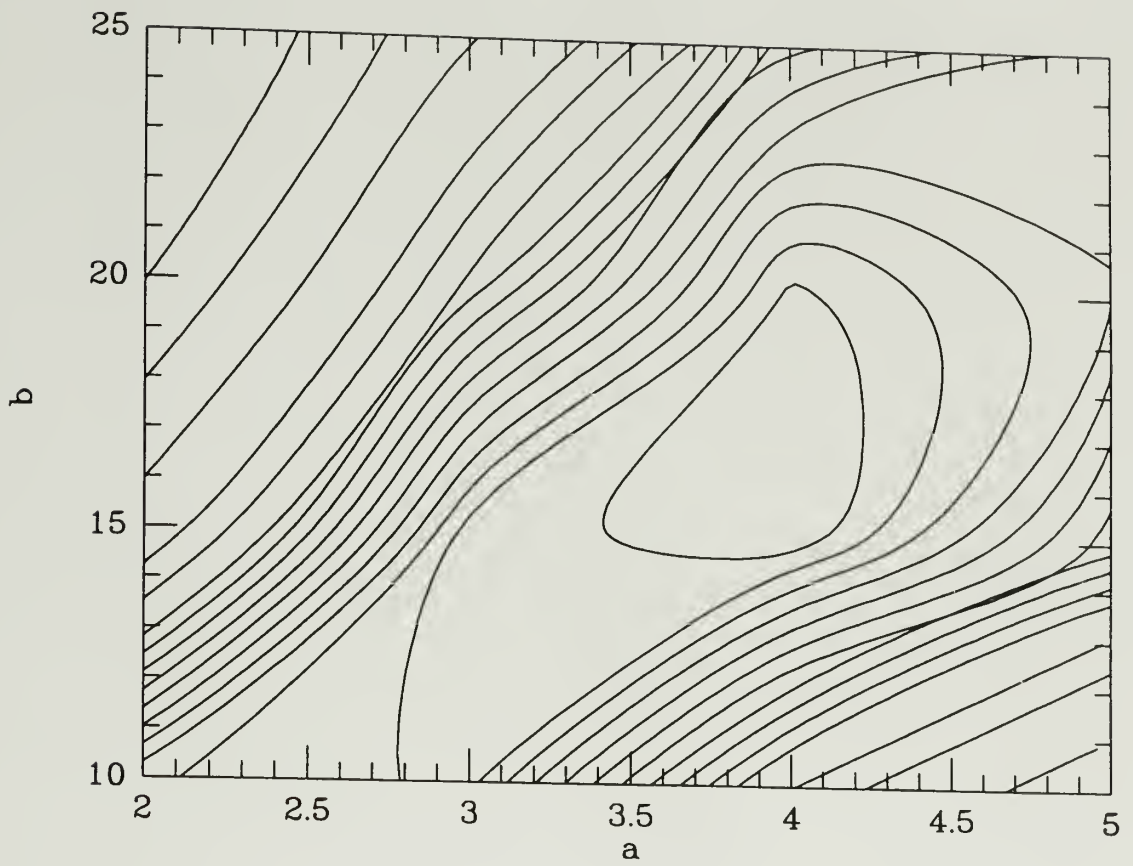


Figure 5.14  $\chi^2$  contour map in a-b space. The equation (5.5) is used as a velocity law. The grid spacing of a is in unit of 1 and b in unit of 5. The contour spacing is 0.06.

theoretical velocity curve and Figure 5.6 shows the theoretical velocity curve scaled for  $r_h$  according to the outflow velocity as a function of inversely square root of heliocentric distance from the Sun. The outflow velocity models obtained from the spectrum fitting are coincide well with the scaled velocity curve in this range, but in the range of  $r < 10^3$  km, the model generally do not agree with the theoretical velocity curve.

However, this apparent disagreement is an artifact of the model fitting procedure since the models are poorly constrained in this region. To illustrate this, we show in Figure 5.15, the distribution of HCN molecules with distance from the nucleus. In the calculation, the velocity of the model 4 has been used and the production distribution is assumed to be symmmatric, that is  $AP=0$ . The figure demonstrates that most HCN molecules reside in the out parts of the coma and therefore, the line of sight velocity distribution is heavily weighted by the results at this location. Thus, our model fitting results really only apply to the  $10^4 - 10^5$  km region, where the behavior of the models is relatively consistent and generally in accord with Combi's theoretical model.

#### **5.1.4 Conclusion**

The results of our analysis demonstrate that the kinematics of the coma can be studied through the HCN  $J=3-2$  rotational lines with high

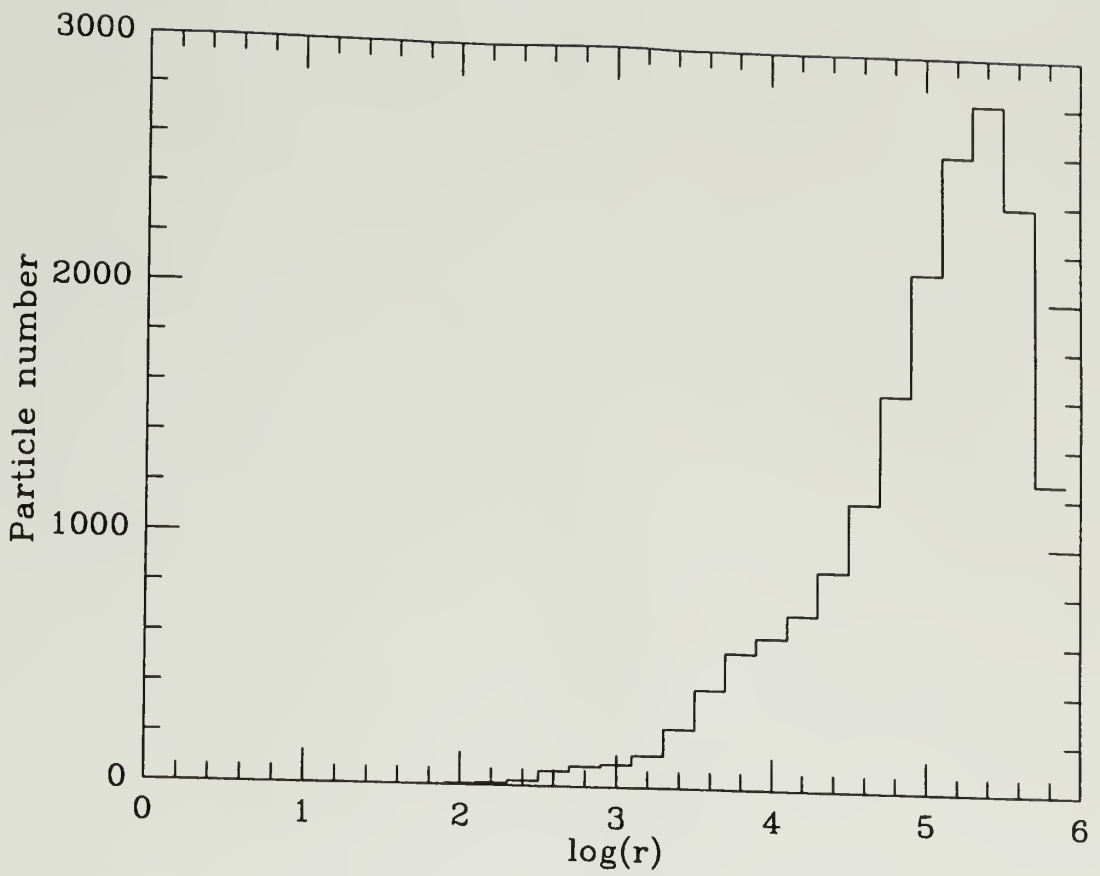


Figure 5.15 The HCN particle number as a function of  $r$ , the distance from the nucleus. The total of 200,000 particles and the velocity of model 4 have been used in the calculation.



spectral resolution obtained in comet Levy, and the map at 13 points over a region of 1.5 arcmin in the coma of comet Levy can be used to constrain the HCN lifetime against photodissociation.

It has been shown that isotropic HCN production from the nucleus with a constant outflow velocity in the coma, which was often adopted in previous models, does not explain the observed data. An anisotropy in the molecular distribution must be involved to account for asymmetry in the observed HCN spectral line profile. Moreover, the outflow velocity is required to be function of radial distance from the nucleus in order to account for the HCN  $J=3-2$  rotational line profile.

The HCN production rate in comet Levy is about  $2.6 \times 10^{26}$  mole.  $s^{-1}$  relative to this outflow velocity, and the abundance of HCN is 0.1% relative to water in comet Levy. This result is in agreement with that obtained in P/Halley and is generally consistent with observations of the HCN  $J=4-3$  spectra line.

As discussed in the chapter 2, the ratios of HCN both  $J=4-3/J=3-2$  and  $J=3-2/J=1-0$  integrated intensities can be used to determine the collisional cross-section and the temperature in the coma. Figure 2.4 shows that the ratios of  $J=4-3/J=3-2$  are relatively insensitive to both the coma temperature and the total collisional cross-section. The temperature of 100 K and the total collisional cross-section of  $10^{-14}$  have

been obtained from the IRAM observed ratio of HCN  $J=3-2/J=1-0$  (Bockelée-Morvan et al. 1990).

## 5.2 H<sub>2</sub>CO Molecule

H<sub>2</sub>CO is a very short-lived molecule with a lifetime of about 3,000 sec when exposed to the solar radiation. H<sub>2</sub>CO has possibly been observed in the optical, infrared, radio, and submillimeter wavelength bands, but despite these observations, it is still unclear whether the observed formaldehyde is coming directly from the nucleus or from a distributed source within the coma.

When recently obtained radio and millimeter observations (Snyder et al. 1989; Colom et al. 1989; Bockelée-Morvan et al. 1990) are interpreted by assuming the formaldehyde issued directly from the nucleus, an unreasonably high H<sub>2</sub>CO production rate relative to water is found. The H<sub>2</sub>CO photodissociation scale length, which is defined by lifetime times outflow velocity, was found to be  $1.44 \times 10^3$  km (Huebner and Carpenter 1979) at  $r_h = 1$  AU from the Sun. It was necessary to extend the H<sub>2</sub>CO scale length in Snyder et al.'s model (1989) to  $10^4$  km in order to obtain a reasonable value of the fractional formaldehyde abundance. This forced extension of the scale length means that gaseous H<sub>2</sub>CO still exists in the zone between  $10^3$  and  $10^4$  km from the nucleus where it

should be have been destroyed by photodissociation. Thus, Snyder et al. suggested that cometary  $\text{H}_2\text{CO}$  was being produced from an extended source in the coma as well as directly from the nucleus. Such an extended source for  $\text{H}_2\text{CO}$  is in agreement with the observations of some other species in comets. For example:

- The in situ measurements of CO and  $\text{N}_2$  in P/Halley made with the Giotto neutral-gas mass spectrometer (NMS) by Eberhardt et al. (1987) found that the NMS signal corresponding to CO had an approximately exponential growth, doubling in intensity within  $10^4$  km, but at distance  $>2 \times 10^4$  km the signal became constant. Eberhardt et al. (1987) can explain their NMS results if CO was produced both as a parent molecule directly from the nucleus and from an extended source in the inner coma such as cometary dust grains.

- Despois et al. (1986) found that CN production rate in Comet Halley is too high for HCN to be the sole source of CN. Moreover, the distribution of CN strongly indicates that a distributed source gives rise to at least part of the observed CN (A' Hearn et al. 1986; Kidger et al. 1987).

The idea of an extended source for molecules in the coma is strengthened by the discoveries of extremely small grains ( $10^{-16}$  g in mass) in P/Halley. Most of the grains are rich in Carbon, Hydrogen, Oxygen, and Nitrogen (Kissel et al. 1986). Of particular interest is the apparent

decrease in the relative amount of C, H, O, and N in the dust with increasing distance from the nucleus (Kissel et al. 1986), which has been invoked to explain the Earth-based observations of CN jets (A' Hearn et al. 1986; Larson et al. 1986). At the same time, infrared observations of a color gradient in the inner coma of P/Halley suggest that there is fragmentation of dust grains which could, in the process, be releasing volatile and thus serving as the dispersed source (Garzon et al. 1987; Rieke and Campins 1987). The polyoxymethylene (POM), as a polymer of  $\text{H}_2\text{CO}$ , has been identified from the periodic mass abundance peaks observed by the heavy ion analyser PICCA of Giotto (Huebner et al. 1987) and suggested as a distributed source of CO and  $\text{H}_2\text{CO}$  throughout the inner coma.

Thus, it is reasonable to examine  $\text{H}_2\text{CO}$  both as a parent and as a possible daughter to analyze the spectra obtained in comet Levy.

### 5.2.1 Spectrum

The same technique that was applied to the HCN spectra has been adapted for the  $\text{H}_2\text{CO}$  analysis. The parameters, for  $\text{H}_2\text{CO}$  as a parent molecule, that need to be determined in the process are:

- The  $\text{H}_2\text{CO}$  production rate  $Q(\text{H}_2\text{CO})$
- The parent outgassing velocity  $V_p$

- The parent lifetime against photodissociation
- The anisotropy parameter AP

Assuming H<sub>2</sub>CO is a parent molecule, we calculate the least values of  $\chi^2_v$  in the AP-V<sub>p</sub> parameter space with several different H<sub>2</sub>CO lifetime values so that we can find the best value of the lifetime to fit the spectrum. Isotropic H<sub>2</sub>CO outflow with a constant velocity has been assumed. Table 5.4 lists the best fitting AP and V<sub>p</sub> values obtained from the calculations. The H<sub>2</sub>CO lifetime against photodissociation is about  $2.9 \pm 0.8 \times 10^3$  sec. These three submillimeter spectral profiles of the H<sub>2</sub>CO rotational transition at 352 GHz have been fitted and shown in Figure 5.16 to Figure 5.18. The H<sub>2</sub>CO production rates found from fitting the spectra on August 30 and 31, 1990, are  $3.75 \pm 0.72 \times 10^{26}$  and  $4.55 \pm 1.1 \times 10^{26}$  molec s<sup>-1</sup>, respectively.

The results in Table 5.4 show large errors in the fitted values of AP due to the poor quality of the spectra. However, it is conceivable that the observed difference in AP values between August 30 and 31 may reflect day-to-day variations in the H<sub>2</sub>CO production distribution. The value of outflow velocity obtained from the averaged spectrum is approximately the same as that we derived from the HCN data.

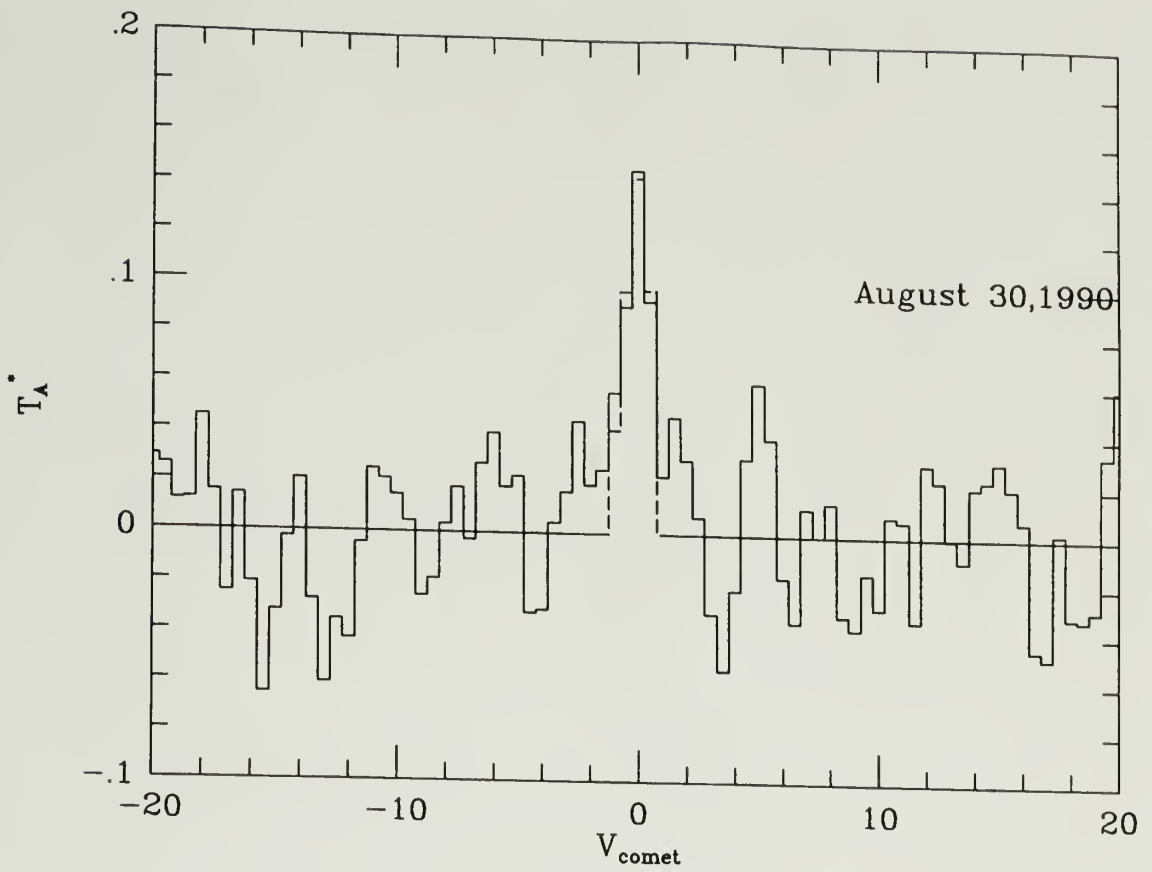


Figure 5.16 Fit to H<sub>2</sub>CO 5<sub>15</sub>-4<sub>14</sub> spectrum of Comet Levy (1990c) obtained on August 30, 1990. The model with the velocity of 0.72 km s<sup>-1</sup> and AP of -0.38 is used.

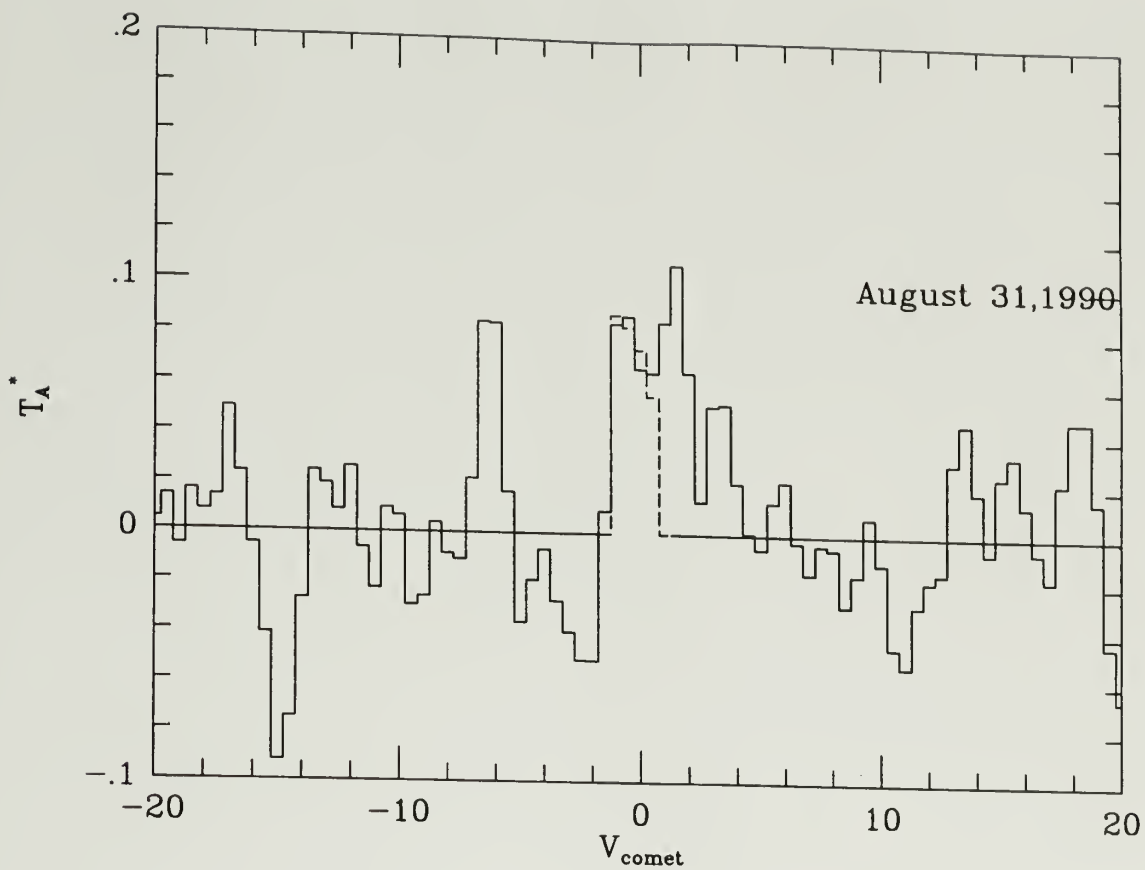


Figure 5.17 Fit to  $\text{H}_2\text{CO } 5_{15}-4_{14}$  spectrum of Comet Levy (1990c) obtained on August 31, 1990. The model with the velocity of  $0.90 \text{ km s}^{-1}$  and AP of 0.20 is used.

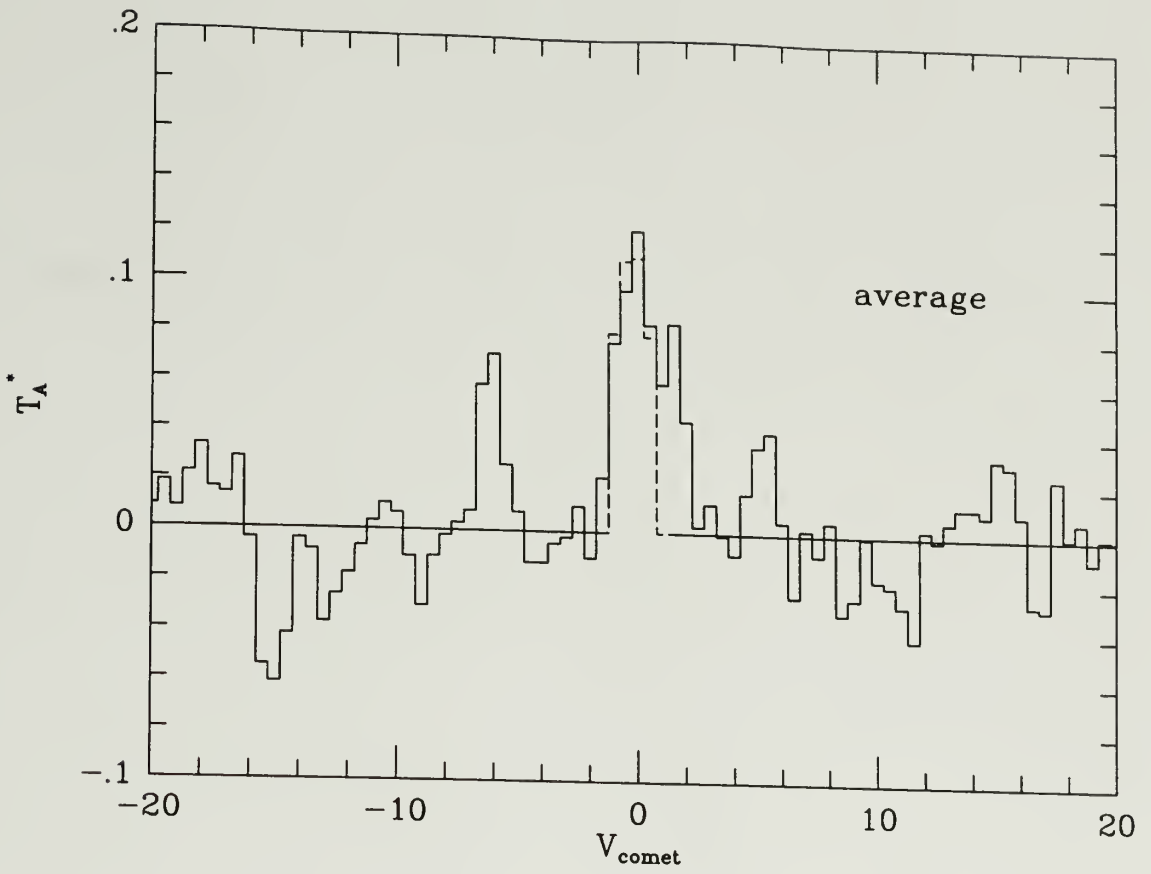


Figure 5.18 Fit to H<sub>2</sub>CO 5<sub>15</sub>-4<sub>14</sub> spectrum of Comet Levy (1990c) obtained on two days average. The model with the velocity of 0.81 km s<sup>-1</sup> is used.



Table 5.4

Parameters in Model fitting

Parameter\Date	August 30	August 31	Average
AP	$-0.38 \pm 0.24$	$0.21 \pm 0.36$	$-0.01 \pm 0.19$
$V_p$	$0.72 \pm 0.11$	$0.90 \pm 0.14$	$0.81 \pm 0.08$
$\chi^2$	1.48	2.30	1.171
$Q(\text{H}_2\text{CO}) 10^{26} \text{ s}^{-1}$	$3.75 \pm 0.72$	$4.55 \pm 1.1$	$4.23 \pm 0.91$

### 5.2.2 Map

The extended emission observed in maps of  $\text{H}_2\text{CO}$  appears to be inconsistent with a parent molecule model (see Figure 4.5) as the molecule has a short-lifetime from the photodissociation. Thus, we have assumed  $\text{H}_2\text{CO}$  as a parent or a daughter molecule respectively in order to fit the map shown in Figure 4.5 and compare the results of these two models. As we discussed in chapter 4, the five-point map has been averaged on the spectra of the offset positions to become a three-point map since its poor quality. The real nucleus position,  $x_{\text{off}}$  and  $y_{\text{off}}$  obtained from the HCN map fit, has been used for both the parent and the daughter models.

A  $2.86 \times 10^3$  sec of the molecular lifetime against photodissociation and  $0.8 \text{ km s}^{-1}$  of outflow velocity have been used in the parent model.

If  $\text{H}_2\text{CO}$  is assumed to be a daughter, the following additional parameters need to be considered:

- Daughter velocity  $V_d$
- Daughter lifetime against photodissociation

Thus, an assumed parent molecule of  $\text{H}_2\text{CO}$  flows out from the nucleus with a constant outflow velocity  $V_p$  and some later time, photodissociation by the solar radiation occurs and an  $\text{H}_2\text{CO}$  molecule is formed. From this position, the  $\text{H}_2\text{CO}$  goes in a random direction until the time of its photodissociation with a velocity  $V_d$ . A value of lifetime  $2.86 \times 10^3 \text{ s}$  is used for  $\text{H}_2\text{CO}$  according to the evaluation by Huebner and Carpenter (1979), and the velocity of the parent molecule is assumed to be the same as the velocity of  $0.8 \text{ km s}^{-1}$  for HCN. In the daughter model, the line width of  $\text{H}_2\text{CO}$  is dependant on the sum of the outflow velocities of parent and daughter molecules. Thus, the daughter outflow velocity can be determined from the width of averaged spectrum shown in Figure 5.18 after giving a value of parent outflow velocity and only the parent lifetime needs to be determined in the model. As discussed before, the dust grains may be the distributed source of  $\text{H}_2\text{CO}$  and in generally, the velocity of dust grain is less than that of molecules in the coma. So the

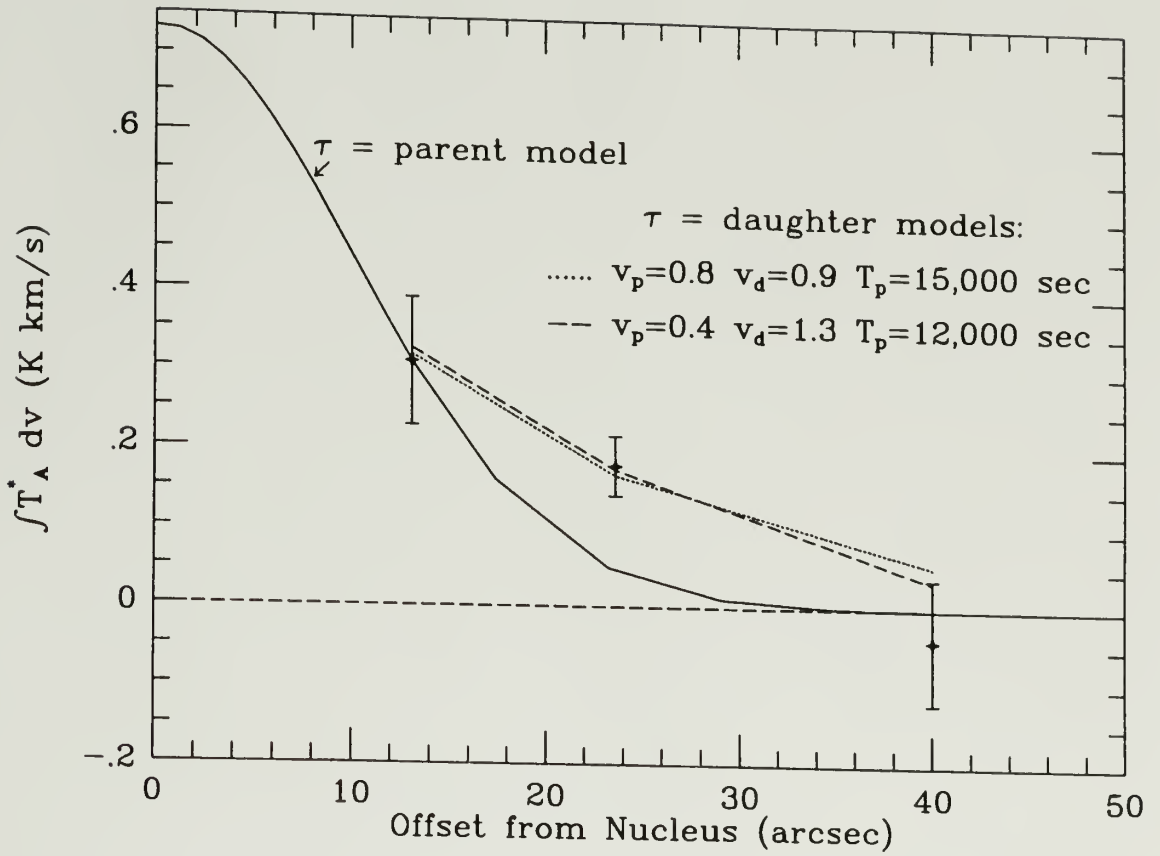


Figure 5.19 Observed distribution of  $H_2CO$   $5_{15}-4_{14}$  emission compared to that of both the parent model (solid line) and the daughter models.

case of  $0.4 \text{ km s}^{-1}$  of parent molecular velocity has been included in the daughter model.

The results in Figure 5.19 display the fitting of  $\text{H}_2\text{CO}$  to the three-point map spectra. The figure indicates that  $1.5 \times 10^4$  and  $1.2 \times 10^4$  sec lifetimes of the parent molecule corresponding to the outflow velocities of  $0.8$  and  $0.4 \text{ km s}^{-1}$  respectively are required to best fit the observed data. Figure 5.19 also shows the results from using the parent model in order to compare the daughter model with the parent one. As we can see from the figure, the parent model is not consistent with the observed data since  $\text{H}_2\text{CO}$  is a short lived molecule under the solar radiation field. A possible explanation of the observed spatial distribution is an over abundance of formaldehyde at  $20 \text{ arcsec}$  from the nucleus, and implying that part of the observed gaseous formaldehyde is produced by a distributed source in the coma.

### 5.2.3 Conclusion

Formaldehyde was detected in comet Levy at submillimeter wavelength through its  $5_{15}-4_{14}$  rotational line at  $355 \text{ GHz}$ , as predicted by the excitation model. Calculations in the assumption of direct release from the nucleus show that the abundance of formaldehyde is variable on the daily basis and close to  $0.2\%$  relative to water in the comet Levy. The

fit of the model to the  $\text{H}_2\text{CO}$  data found a value of  $0.8 \text{ km s}^{-1}$  for the outflow velocity, which is in agreement with that derived from the HCN data.

The observed spatial distribution of the 355 GHz line intensity suggests that a daughter model for  $\text{H}_2\text{CO}$  can better explain the data. The results support the assumption that  $\text{H}_2\text{CO}$ , in addition to its release from the nucleus, also originates from a distributed source in the coma. A distributed source with a 15,000 sec lifetime against photodissociation if the outflow velocity  $0.8 \text{ km s}^{-1}$  is assumed fits the observations of comet Levy.

That formaldehyde might originate from a distributed source has been suggested by Snyder et al. (1989) in order to explain the detection of the 6 cm  $\text{H}_2\text{CO}$  line in comet Halley with the VLA and by Colom et al. (1992) in order to fit IRAM observation of the 226 GHz line intensity. The discovery of dust grains consisting of carbon, hydrogen, oxygen, and nitrogen (Kissel et al 1986) suggests that there is a connection between molecules in the coma and the dust grains. Huebner et al. (1987) have suggested the identification of polyoxymethylene (POM), a polymer of  $\text{H}_2\text{CO}$ , acting as a distributed source throughout the inner coma.

## CHAPTER 6

### SUMMARY

Comets are believed to be the most pristine remnants of the material present at the time of the formation of the solar system, and important information about the chemical and physical processes early in the evolution of a planetary system can be obtained from the study of their composition. The molecules in the coma can give the direct information on the composition of cometary ices. The determination of their production rate, spatial distribution, and kinematics are the primary goals for spectral studies of comets.

Observations with high spectral resolution are most desirable in order to probe the physical and kinematic conditions in the coma. The high quality of spectra for both HCN and H<sub>2</sub>CO molecules in comet Levy offer an opportunity to acquire the information.

We have developed models for the excitation of cometary hydrogen cyanide and formaldehyde in order to interpret their rotational lines observed in comets. The main excitation mechanisms included in our models are thermal excitation by collision and radiative excitation by infrared solar radiation. In our model, we have treated collisional cross-sections for both molecules as depending on the rotational quantum numbers in the calculations. This method results in only a 10% difference

in derived HCN integrated intensities compared with previous models. The model for excitation of formaldehyde shows that both rotational transitions,  $3_{12}-2_{11}$  and  $5_{15}-4_{14}$ , should be observable in comets. However, the model fails to produce the strong the  $\text{H}_2\text{CO}$  6-cm line obtained in P/Halley by Snyder et al (1989) with VLA.

The distribution of molecules in the comet coma is discussed in order to interpret the observed integrated intensity. We have adapted the vectorial model for the behavior of daughter molecules in cometary comae to generate synthetic spectra of both parent molecules and possible daughter molecules. The model is sufficiently complex that the Monte Carlo method has been used to facilitate the calculations.

We have used our excitation and coma models to analyze both HCN and  $\text{H}_2\text{CO}$  molecules. The kinematics of the coma can be studied through the HCN  $J=3-2$  rotational lines obtained with high spectral resolution in comet Levy and the spectral line map. It has been shown that a varying outflow velocity as a function of radial distance from the nucleus is required to fit the HCN  $J=3-2$  rotational line profile. The HCN production rate in comet Levy is about  $2.6 \times 10^{26}$  mole.  $\text{s}^{-1}$  and the derived abundance is in agreement with that obtained in P/Halley.

Formaldehyde was detected for the first time in comets at millimeter and submillimeter wavelengths through the  $3_{12}-2_{11}$  (Colom et al. 1990) and  $5_{15}-4_{14}$  transitions (Schloerb and Ge 1990). It appears that

$\text{H}_2\text{CO}$  is a relatively minor species with a production rate relative to water of less than 1%. Both a parent model and daughter model have been used in order to explain its emission distribution in comet Levy. A daughter model with a lifetime of  $6 \times 10^4$  sec provides the most reasonable fit to the observations and suggests that  $\text{H}_2\text{CO}$  may be produced by an extended source in the coma.



## BIBLIOGRAPHY

- A'Hearn, M.F., S. Hoban, P.V., Birch, C., Bowers, R., Martin, and D.A. Klinglesmith III 1986, *Nature* 327, 649-651.
- Bockelée-Morvan, D. 1987, *Astron. Astrophys.* 181, 169.
- Bockelée-Morvan, D. 1990 In *Asteroids, Comets and Meteors III* 259.
- Bockelée-Morvan, D., Colom, P., and Crovisier, J. 1991 *Nature* 350, 318.
- Bockelée-Morvan, D. and Crovisier, J. 1986, in "Asteroids, comet MeteorsII" P279.
- Bockelée-Morvan, D., Gérard, E. 1984 *Astron. Astrophys.* 131, 111.
- Bockelée-Morvan, D., Crovisier, J., Baudry, A., Despois, D., Perault, M., Irvine, W.M., Schloerb, F.P., and Swade, D. 1984, *Astron. Astrophys.*, 141, 411.
- Bockelée-Morvan, D. and Crovisier, J. 1987a, *Astron. Astrophys.* 187, 425.
- Bockelée-Morvan, D. and Crovisier, J. 1987b, in "Proc. Symposium on the Diversity and similarity of Comets", ESA SP-278,235.
- Bockelée-Morvan, D. and Crovisier, J. 1992, (in press).
- Bockelée-Morvan, D., Crovisier, J., Despois, D., Forveille, T., Gérard, E., Schraml, J., Thum, C. 1987, *Astron. Astrophys.* 180, 253.
- Brooke, T.Y., Knacke, R.F., Owen, T.C., Tokunaga, A.T. 1989, *Astrophys.* 336, 971.
- Brooke, T.Y., Tokunaga, A.T., Knacke, R.F. 1991, *Astron.* 101, 268.
- Claussen, M.J., and Schloerb, F.P. 1987, NRAO Workshop No. 17, Green Bank, W. Virginia, 135-141.

- Clouthier, D.J., Ramsay, D.A. 1983, *Ann. Rev. Phys. Chem.* **34**, 31.
- Colom, P., Crovisier, J., Bockelée-Morvan, D., Despois, D.,  
Paubert, G. 1992, *Astron. Astrophys.* (in press).
- Combes, M., Moroz, V.I., Crovisier, J. 1988, *ICARUS* **76**, 404.
- Combi, M.R. 1980, *astrophys. J.* **237**, 633.  
-----1980b, *Astrophys. J.* **237**, 641.
- Combi, M.R. 1989, *ICARUS* **81**, 41.
- Combi, M.R. and Smyth, W.H. 1988a, *Astrophys.* **327**, 1026.  
-----1988b, *Astrophys.*, **327**, 1044
- Cosmovici, C. B., Ortolani, S. 1984 *Nat* **310**, 122.
- Crovisier, J. 1984, *Astron. Astrophys.*, **130**, 361.
- Crovisier, J. 1987, *Astron. Astrophys. Suppl.*, **68**, 223.
- Crovisier, J., Despois, D., Bockelée-Morvan, D., Colom, P.,  
Paubert, G. 1991, *ICARUS* **93**, 246.
- Crovisier, J. and Encrenaz, T. 1983, *Astron. Astrophys.*, **126**, 170.
- Crovisier, J. and Schloerb, F.P. 1991, In *Comets in the post-Halley  
Era*, Edts R. Newburn et al., Kluwer Academic Publishers, p.  
149.
- Delsemme, A.H. 1982, Chemical composition of cometary nuclei. In  
*comets*(L.L. Wilkening, ED), PP. 85-130.
- Despois, D., Crovisier, J., Bockelée-Morvan, D., Schraml, J.,  
Forveille, T., and Gérard, E. 1986, *Astron. Astrophys.* **160**,  
L11.
- Eberhardt, P., D. Krankowsky, W. Schulte, U. Dolder, P.  
Lammerzahl, J.J. Berthelier, J. Woweries, U. Stubbemann,  
R.R. Hodges, J.H. Hoffman, and J.M. Illiano 1987, *Astron.  
Astrophys.* **187**, 481.
- Green, S. and Thaddeus, P. 1974, *Astrophys. J.*, **191**, 653.

- Green, S., Garrison, B.J. and Lester, W.A. 1978, *Astrophys. Suppl.* **37**, 321.
- Haser, L. 1957, *Bull. Acad. Roy. Soc. Belgique*, **43**, 740.
- Haser, L. 1966, *Mém. Soc. Roy. Sci. Liège*, **12**, series 5, 233.
- Hu, H.-Y., 1990, Ph.D. dissertation, University of Arizona.
- Huebner, W.F. and Carpenter, C.W. 1979, Los Alamos Informal Report LA-8065-MS.
- Huebner, W.F., Snyder, L.E., and Buhl, D. 1974, *Icarus* **23**, 580.
- Huggins, W. 1882, *Proc. Roy. Soc.* **33**, 1.
- Jaruschewski, S., Chandra, S., Varshalovich, D.A., Kegel, W.H. 1986, *Astron. Astrophys. Suppl.* **63**, 307.
- Keller, H.U. et al. 1987, *Astron. Astrophys.* **187**, 807.
- Kidger, M.R., Acosta, J.A., Garzón, F., Prieto, M., Gómez, R. *Astron. Astrophys.* **187**, 363.
- Lämmerzahl, P., Krankowsky, R.R. Hodges, U. Stubbemann, J. Woweries, I. Herrwerth, J.J. Berthelier, J.M. Illiano, P. Eberhardt, U. Dolder, W. Schulte, and J. H. Hoffman 1987, *Astron. Astrophys.* **187**, 169.
- Larson, H.P., H.-Y. Hu, M.J. Mumma, and H.A. Weaver 1990, *Icarus* **82**, 379.
- Larson, H.P., Mumma, M.J., Weaver, H.A. 1987, *Astron. Astrophys.* **187**, 391.
- Mumma, M.J., Weaver, H.A., Larson, H.P., Davis, D.S., Williams, M. 1986, *Science* **232**, 1523.
- Reuter, D., Mumma, M., Nadler, S. 1989a, *Astrophys.* **341**, 1045.
- Schloerb, F.P. and Ge, W. 1990, *IAU Circ. No.* 5086.
- Schloerb, F.P., Kinzel, W.M., Swade, D.A., and Irvine, W.M. 1986a, *Astrophys. J.* **310**, L55.

- Schloerb, F.P., Kinzel, W.M., Swade, D.A., and Irvine, W.M. 1987, *Astron. Astrophys.* **187**, 475.
- Snyder, L.E. 1982, *Icarus* **51**, 1.
- Snyder, L.E. and Buhl, D. 1971, *Astrophys. J.* **241**, L123.
- Snyder, L.E., Palmer, P., and Pater, I.D. 1989, *Astron. J.* **97**, 246.
- Tacconi-Garman, L.E. 1989, Ph.D. dissertation, University of Massachusetts.
- Tacconi-Garman, L.E., and Schloerb, F.P. 1987, NRAO Workshop No. 17, 143.
- Tacconi-Garman, L.E., Schloerb, F.P., and Claussen, M.J. 1990, *Astrophys. J.* **364**, 672.
- Valk, J.H., O'Dell, C.R., Cochran, A.L., W.D., Opal, C.B. 1992, *Astrophys. J.* **388**, 621.
- Weaver, H.A., and Mumma, M.J. 1984, *Astrophys. J.* **276**, 782.
- Weaver, H.A., Mumma, and H.P. Larson 1987, *Astron. Astrophys. J.* **187**, 411.
- Whipple, F.L. 1950, *Astrophys. J.* **111**, 375.
- Winnberg A., Ekelund, L., Ekelund, A. 1987, *Astron. Astrophys.* **172**, 476.
- Wyckoff, S., Tegler, S., Wehinger, P.A., Spinrad, H. and Betton, M.J.S. 1988, *Astrophys. J.* **325**, 927.

